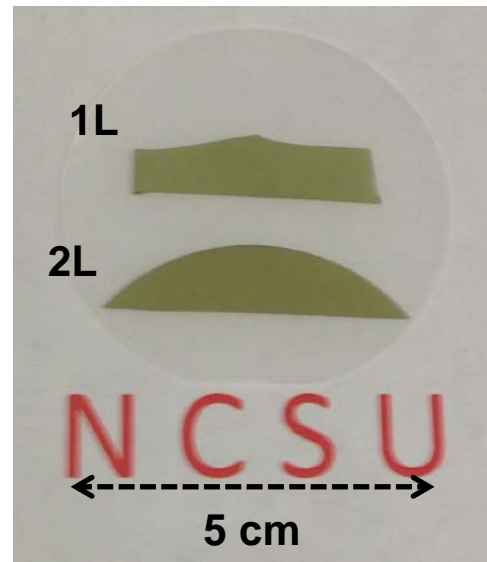


# **2D Transition Metal Dichalcogenide (TMDC) Materials : Synthesis, Properties, and Applications**



**Linyou Cao**

Department of Materials Science and Engineering, North  
Carolina State University

**Oct. 3, 2015 CCDM Tutorial**

# Outline

## **I. Introduction of 2D TMDC materials**

## **I. Synthesis and transfer of 2D TMDC materials**

- Synthesis
- Transfer

## **II. Fundamental Properties**

- Raman
- Catalytic
- Electrical
- Optical

# **I. Introduction of 2D TMDC Materials**

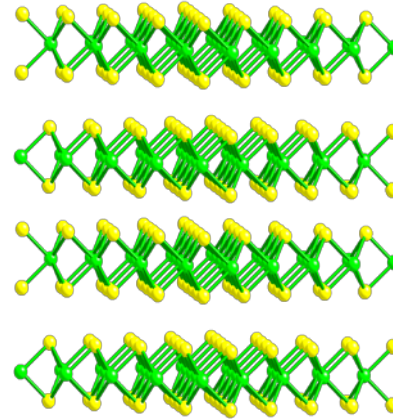
# Transition Metal Dichalcogenide (TMDC)

## Materials: Compositions



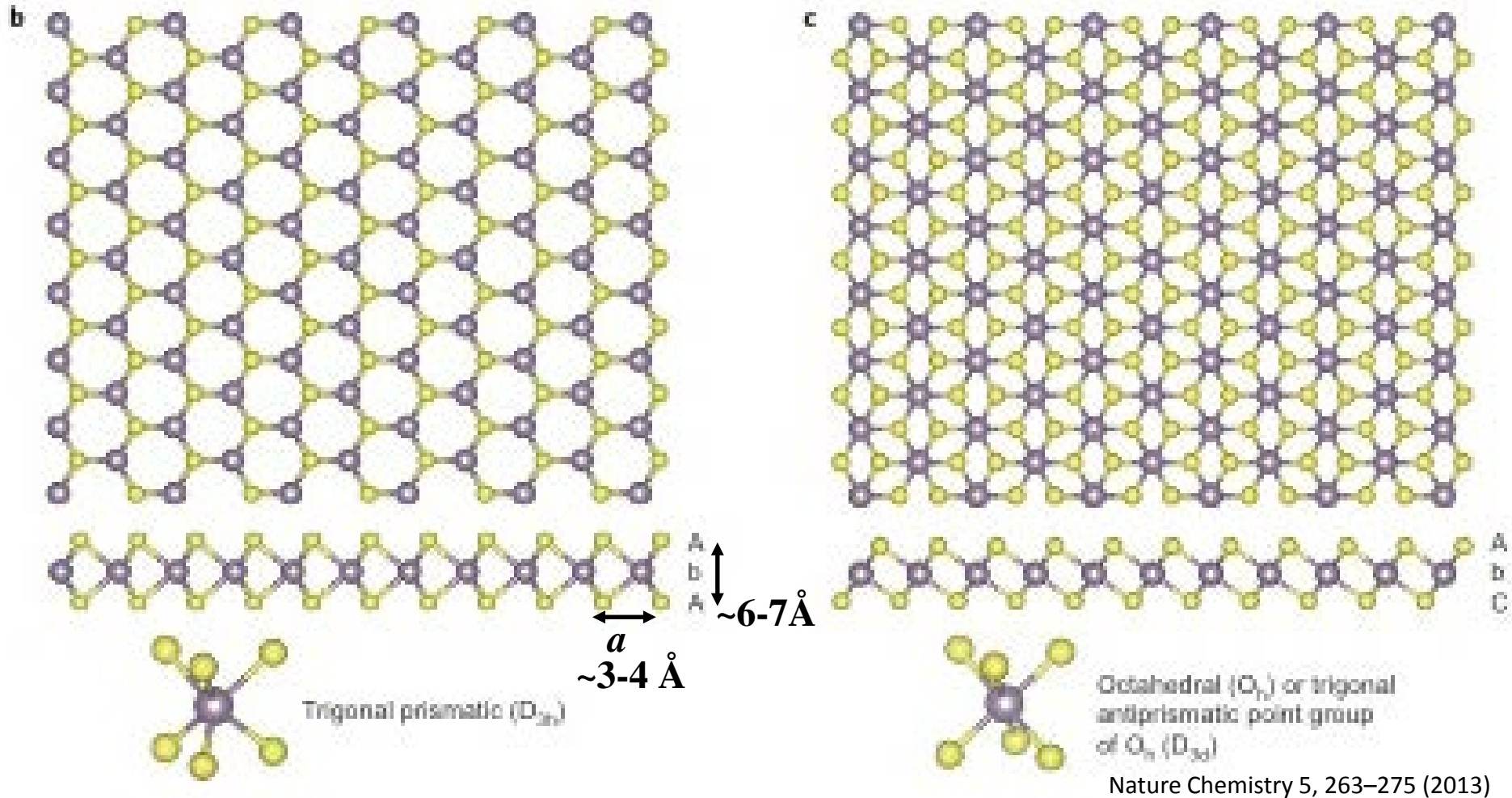
M = Transition metal

X = Chalcogen



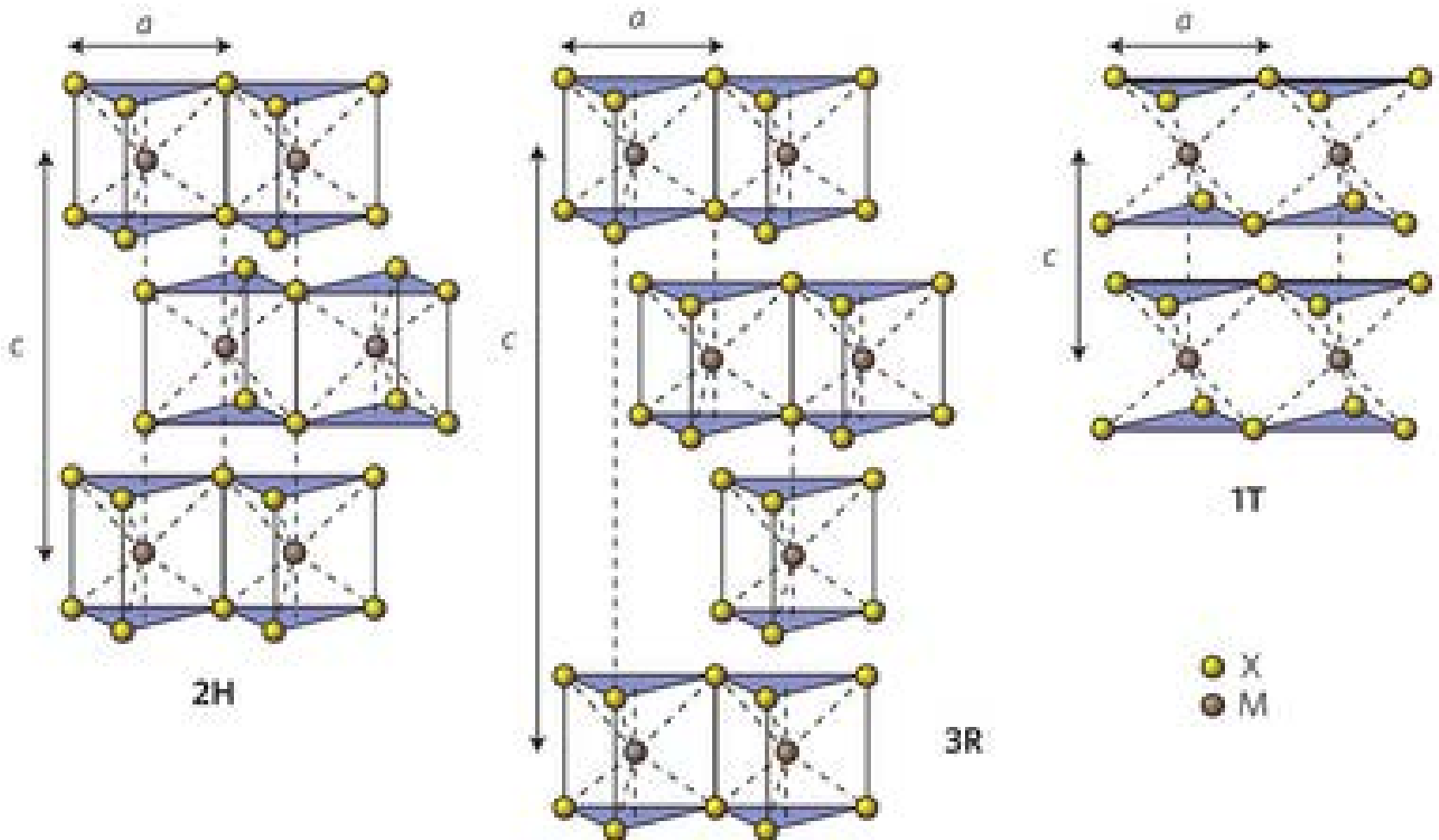
H																	He
Li	Be											B	C	N	O	F	Ne
Na	Mg	3	4	5	6	7	8	9	10	11	12	Al	Si	P	S	Cl	Ar
K	Ca	Sc	Ti	V	Cr	Mn	Fe	Co	Ni	Cu	Zn	Ga	Ge	As	Se	Br	Kr
Rb	Sr	Y	Zr	Nb	Mo	Tc	Ru	Rh	Pd	Ag	Cd	In	Sn	Sb	Te	I	Xe
Cs	Ba	La-Lu	Hf	Ta	W	Re	Os	Ir	Pt	Au	Hg	Tl	Pb	Bi	Po	At	Rn
Fr	Ra	Ac-Lr	Rf	Db	Sg	Bh	Hs	Mt	Ds	Rg	Cn	Uut	Fl	Uup	Lv	Uus	Uuo

# TMDC Materials: Crystal Structures



**Two polymorphs in monolayer : trigonal prismatic (1H) and octahedral (1T).**

# TMDC Materials: Crystal Structures

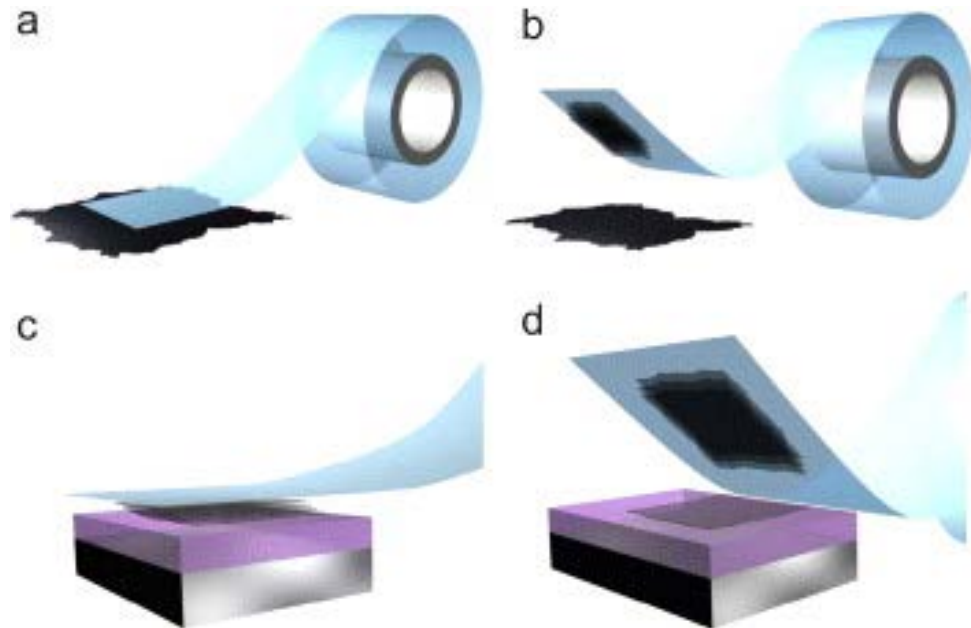


**Bulk TMDCs exhibit a wide variety of polymorphs and stacking polytypes**

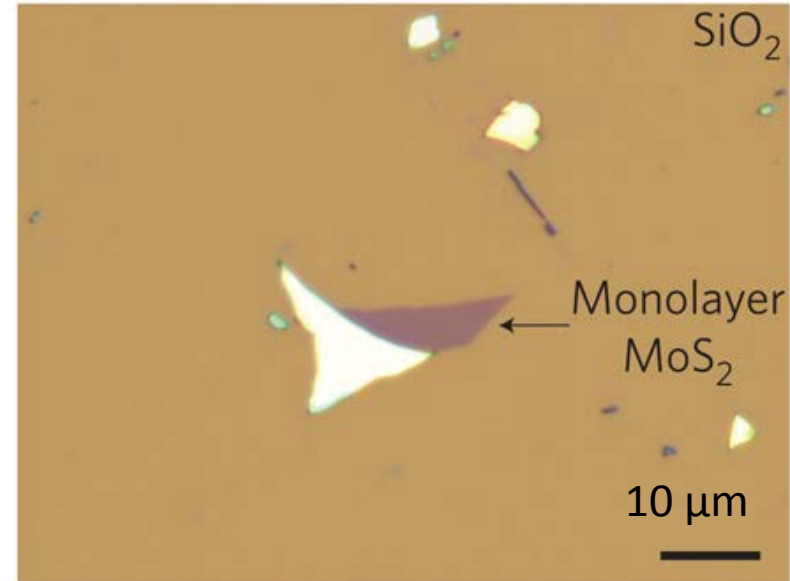
# **II. Synthesis and Transfer of 2D TMDC Materials/Heterostructures**

## **II.1 Synthesis**

# Mechanical Exfoliation



Credit: K S Novoselov and A H Castro Neto



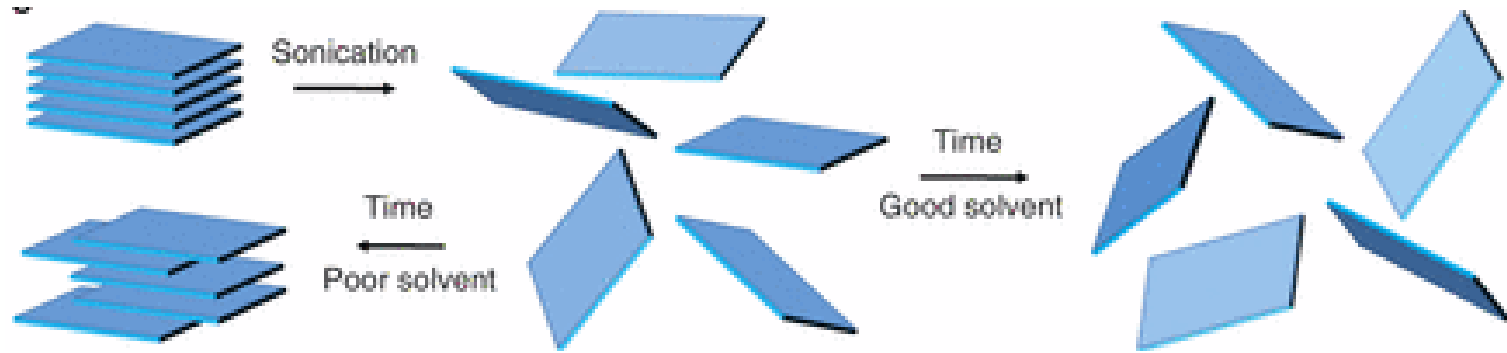
Nature Nanotechnology 6, 147–150 (2011)

- Low yield, not scalable
- Limited control in layer number
- Low uniformity (mixed layer numbers)
- Small size



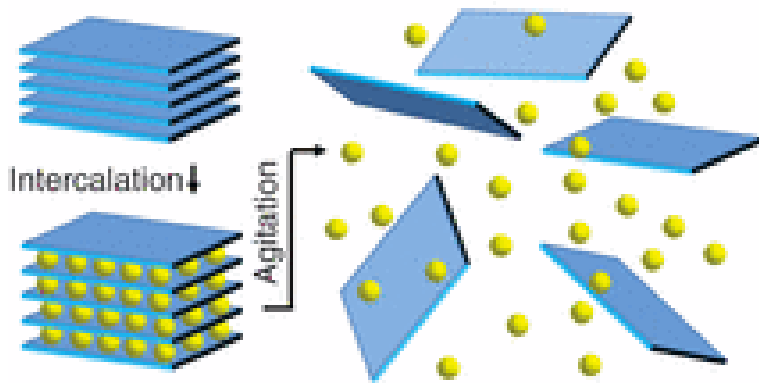
# Liquid Exfoliation

## Sonication-assisted exfoliation (both monoalyer and fewlayers)



Key: good solvent (its surface energy is similar to that of the layered material, dimethylformamide or N-methyl-pyrrolidone), surface surfactant or polymer

## Ion intercalation - assisted exfoliation



Intercalants such as n-butyllithium in hexane (exclusively monolayers)

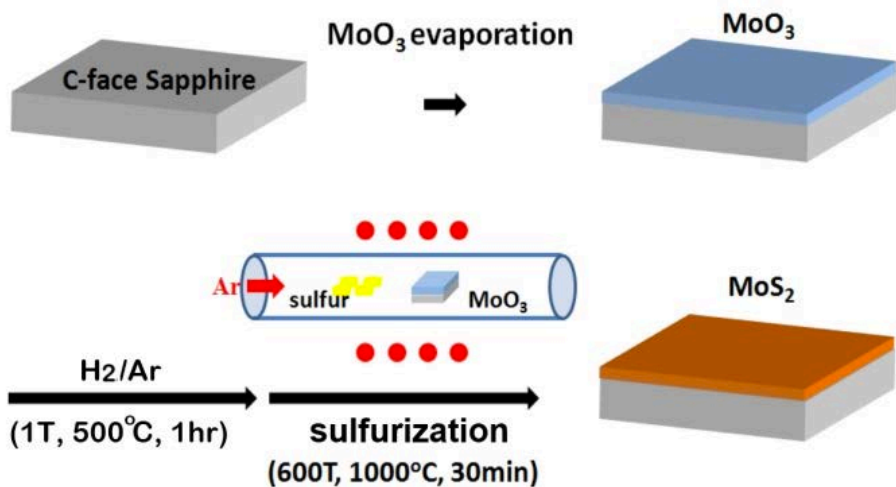


Nature Chemistry 5, 263–275 (2013)

- Surface contamination
- Structure distortion or damage

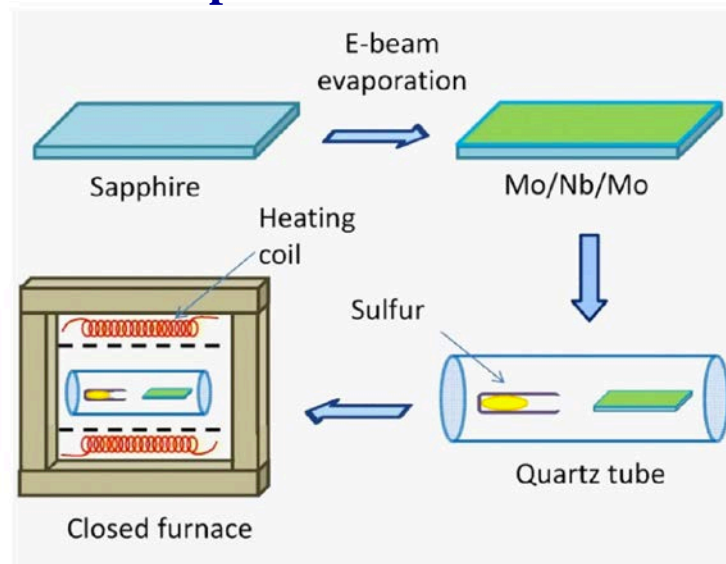
# Sulfurization of Pre-deposited Precursors

## Oxide precursor: $\text{MoO}_3$ or $\text{WO}_3$



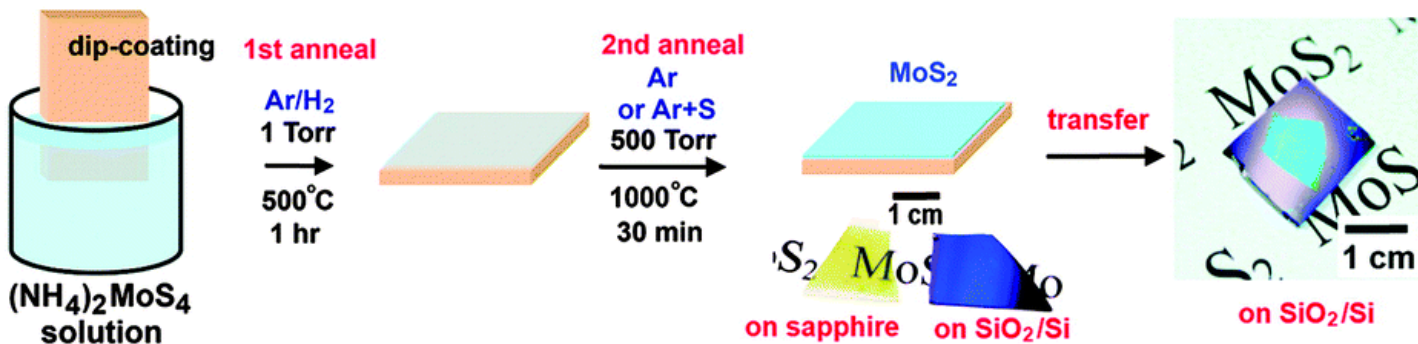
Nanoscale 4, 6637-6641 (2012)

## Metal precursor: Mo or W



Applied Physics Letters, 102, 252108 (2013)

## Thiosalt

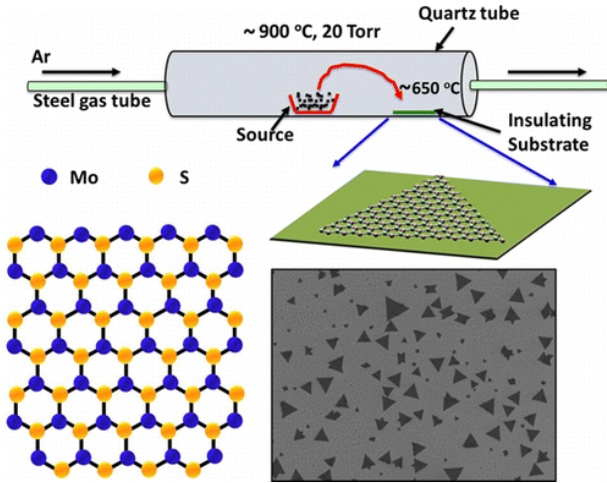


Nano Letters 12 (3), 1538-1544 (2012)

Uniformity & Control of layer number?

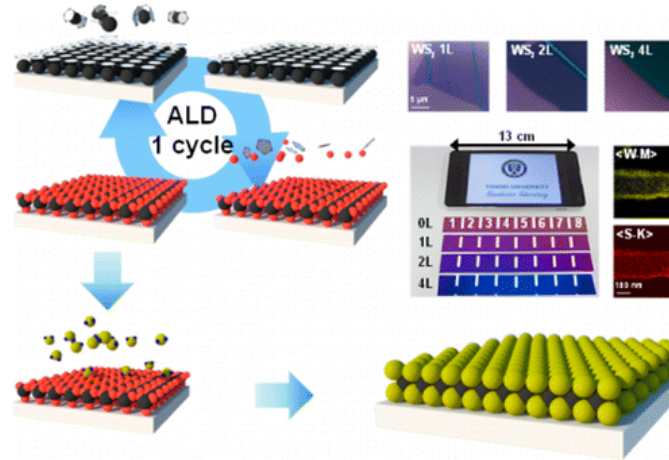
# PVD, ALD, and MBE Growth

## Physical vapor deposition

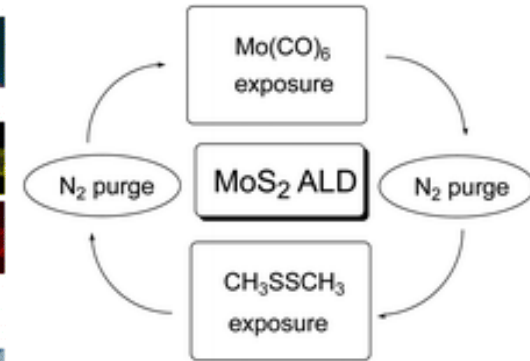


ACS Nano, 2013, 7 (3), pp 2768–2772

## Atomic layer deposition

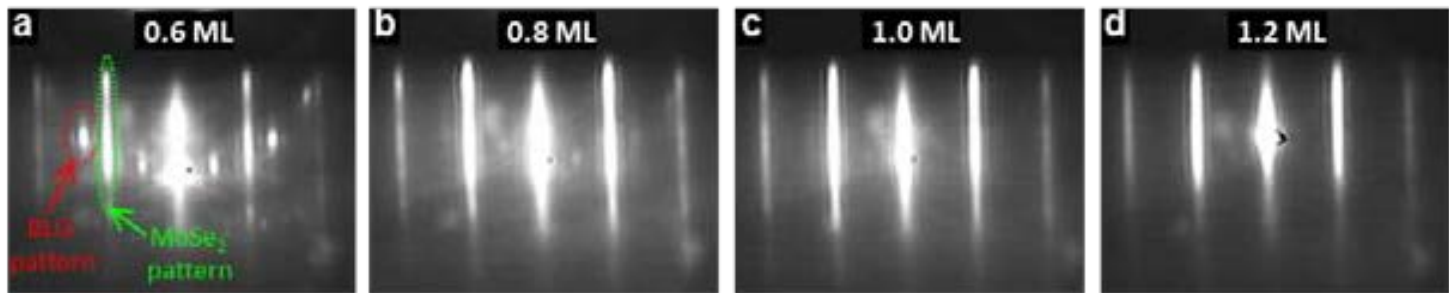
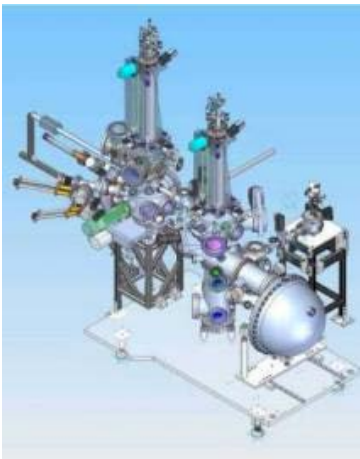


ACS Nano, 2013, 7 (12), pp 11333–11340



Nanoscale, 2014, 6, 14453–14458

## Molecular beam epitaxy (only MoSe2 reported to date)



Nature Nanotechnology 9, 111–115 (2014)

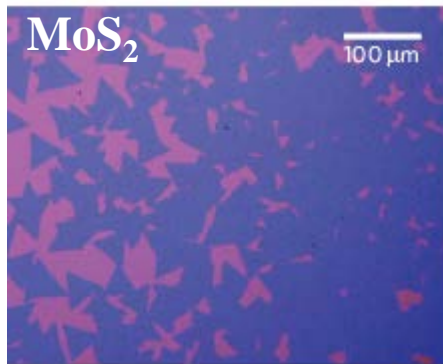
**Cost, Uniformity & Control of layer number?**

# Chemical Vapor Deposition: Oxide Precursor

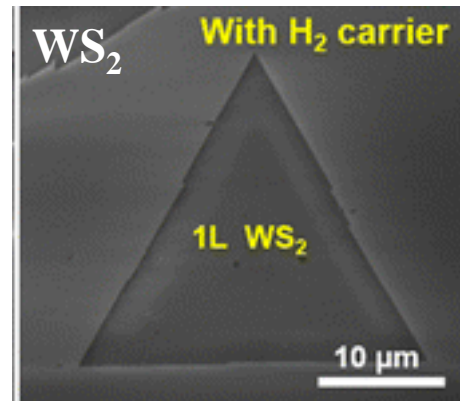


Precursor 1: S or Se  
Precursor 2: MoO<sub>3</sub> or WO<sub>3</sub>

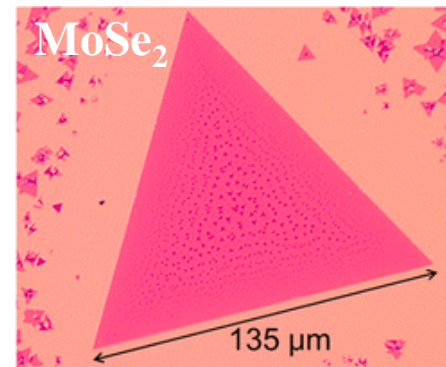
Credit: Lain-Jong Li



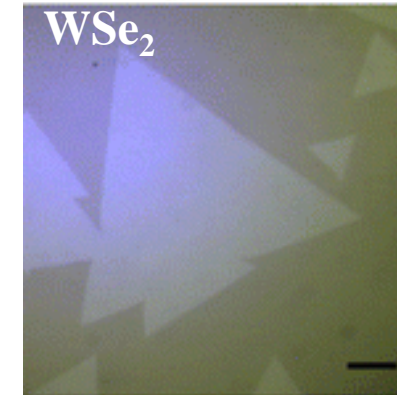
Nat. Mater. 12, 554, 2013  
Nat. Mater. 12, 754, 2013



ACS Nano, 2013, 7 (10), 8963–8971



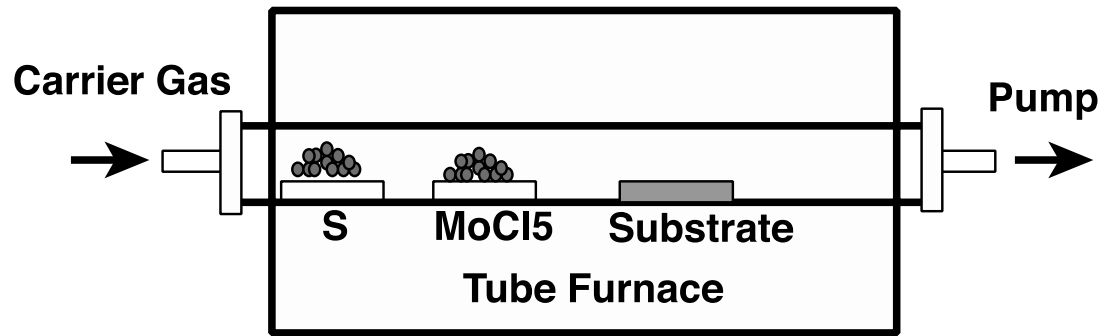
ACS Nano, 2014, 8 (5), 5125–5131  
ACS Nano, 2014, 8 (8), 8582–8590



ACS Nano, 2014, 8 (1), 923–930

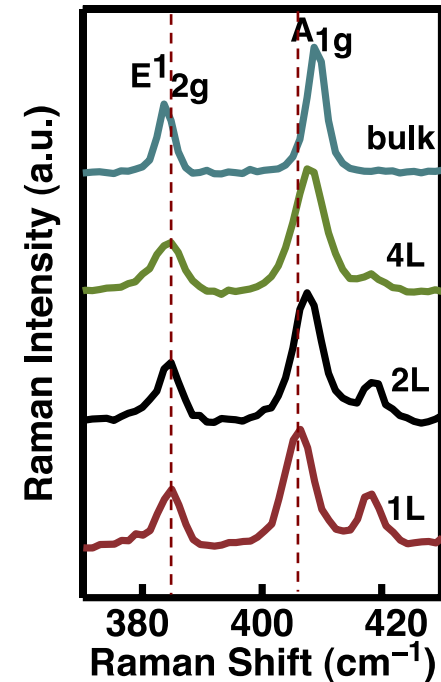
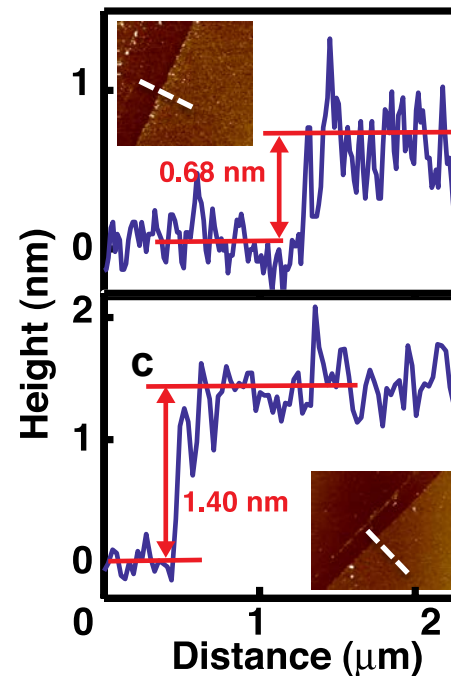
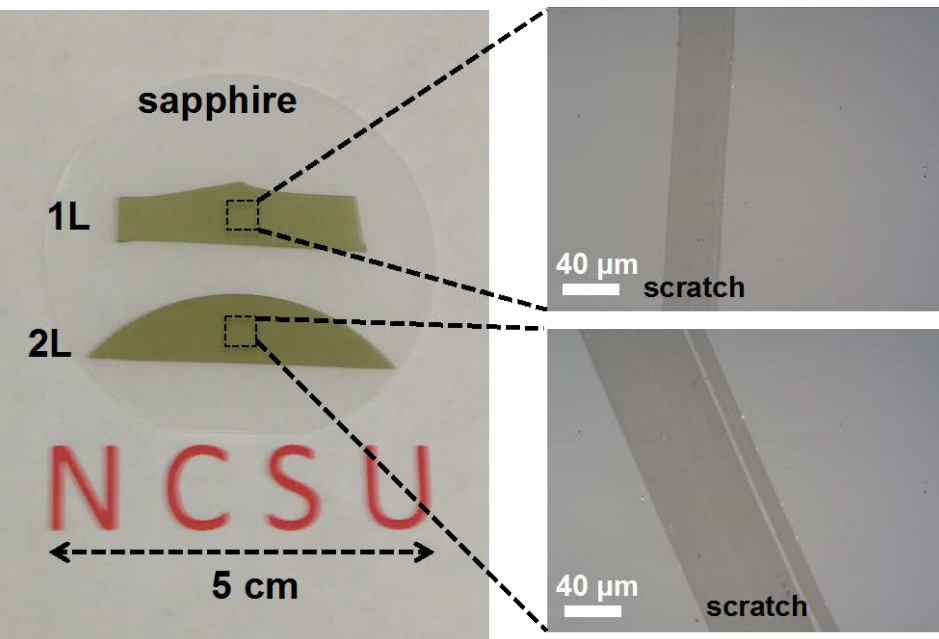
**Large size & Control of layer number?**

# Self-limiting CVD Growth



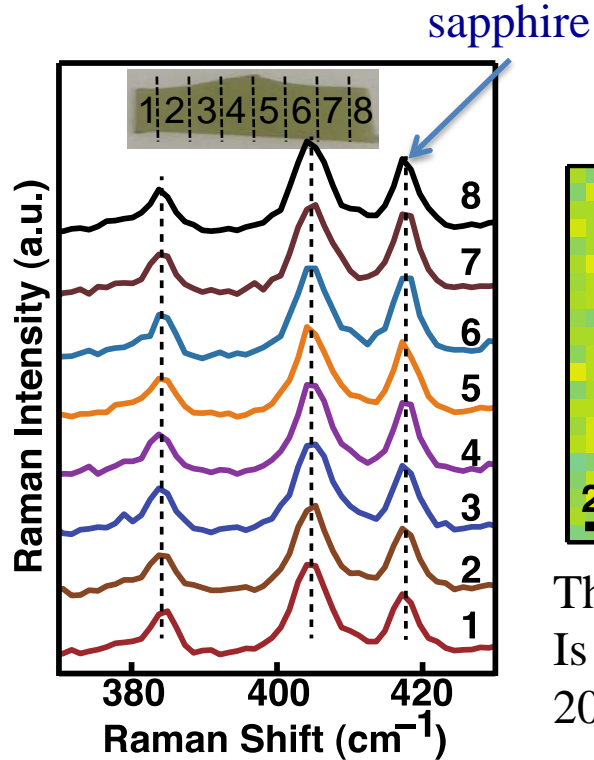
Conditions:

- 850 °C
- 1-2 Torr
- 1-20 mg MoCl<sub>5</sub>
- 1 g sulfur
- Carrier gas: Ar

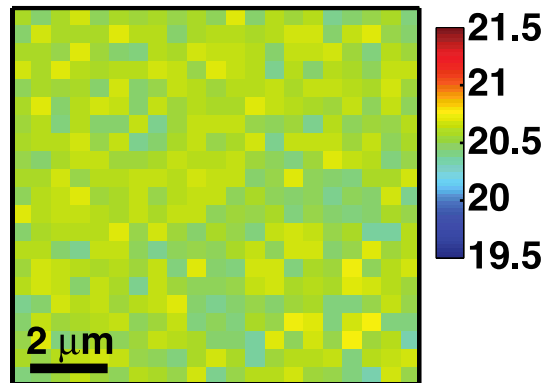


Growth of large-area, uniform monolayer and fewlayer MoS<sub>2</sub>.

# Remarkable Uniformity



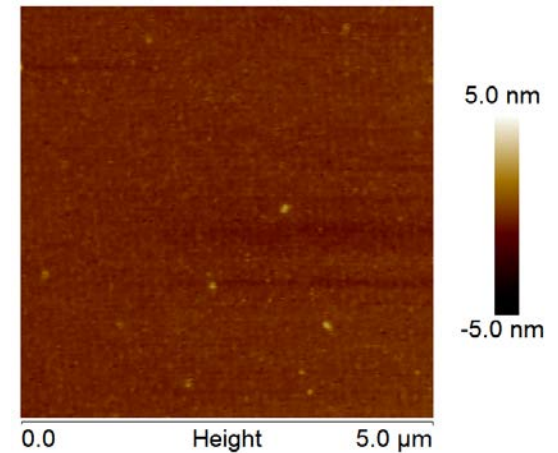
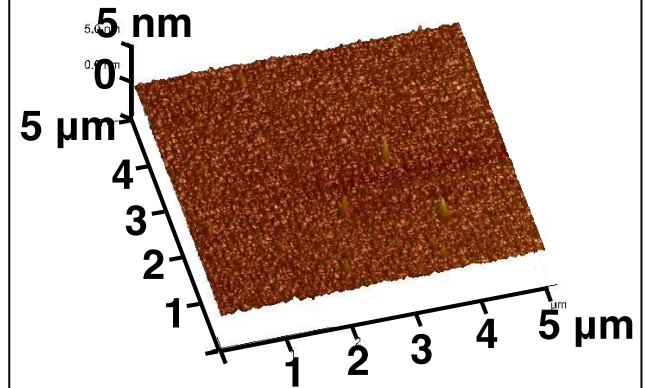
Raman mapping



The frequency difference  
Is in the range of 20.3 -  
20.7  $\text{cm}^{-1}$

The frequencies of the  $A_{1g}$  and  $E_{2g}^1$  peaks  
remain constant cross the entire film!

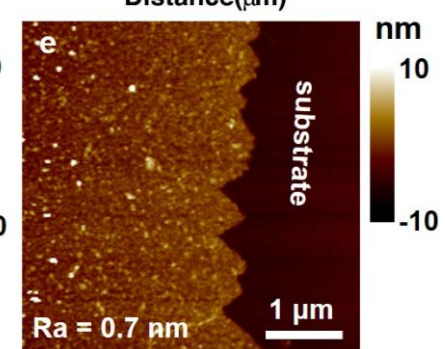
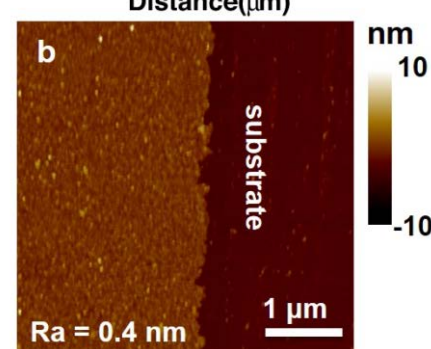
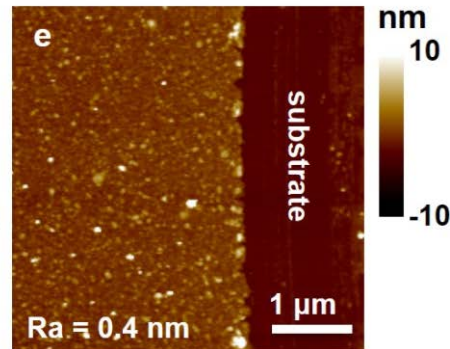
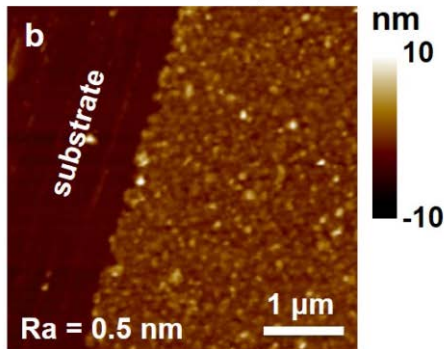
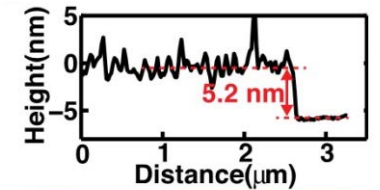
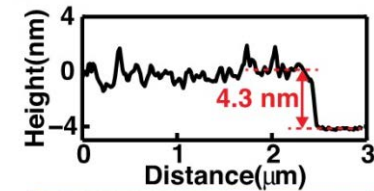
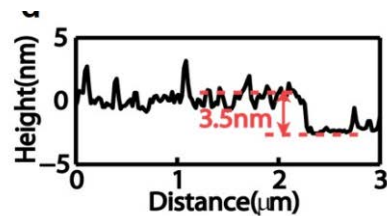
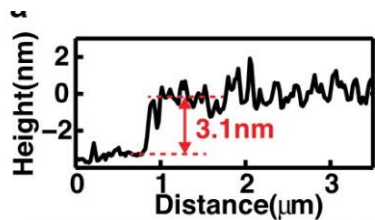
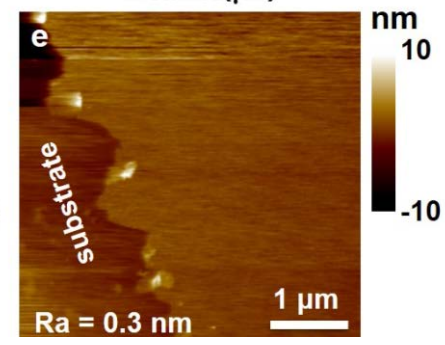
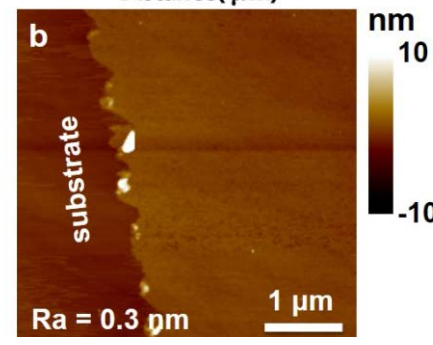
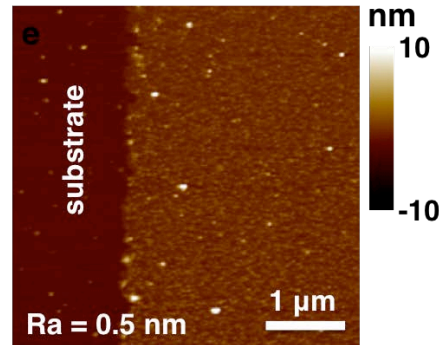
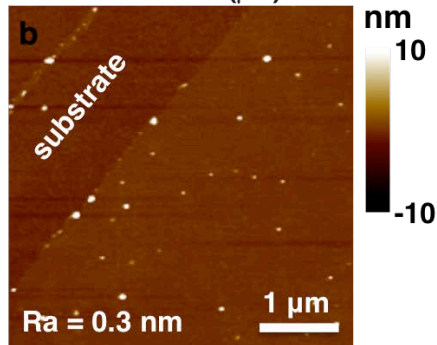
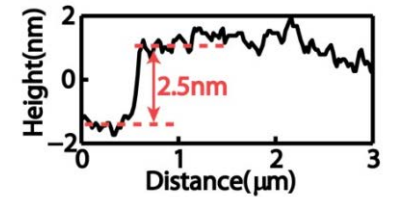
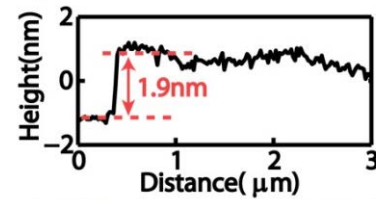
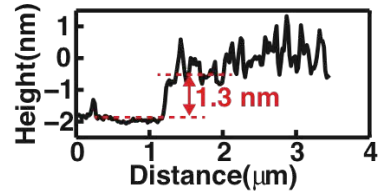
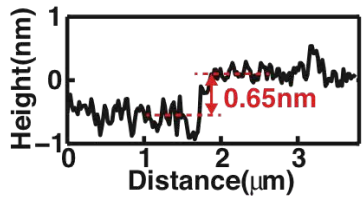
**Roughness < 0.2 nm**



**No void, step, edge!**

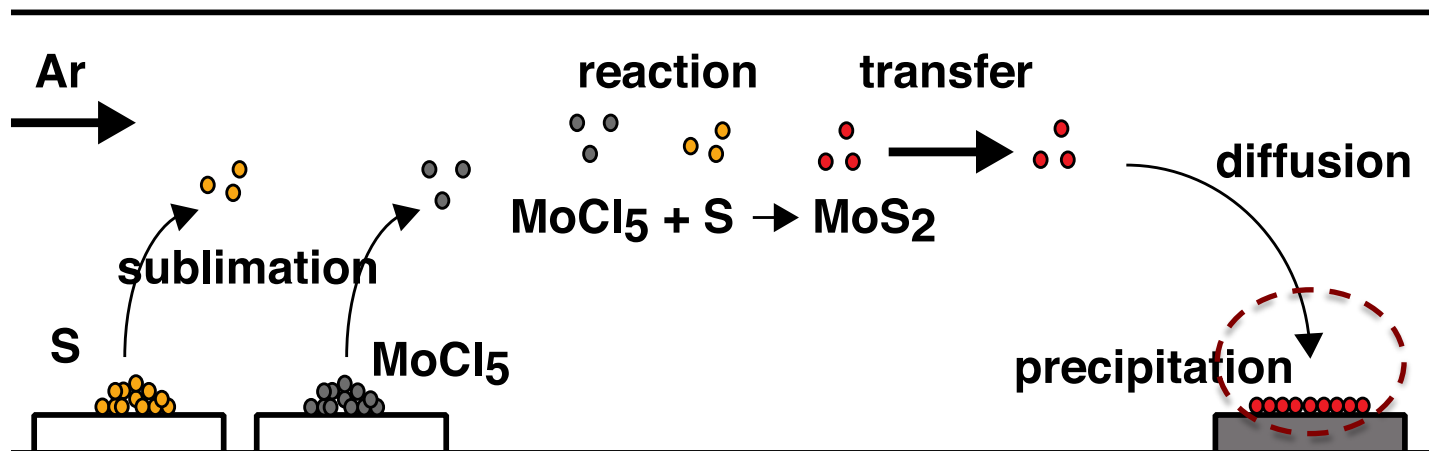
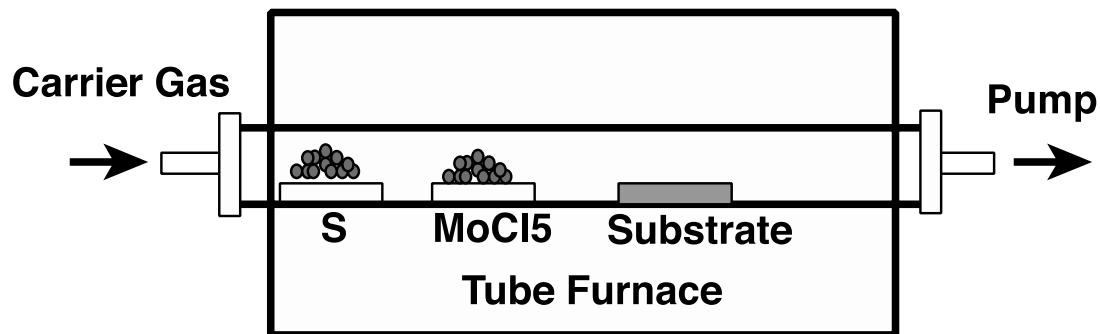
**The synthesized MoS2 film shows remarkable uniformity.**

# Precise Control of Layer Number



# Key of Self-limiting Growth

## Synthetic Setup

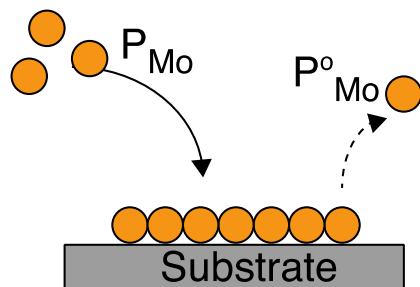


The rate-determining step is the precipitation reaction:





# Key of Self-limiting Growth

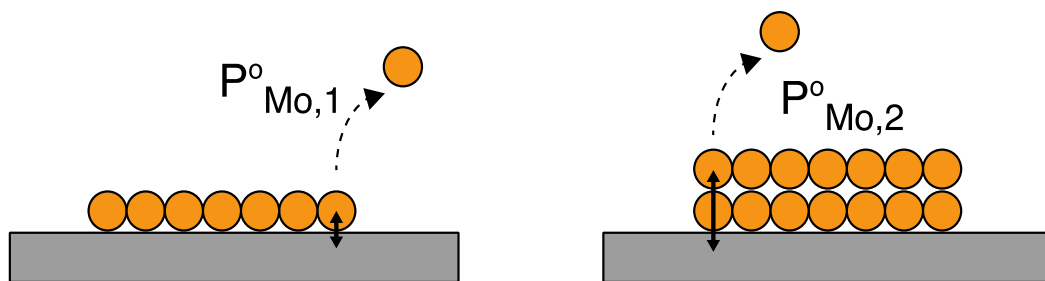


Two pressures dictate the precipitation:

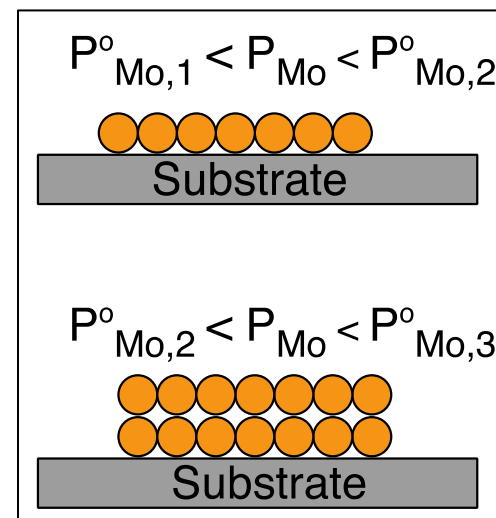
1. partial pressure of the gaseous MoS<sub>2</sub>,  $P_{\text{Mo}}$
2. vapor pressure of the MoS<sub>2</sub> film.  $P_{\text{Mo}}^{\circ}$

To drive the precipitation,  $P_{\text{Mo}} > P_{\text{Mo}}^{\circ}$

**The balance between the partial pressure and the vapor pressure provides the self-limiting growth mechanism.**



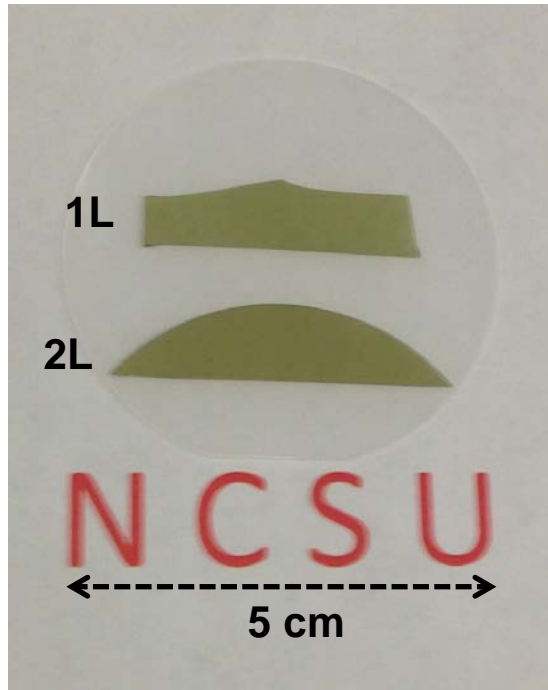
Layer dependent vapor pressure of the film due to interaction with the substrate.



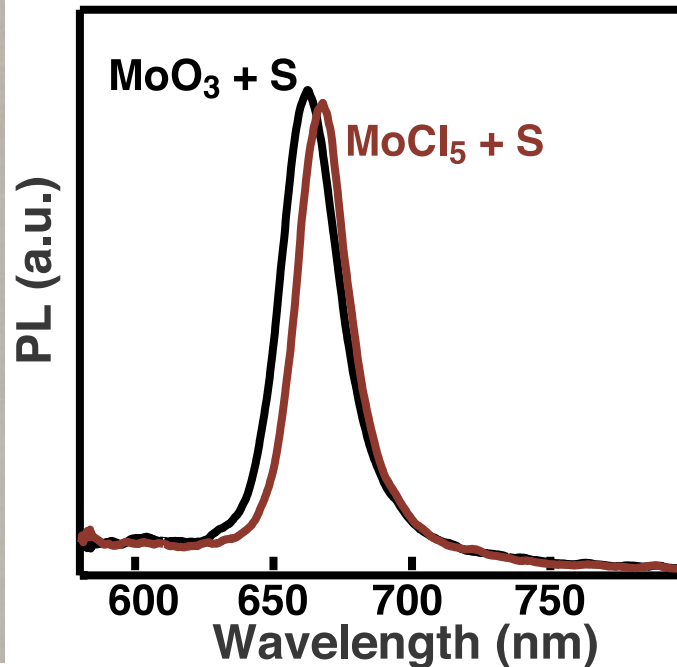
# Key Advantages of Self-limiting CVD Growth

Self-limiting CVD

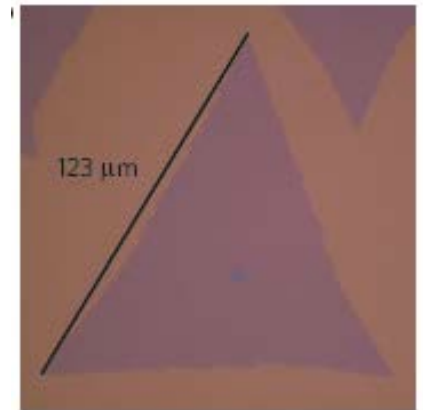
MoCl<sub>5</sub> + S



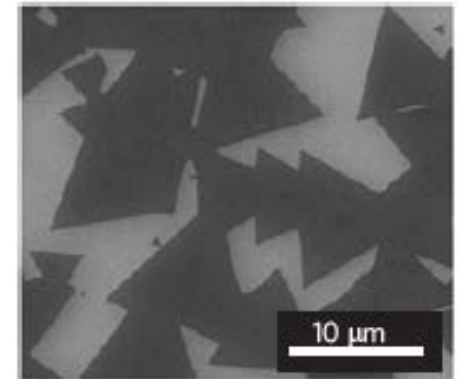
Comparable Quality



Other CVD Method  
MoO<sub>3</sub> + S



Nat. Mater. 12, 554, 2013



Nat. Mater. 12, 754, 2013

Key advantage of the self-limiting CVD approach :

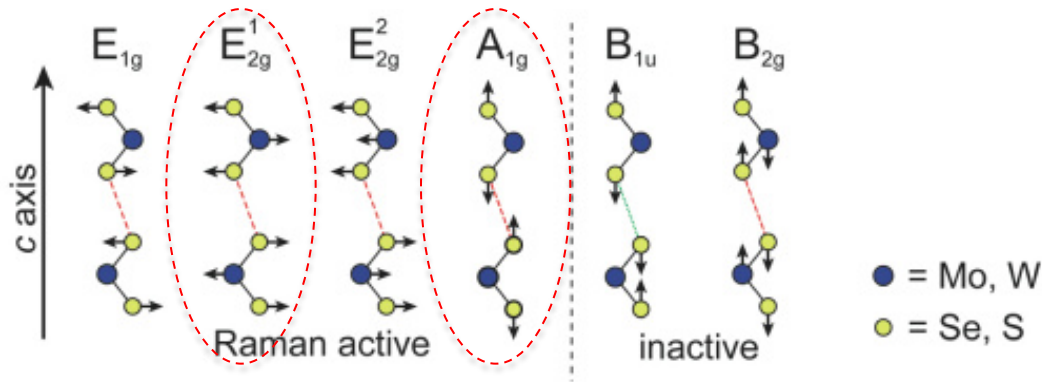
- Much larger size (5 cm vs mm)
- Control of layer numbers

# **II. Fundamental Properties**

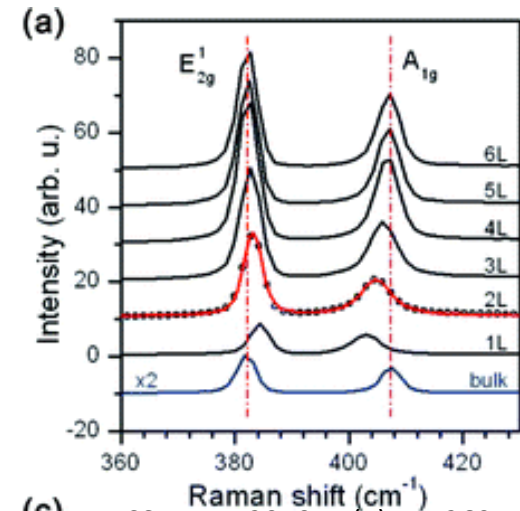
## **III.1 Raman**

# Raman vs. Layer Number

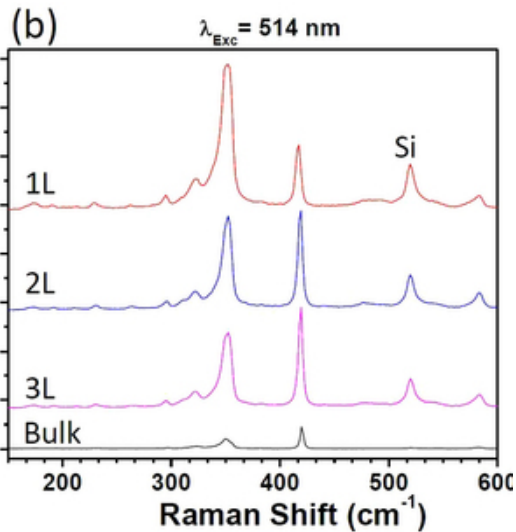
## Two most important modes



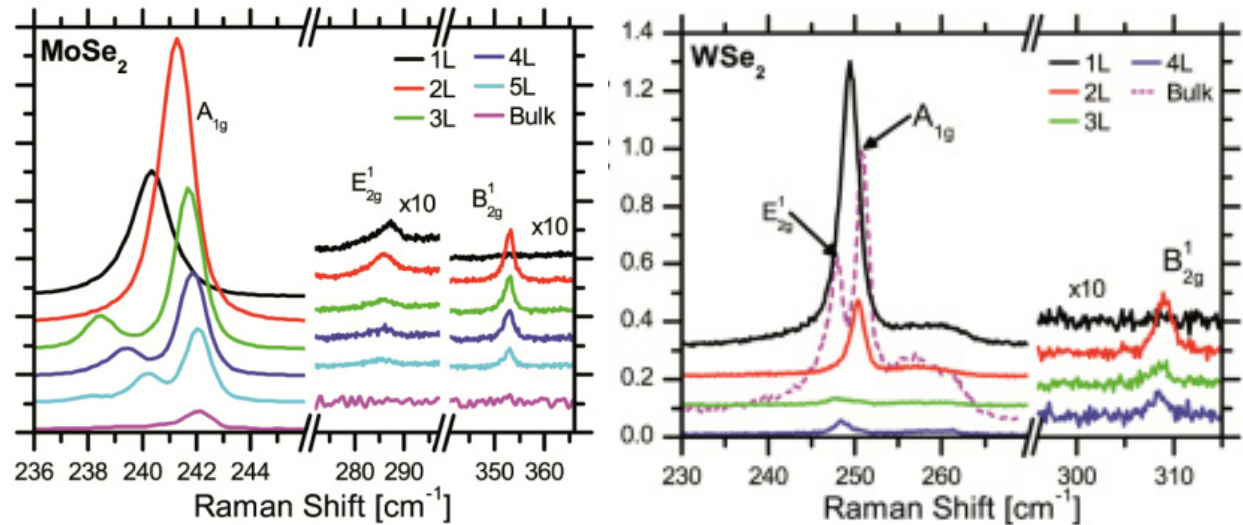
Optics Express, Vol. 21, Issue 4, pp. 4908-4916 (2013)



(c) ACS Nano, 2010, 4 (5), pp 2695–2700



Scientific Reports 3, Article number: 1755

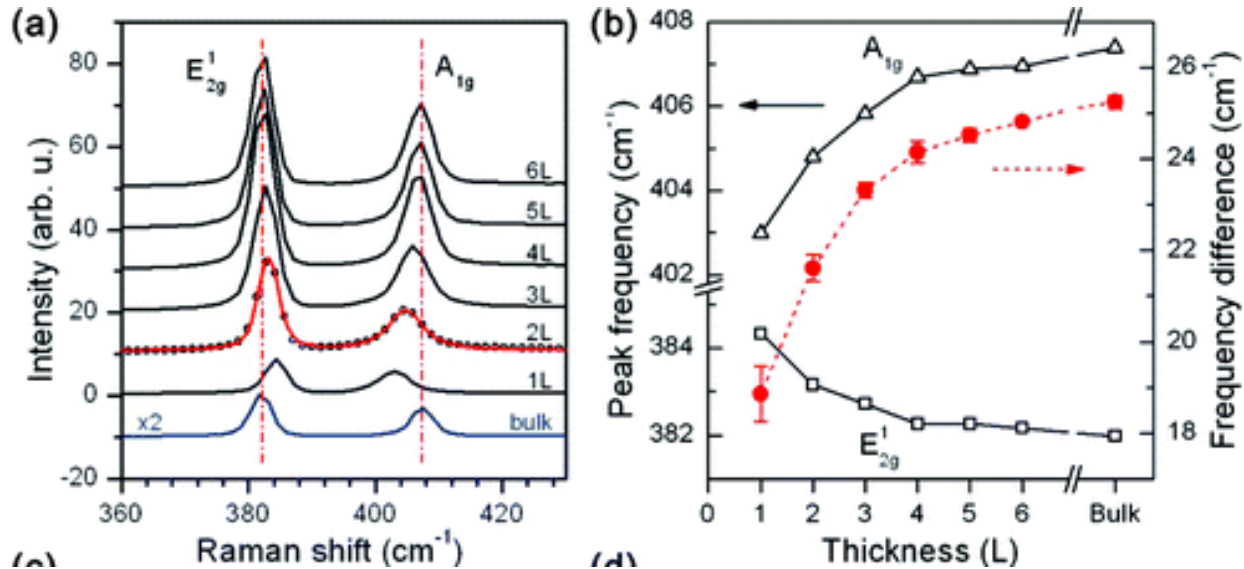


Optics Express, Vol. 21, Issue 4, pp. 4908-4916 (2013)

**Raman intensity and peak position depend on the layer number.**

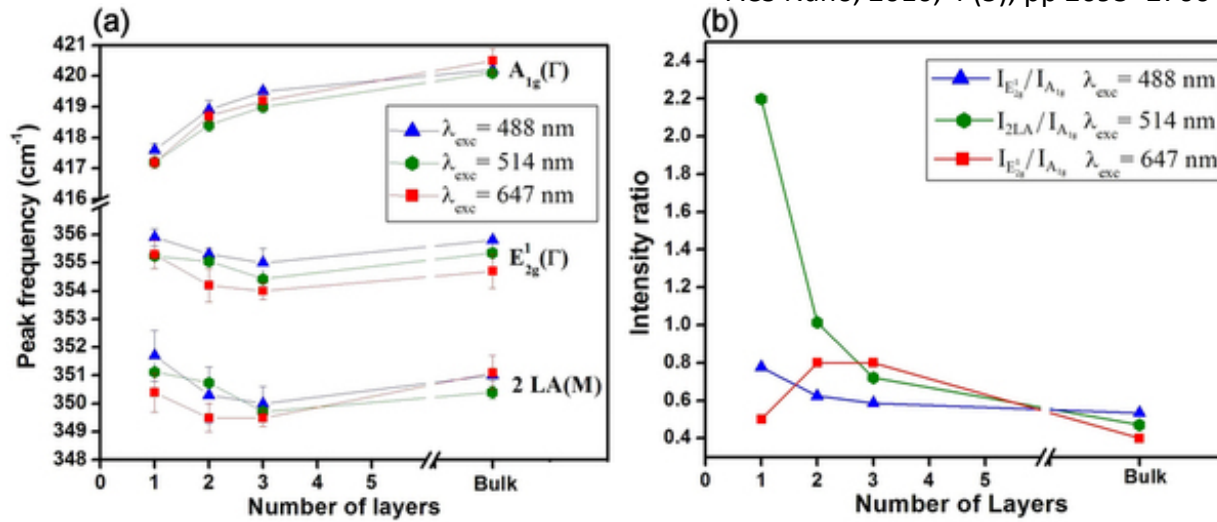
# Raman vs. Layer Number

MoS2



ACS Nano, 2010, 4 (5), pp 2695–2700

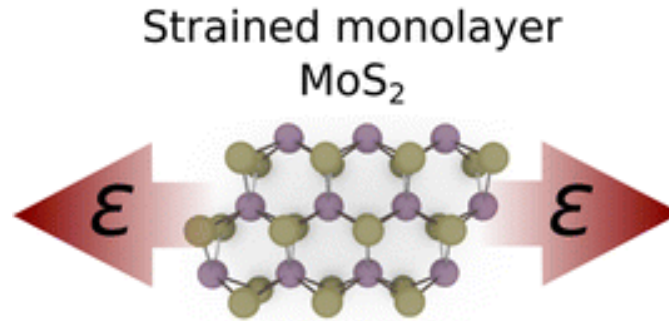
WS2



Scientific Reports 3, Article number: 1755

**Raman can serve as a credible tool to identify the layer number.**

# Raman vs. Strain

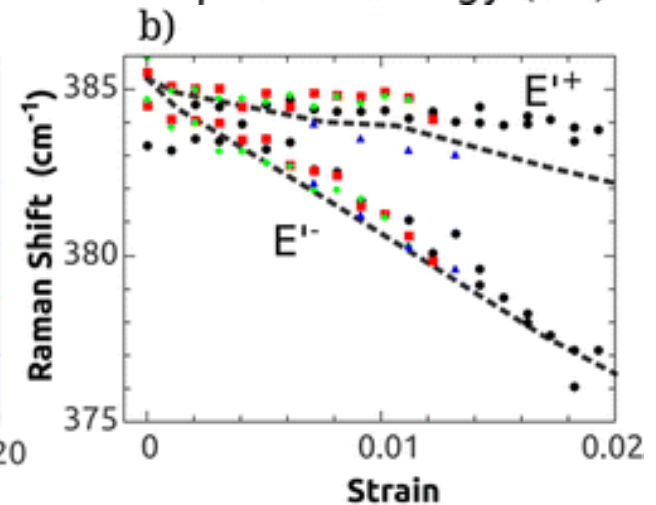
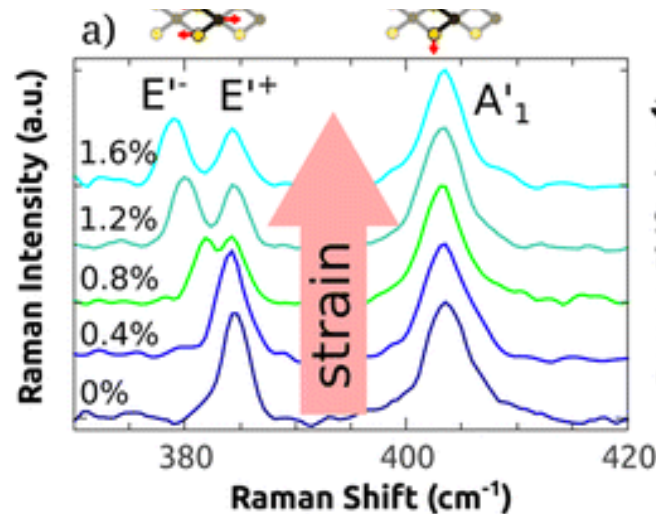
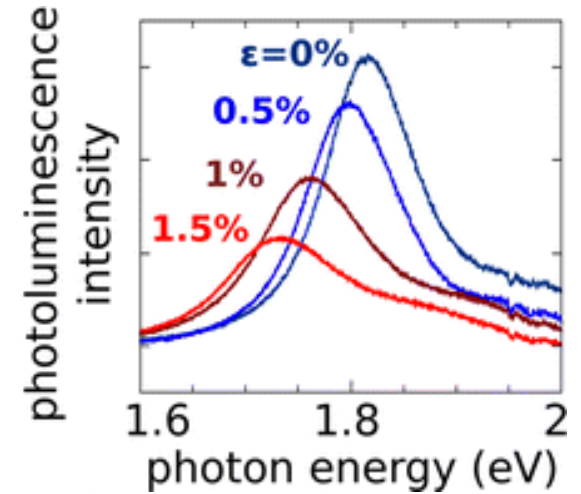


E'−:

$4.5 \pm 0.3 \text{ cm}^{-1}/\%$  strain 1L  
 $4.6 \pm 0.4 \text{ cm}^{-1}/\%$  strain 2L

E'+:

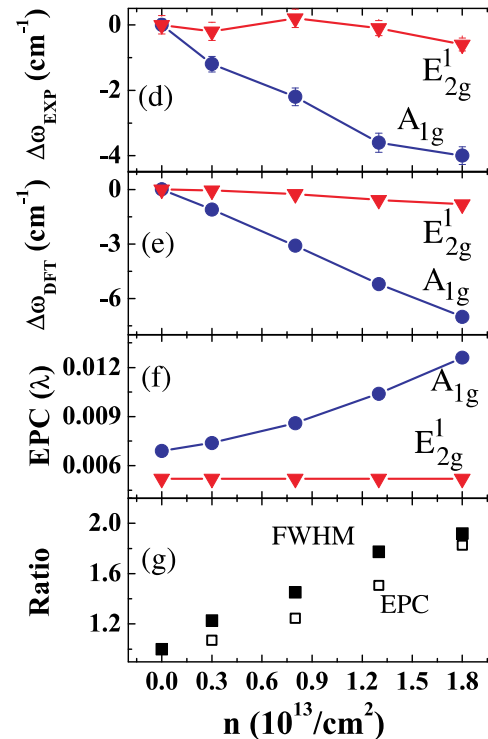
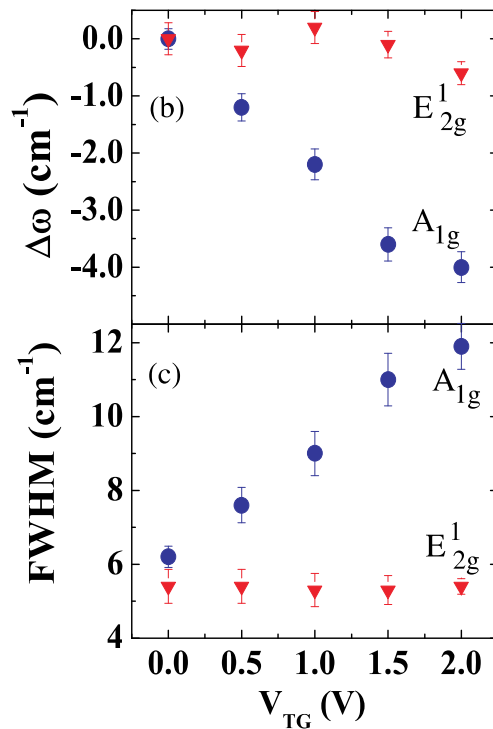
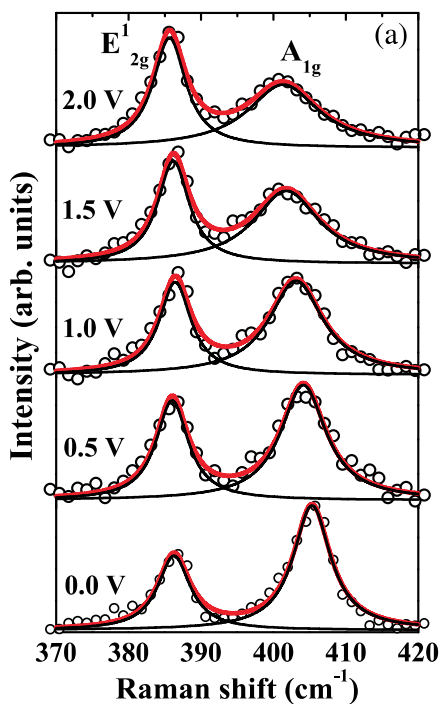
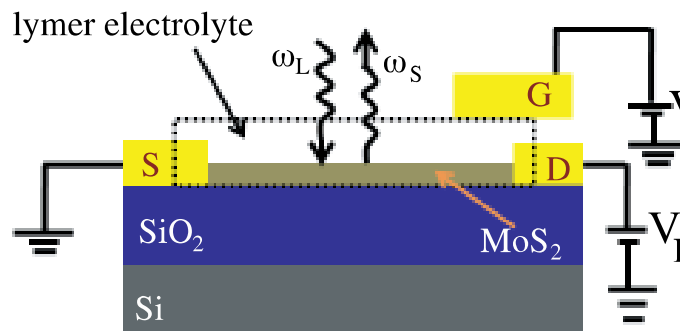
$1.0 \pm 1 \text{ cm}^{-1}/\%$  strain 1L  
 $1.0 \pm 0.9 \text{ cm}^{-1}/\%$  strain 2L



Nano Lett., 2013, 13 (8), pp 3626–3

- the A<sub>1g</sub> peak shows no measurable shift in position
- the degenerate E' peak splits into two subpeaks

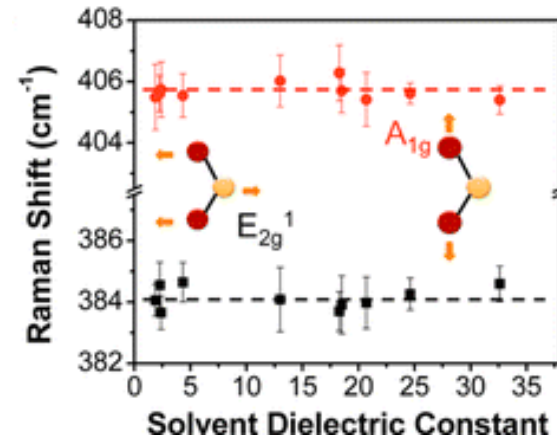
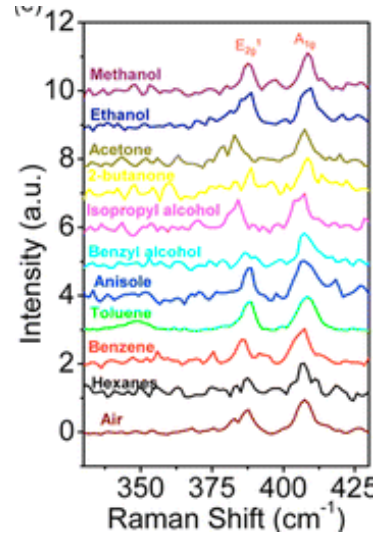
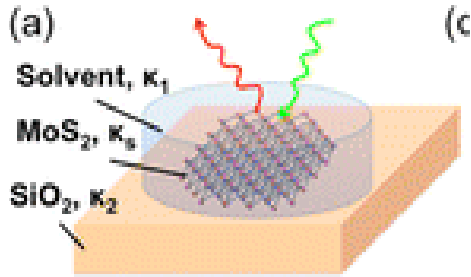
# Raman vs. Carrier Concentration



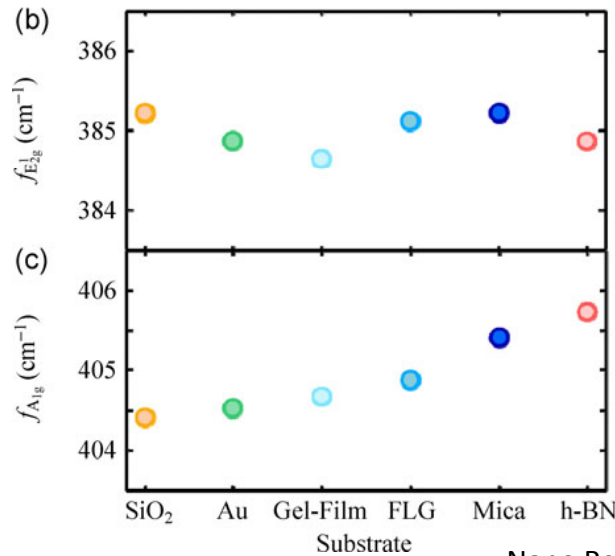
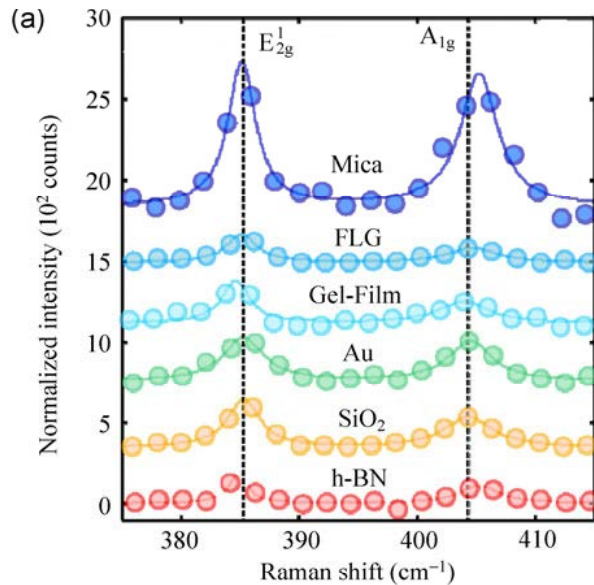
Phys. Rev. B 85, 161403(R), 2012

**A<sub>1g</sub> strongly depends on the carrier concentration.**

# Raman vs. Substrate/Dielectric Screening



Nano Lett., 2014, 14 (10), pp 5569–5576



Nano Research 2014, 7(4): 561–571

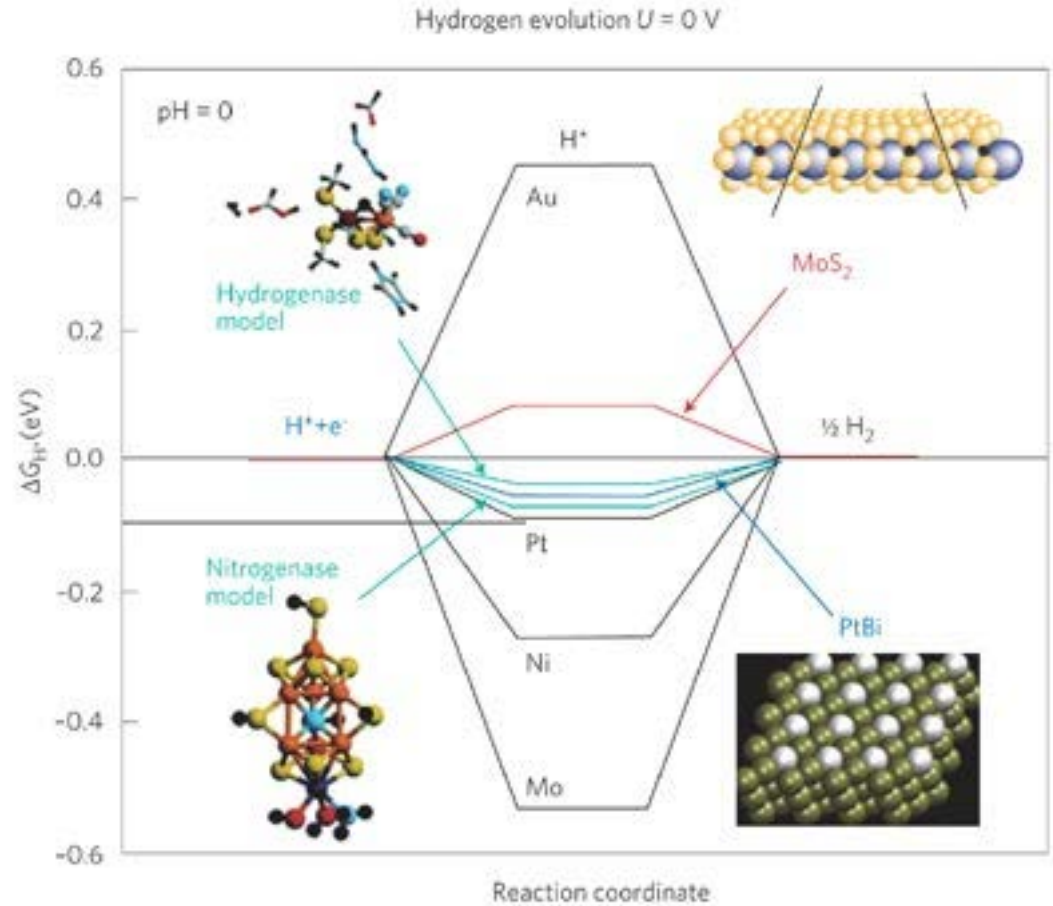
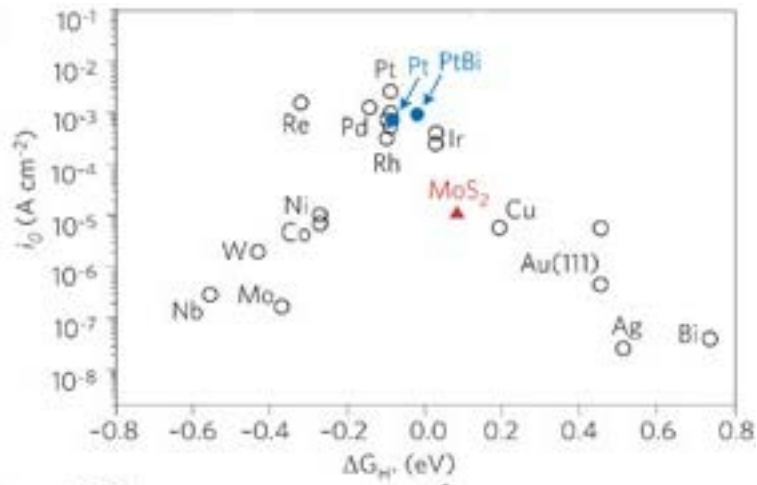
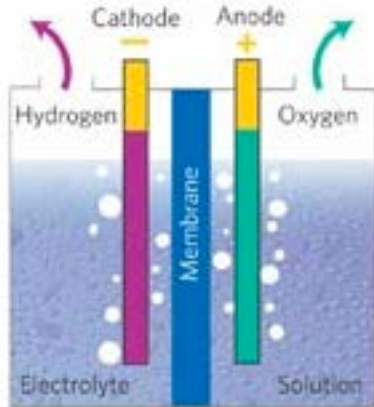
- **No obvious dependence on the dielectric environment, but substantial dependence on the substrate (doping, strain).**



# **III. Fundamental Properties**

## **III.2 Catalytic Properties**

# MX<sub>2</sub> (M= Mo, W, X= S, Se): HER Catalyst

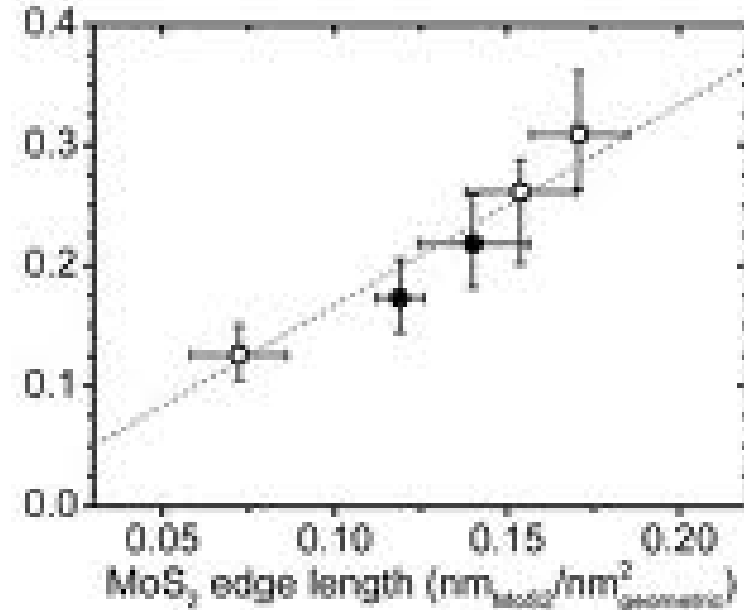
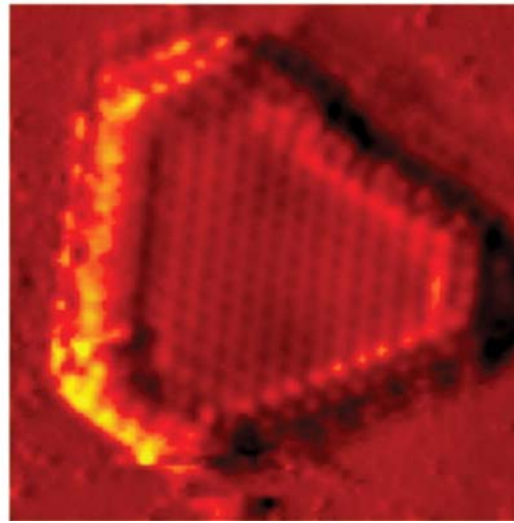
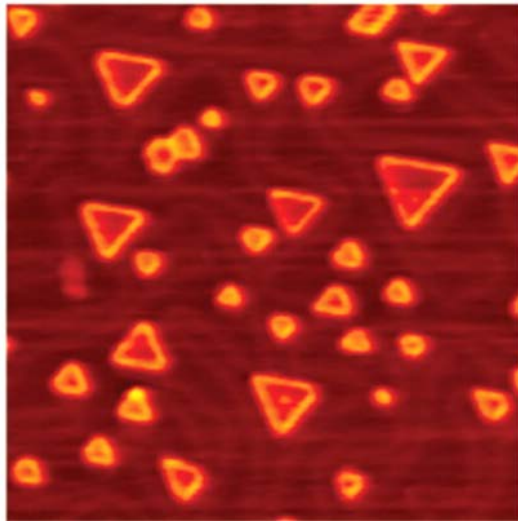


Nature Chemistry 1, 37 - 46 (2009)

**MX<sub>2</sub> (M= Mo, W, X= S, Se) are predicted as good catalysts for the hydrogen evolution reaction (HER)**

# Current Theory: Edge Sites Matter.

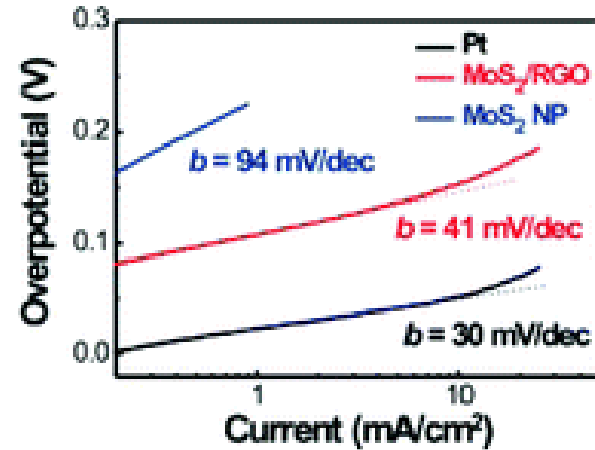
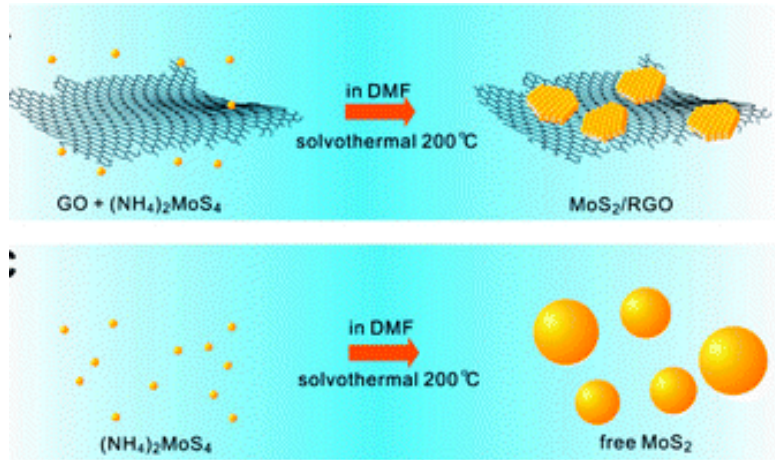
MoS<sub>2</sub>



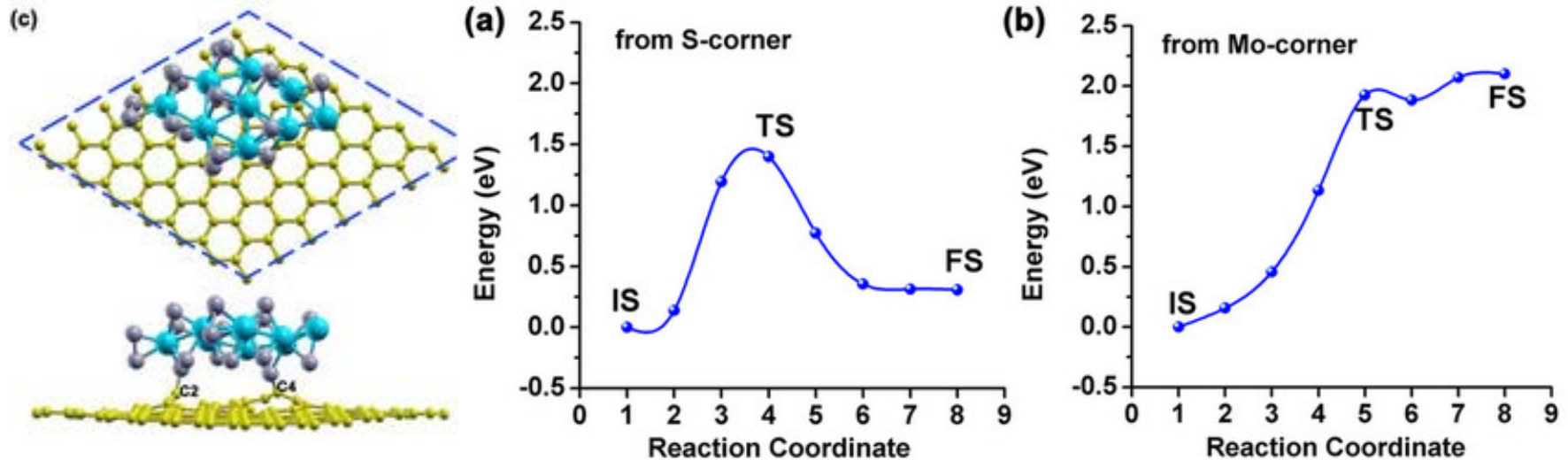
Science 6 July 2007:  
vol. 317 no. 5834 100-102

**Conventional wisdom:** exchange current density is proportional to the number of edge sites.

# Recent Studies: Coupling with Graphene



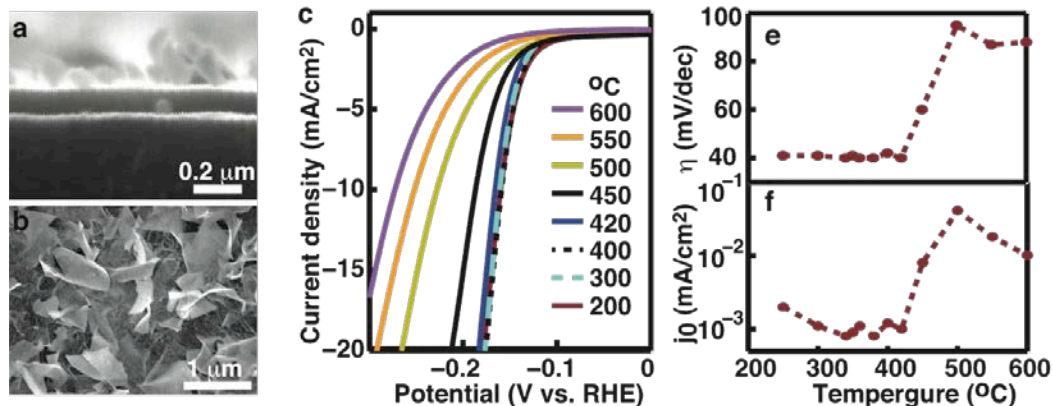
J. Am. Chem. Soc., 2011, 133 (19), pp 7296–7299



Scientific Reports 4, Article number: 6256

**The electronic coupling with graphene is helpful.**

# Recent Studies: Composition and Crystallinity



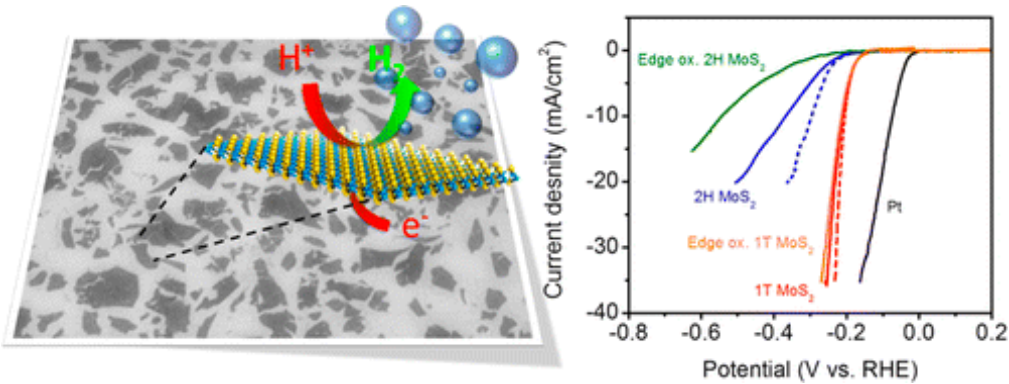
	Composition	Structure	Tafel slope (mV/dec)	$J_0$ ( $\mu\text{A}/\text{cm}^2$ )	Capacitance (mF/ $\text{cm}^2$ )	TOF ( $10^{-3} \text{s}^{-1}$ )
200°C - 380°C	$\text{MoS}_3$	amorphous	39	~1-2	10-20	0.01-0.03
400°C	$\text{MoS}_3$ (70%) $\text{MoS}_2$ (30%)	amorphous nanocrystalline	42	1.2	10	0.027
420°C	$\text{MoS}_3$ (40%) $\text{MoS}_2$ (60%)	amorphous nanocrystalline	40	1.0	12	0.012
450°C	$\text{MoS}_2$	polycrystalline	50-60	8	8	0.14
500°C - 600°C	$\text{MoS}_2$	single crystalline	80-90	10-40	0.5-1.5	2.5-3.5

ACS Catal., 2015, 5 (1), pp 448–455

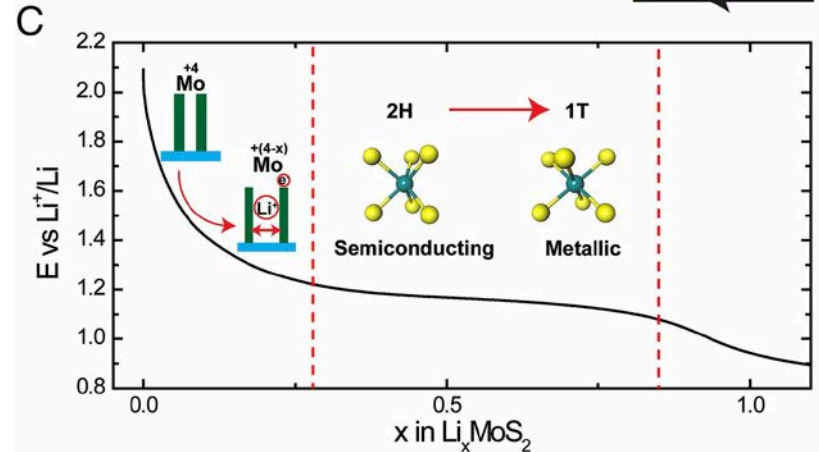
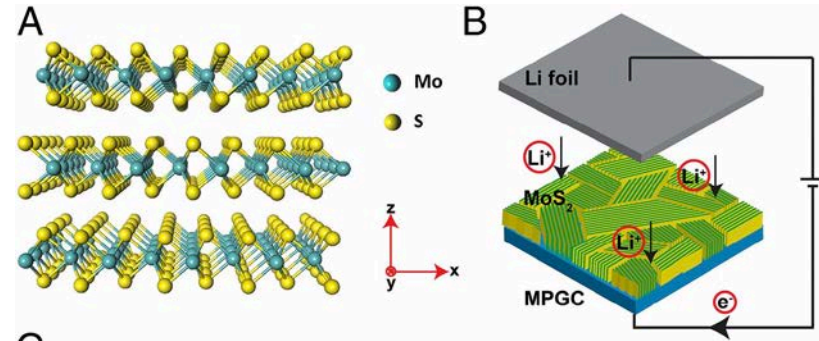
1. The stoichiometric ratio of Mo: S does not matter much.
2. The crystallinity may affect the Tafel Slope and TOF in opposite ways  
 Low crystallinity: 40 mV/dec and low TOF  
 Highly crystalline : 80-90 mV/dec and high TOF

**Does Edge Sites Really Matter?**

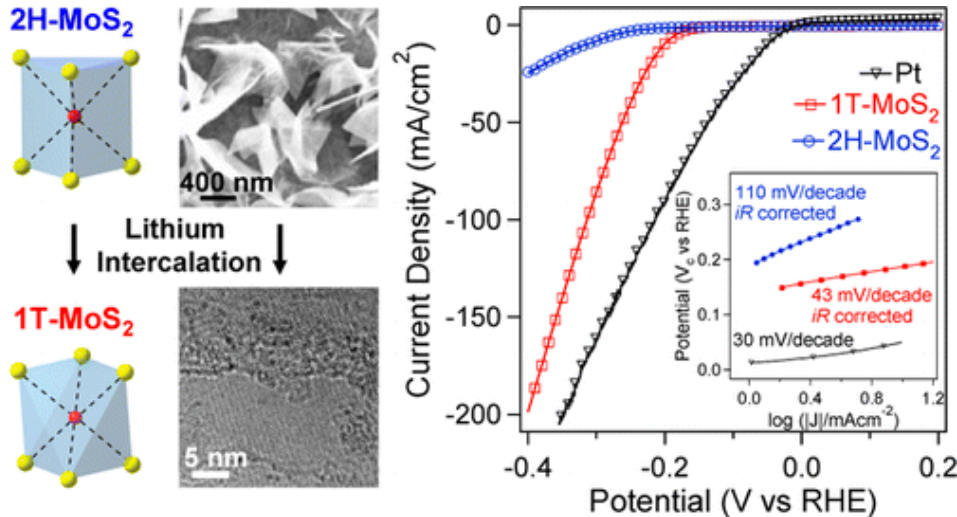
# Recent Studies: Not Just Edge Sites



Nano Lett., 2013, 13 (12), pp 6222–6227



PNAS, 2013, vol. 110, 19701–19706

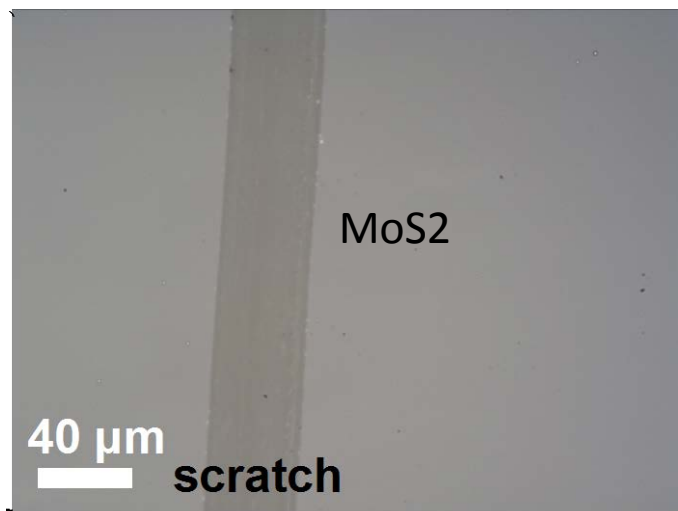


J. Am. Chem. Soc., 2013, 135 (28), pp 10274–10277

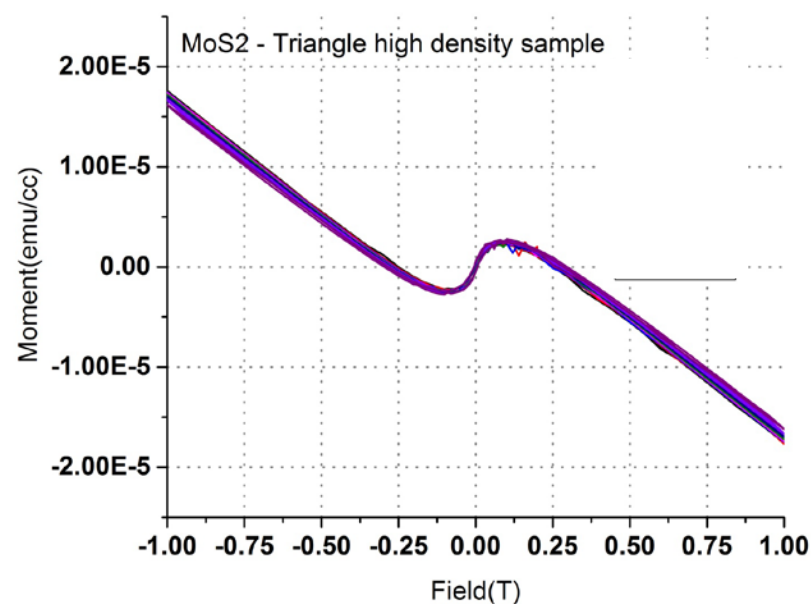
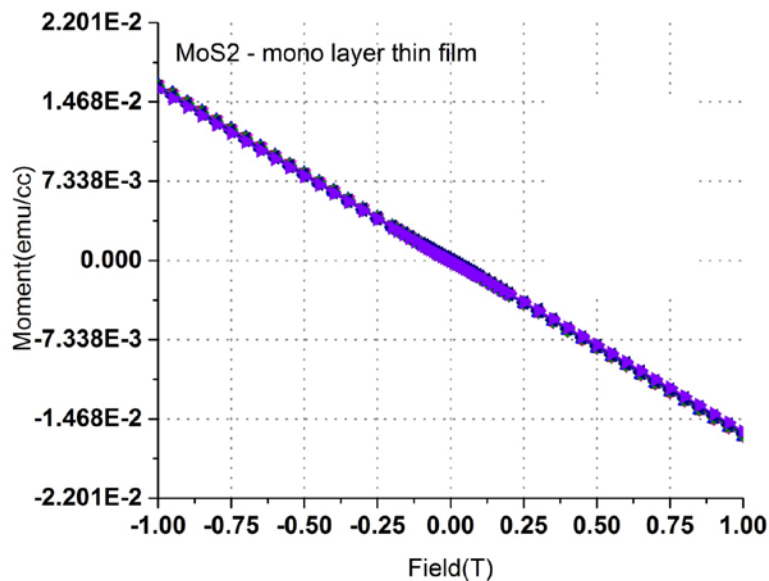
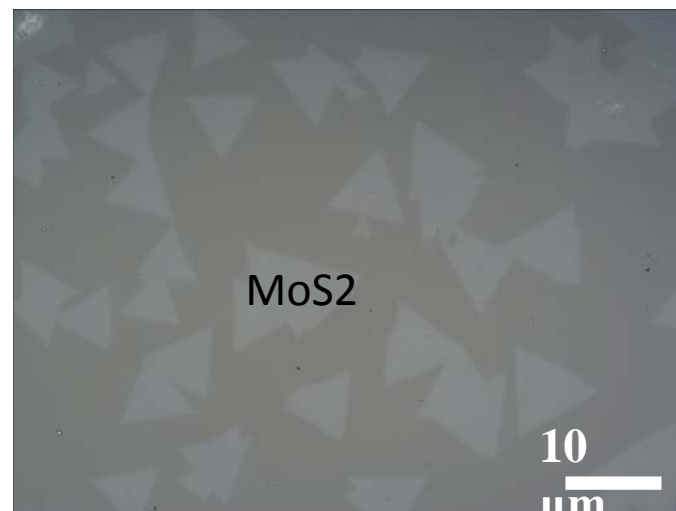
**1T-MoS<sub>2</sub> is better than 2H-MoS<sub>2</sub> in terms of catalyzing the HER.**

# Does The Edge Sites Really Matter?

Continuous Film



Discontinuous MoS2 Flakes



**Magnetic measurements indicate No substantial edge sites in the film**

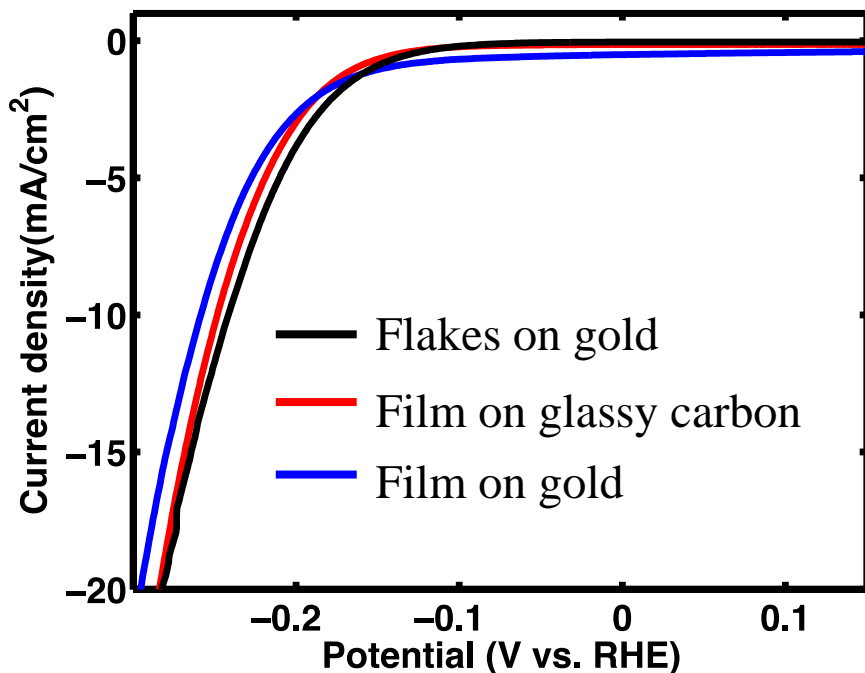
Unpublished Results



# Does The Edge Sites Really Matter?

Exchange current density: 25-40  $\mu\text{A}/\text{cm}^2$

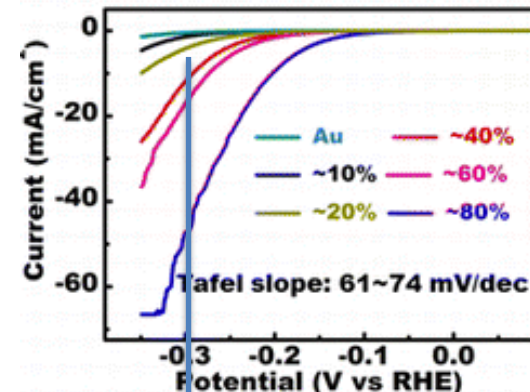
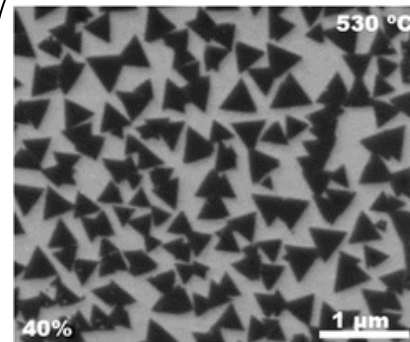
Tafel slope: 75mV/dec



Submitted

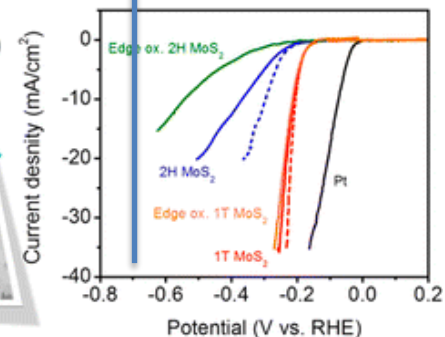
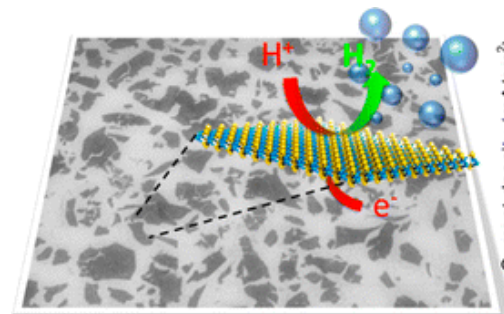
**No substantial difference in the exchange current density at the edge site and basal plane of MoS<sub>2</sub>**

36.8  $\mu\text{A}/\text{cm}^2$  and 61-74 mV/dec



ACS Nano, 2014, 8 (10), pp 10196-10204

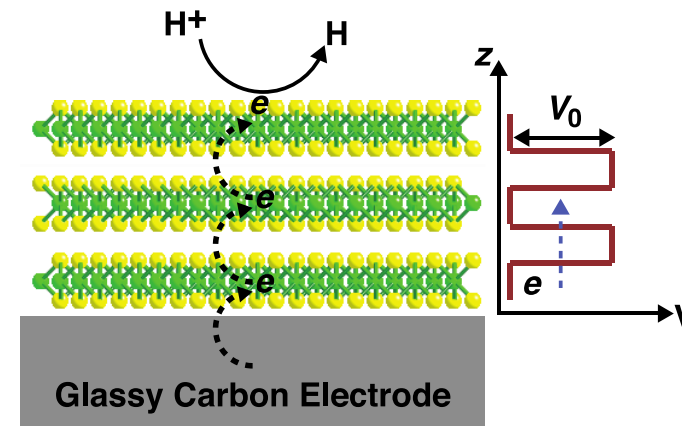
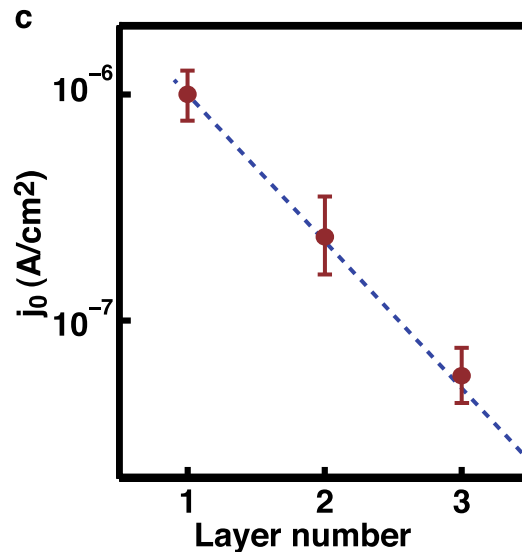
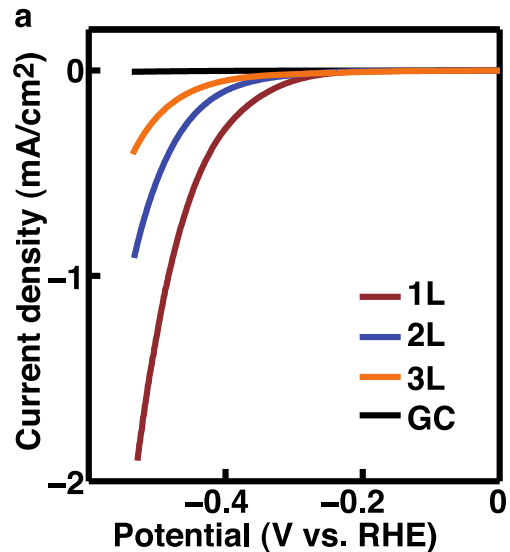
??  $\mu\text{A}/\text{cm}^2$  and 75-85 mV/dec



Nano Lett., 2013, 13 (12), pp 6222-6227

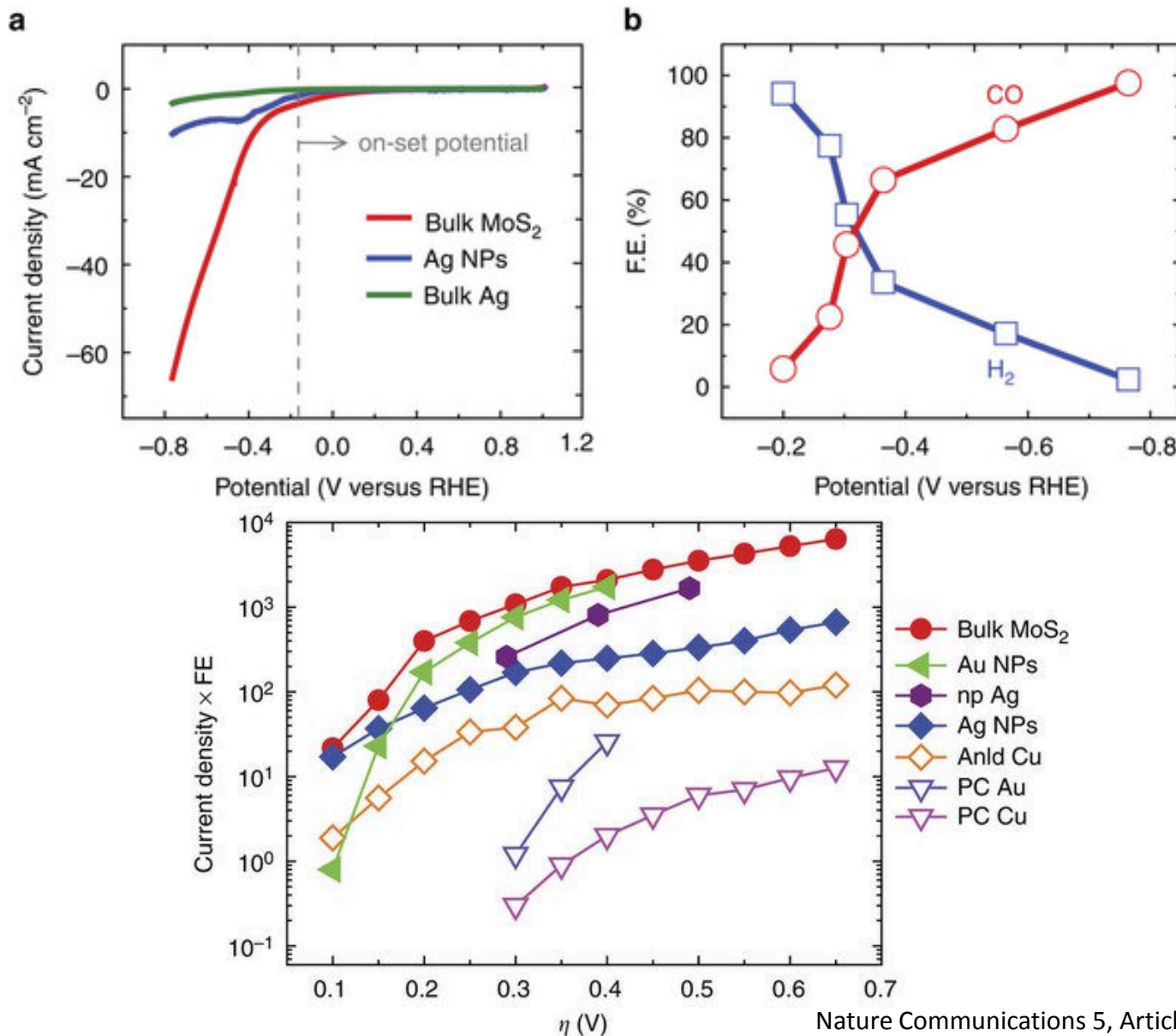
Unpublished Results

# Recent Studies: Layer Dependence Electrocatalysis



**Efficiency of electron hopping plays an important role**

# MoS<sub>2</sub>: Catalyst for Carbon Dioxide Reduction



Nature Communications 5, Article number: 4470

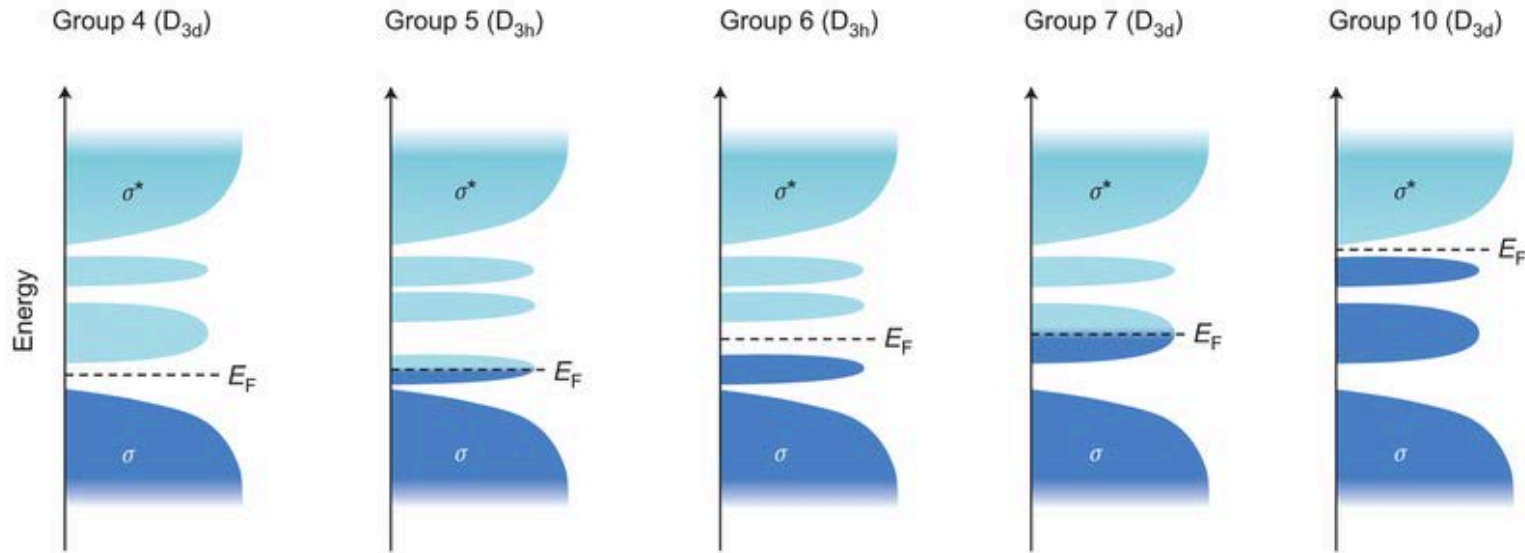
**MoS<sub>2</sub> is a promising catalyst for the reduction of carbon dioxide**

# **III. Fundamental Properties**

## **III.3 Electronic Structures/Properties**

## **III.3.1 Band Structures**

# Electronic character of TMDCs: d-Orbital filling



Nature Chemistry 5, 263–275 (2013)

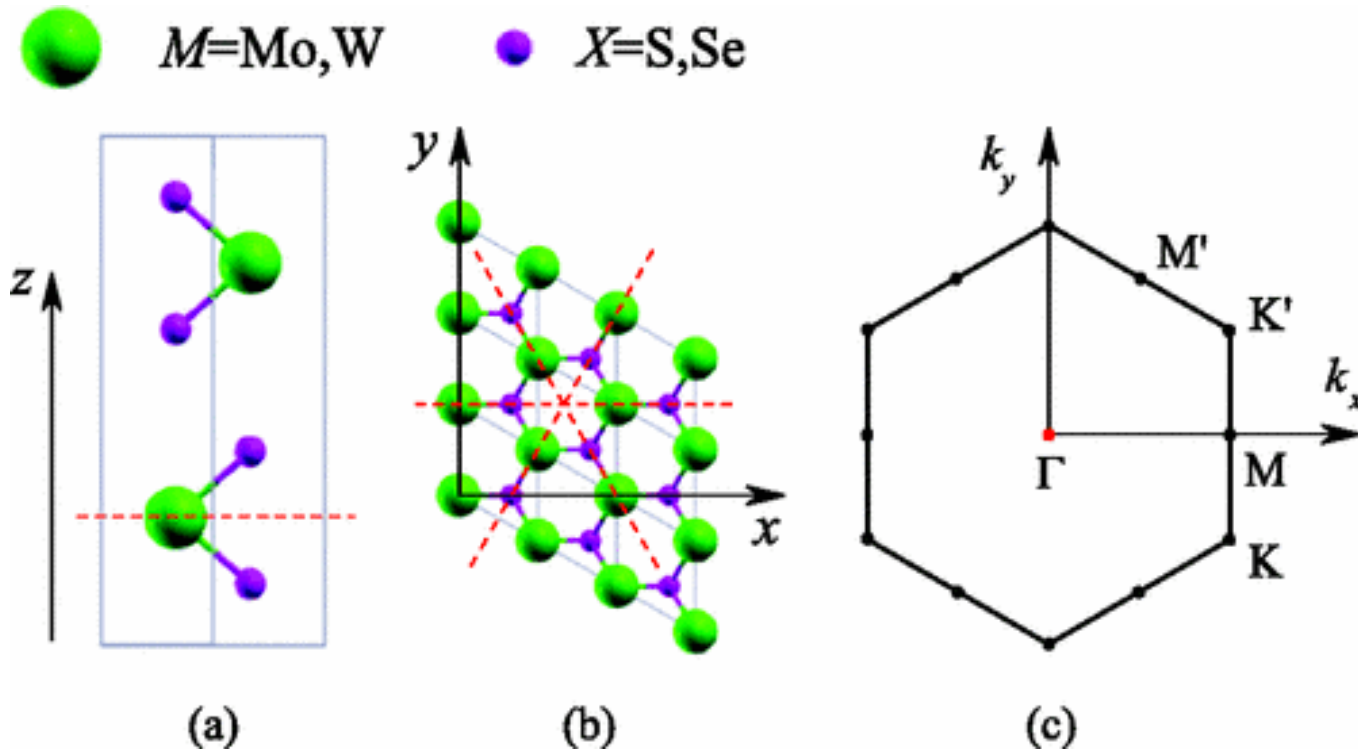
**Table 1 | Electronic character of different layered TMDCs<sup>25</sup>.**

Group	M	X	Properties
4	Ti, Hf, Zr	S, Se, Te	Semiconducting ( $E_g = 0.2\text{--}2\text{ eV}$ ). Diamagnetic.
5	V, Nb, Ta	S, Se, Te	Narrow band metals ( $\rho \sim 10^{-4}\ \Omega\cdot\text{cm}$ ) or semimetals. Superconducting. Charge density wave (CDW). Paramagnetic, antiferromagnetic, or diamagnetic.
6	Mo, W	S, Se, Te	Sulfides and selenides are semiconducting ( $E_g \sim 1\text{ eV}$ ). Tellurides are semimetallic ( $\rho \sim 10^{-3}\ \Omega\cdot\text{cm}$ ). Diamagnetic.
7	Tc, Re	S, Se, Te	Small-gap semiconductors. Diamagnetic.
10	Pd, Pt	S, Se, Te	Sulfides and selenides are semiconducting ( $E_g = 0.4\text{ eV}$ ) and diamagnetic. Tellurides are metallic and paramagnetic. PdTe <sub>2</sub> is superconducting.

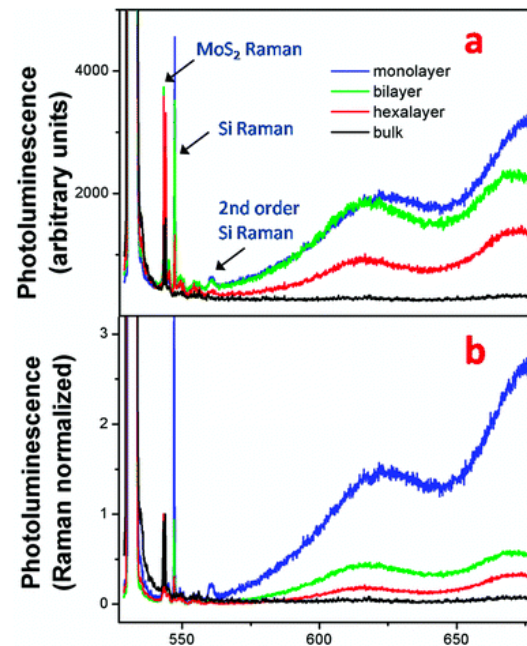
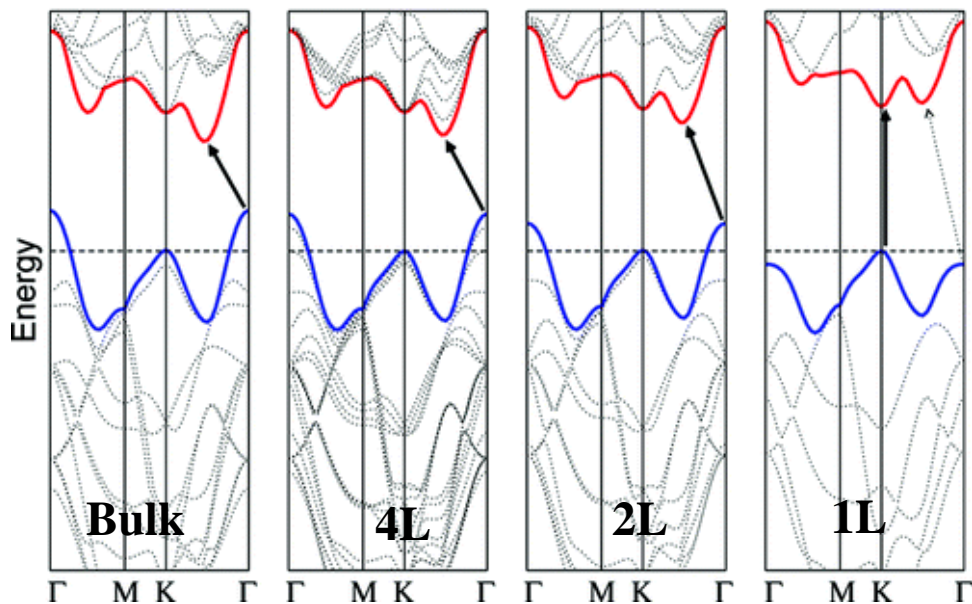
$\rho$ , in-plane electrical resistivity.

- The non-bonding *d* bands between the bonding ( $\sigma$ ) and antibonding ( $\sigma^*$ ) bands are very important.
- The diverse electronic properties arise from the progressive filling of the non-bonding *d* bands
- The effect of chalcogen atoms on the electronic structure is minor compared with that of the metal atoms

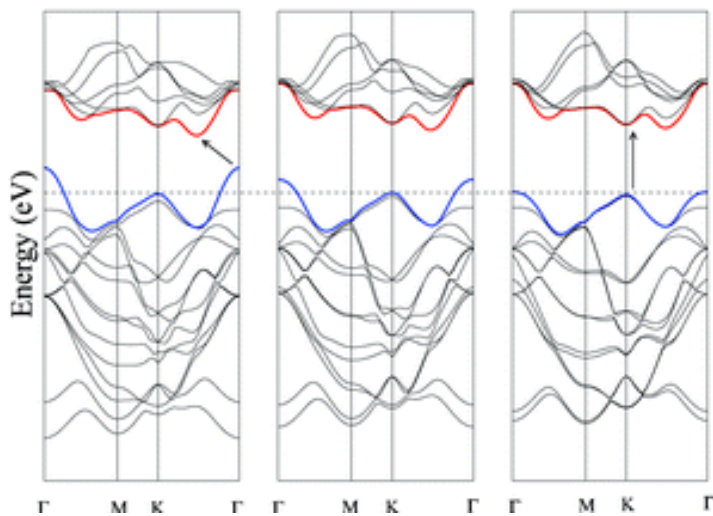
# Hexagonal Brillouin Zone of TMDCs (MoS2)



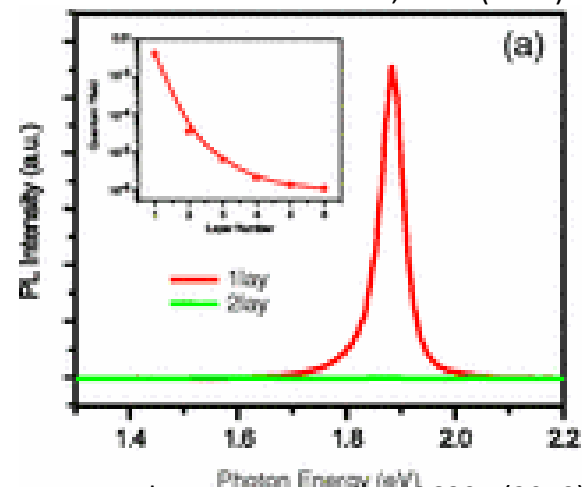
# Evolution of Band Structure: Indirect to Direct



Wavelength  $\lambda$  (nm)  
Nano Lett. 10, 1271 (2010)



J. Phys. Chem. C, 2007, 111 (44), pp 16192–16196

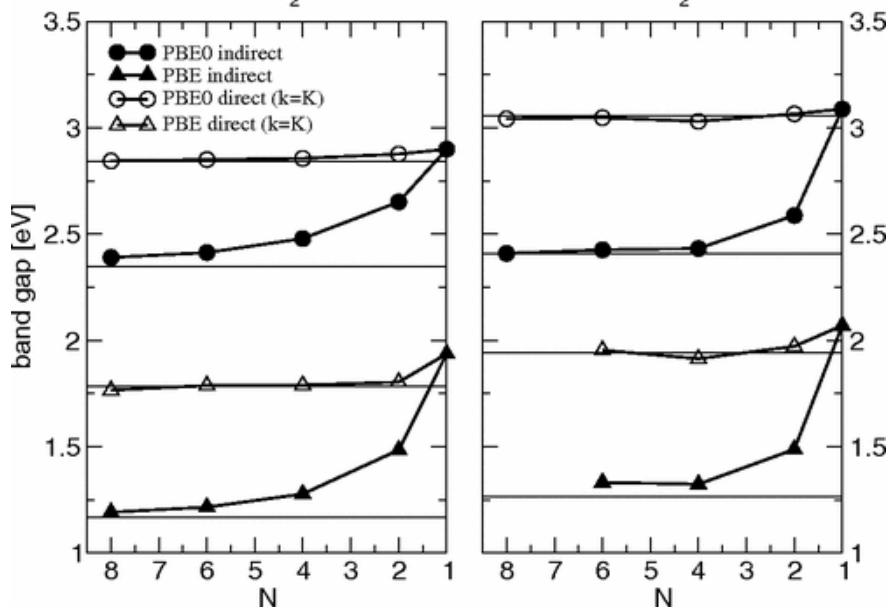
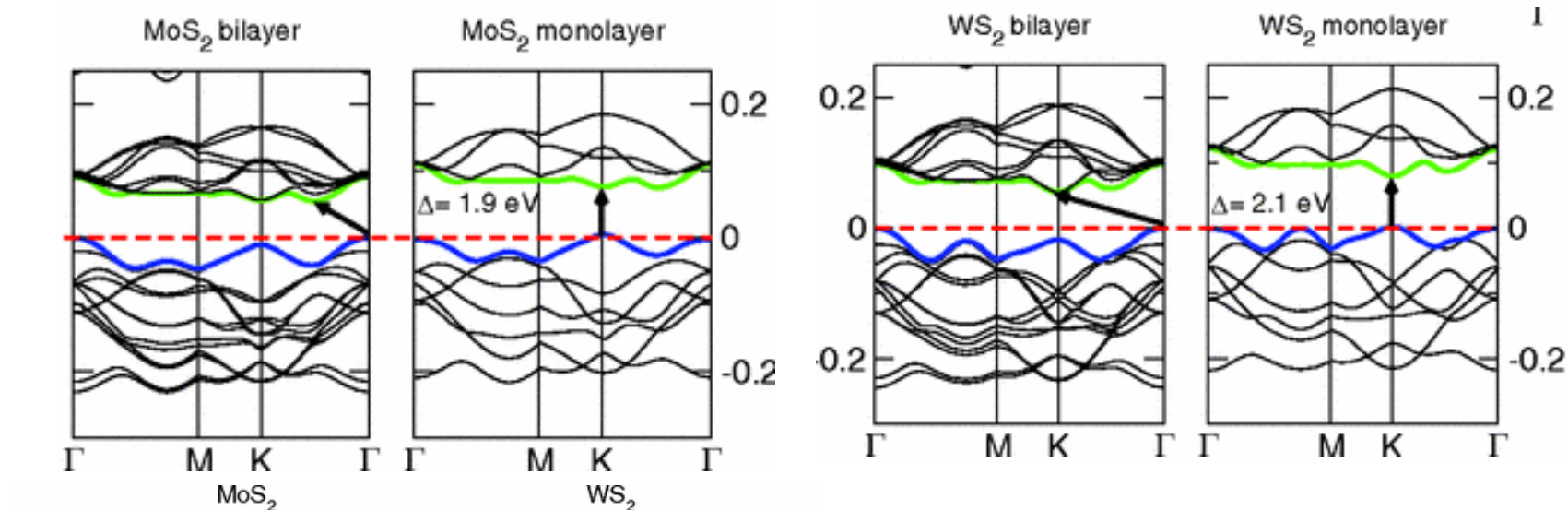


Phys. Rev. Lett. 105, 136805 (2010)

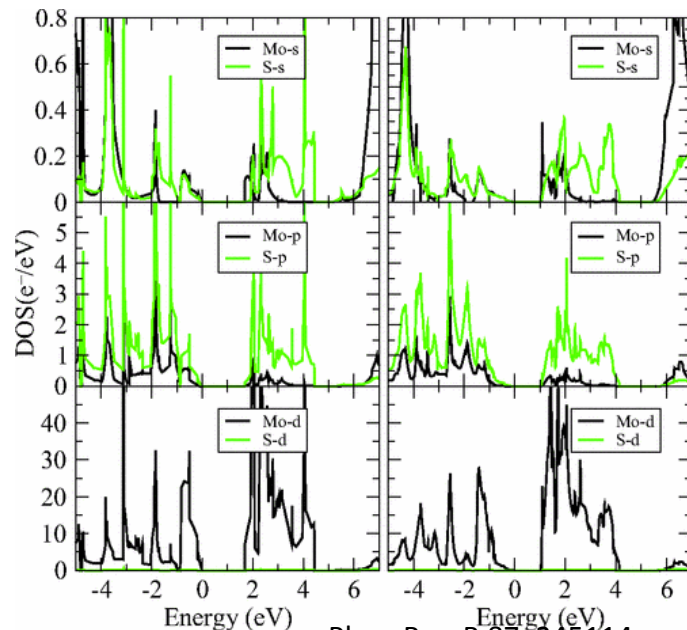
**An indirect to direct bandgap transition at monolayer MoS<sub>2</sub>**



# Evolution of Band Structure: Indirect to Direct



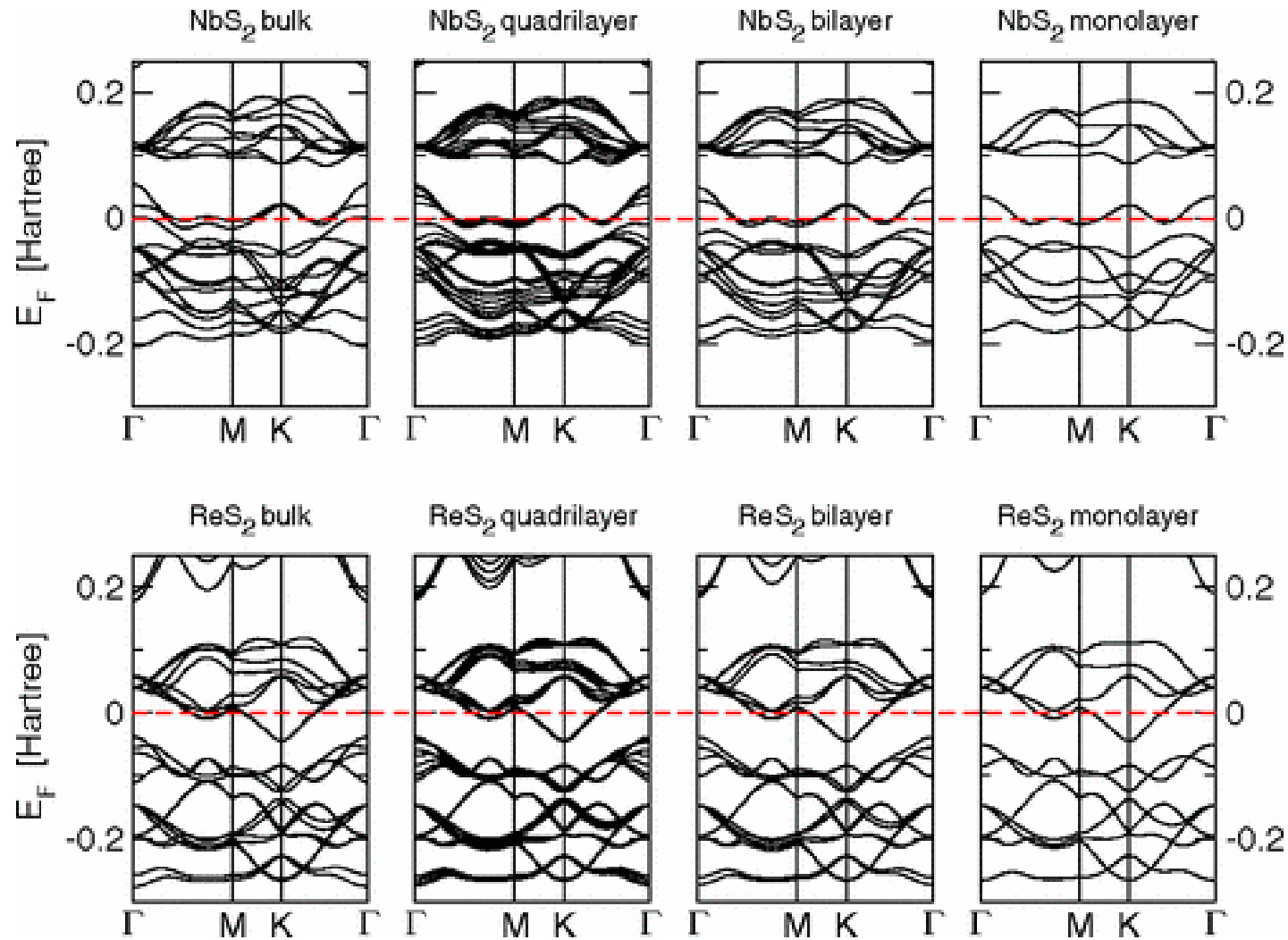
Phys. Rev. B 83, 245213



Phys. Rev. B 87, 245114

**The d-electron orbitals dominate the valence and conduction bands**

# The Crossover of Indirect to Direct Not Universal

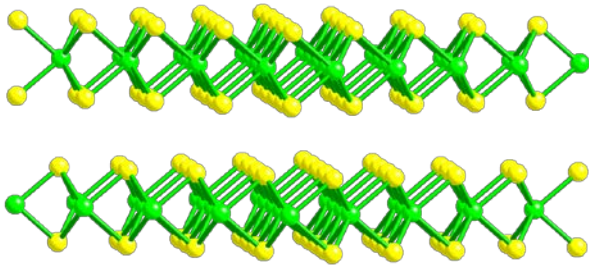


Phys. Rev. B 83, 245213

**NbS<sub>2</sub> and ReS<sub>2</sub> are metallic because the 4d<sub>z<sub>2</sub></sub> orbital is half-filled. No layer dependence crossover.**

# Key Points

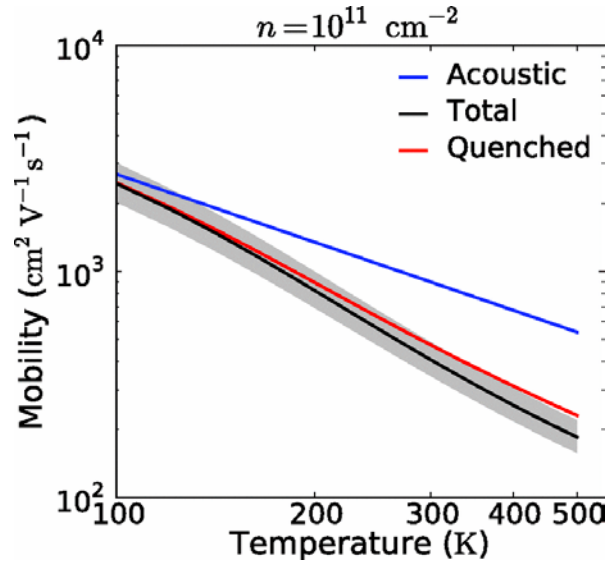
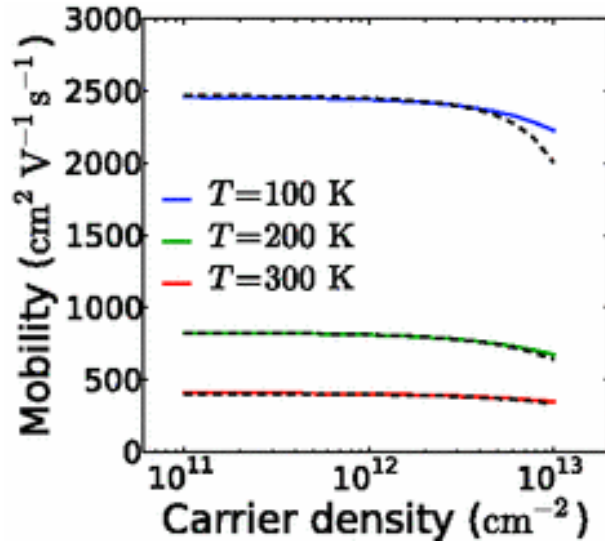
- Mo  $4d$  and S  $3p$  atomic orbitals play a decisive role in the band structure



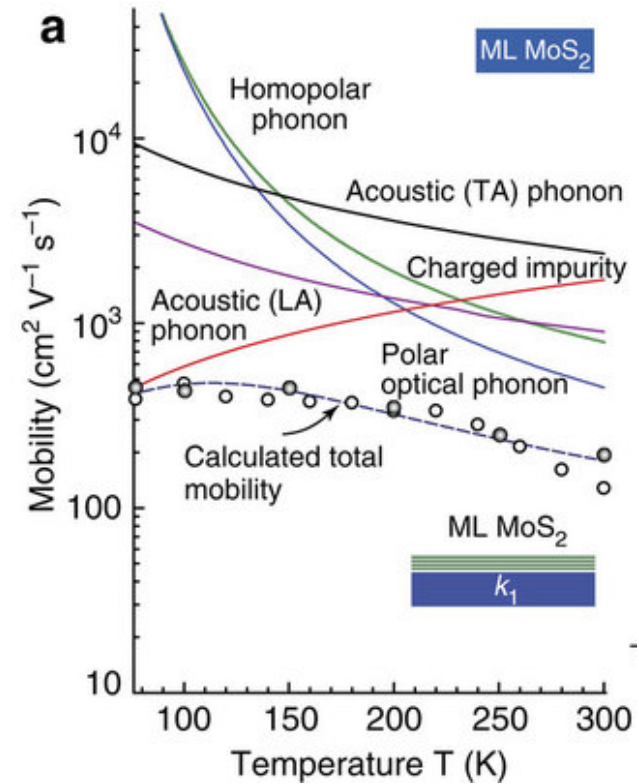
- The energy levels dominated by the S  $p$ -orbitals is subject to the influence of interlayer interactions, while those mainly consisting of Mo  $d$ -orbitals not
- The valence band edge at  $\Gamma$  point involves the contribution from S  $3p$  orbitals, while the band edges at  $K$  point are mainly made of Mo  $4d$  orbitals

## **III.3.2 Mobility**

# Phonon-limited Charge Mobility in MoS2



Phys. Rev. B 85, 115317



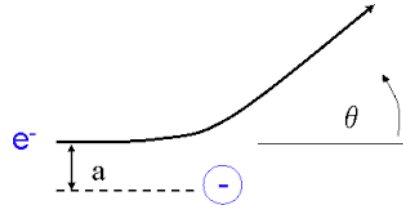
Nature Communications 3, 1011

**The room-temperature mobility is dominated by optical phonon scattering.**

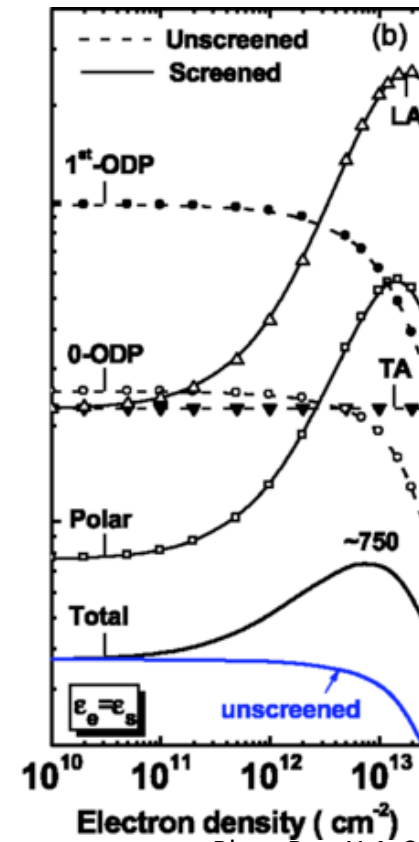
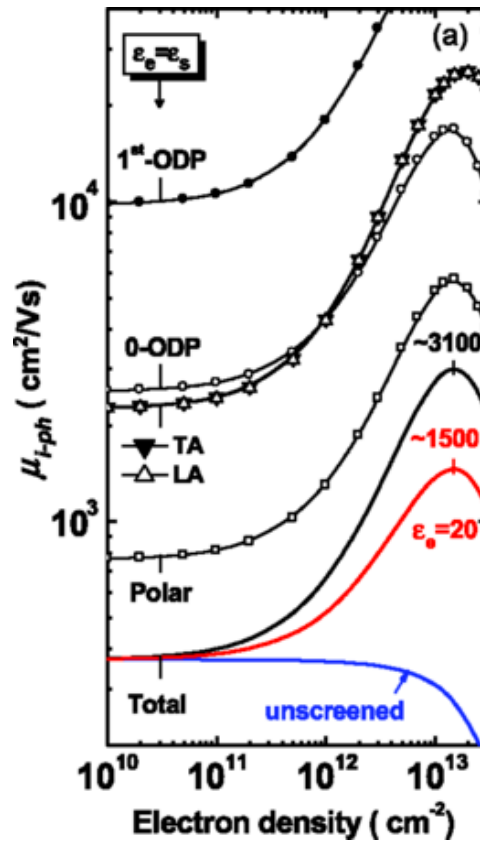
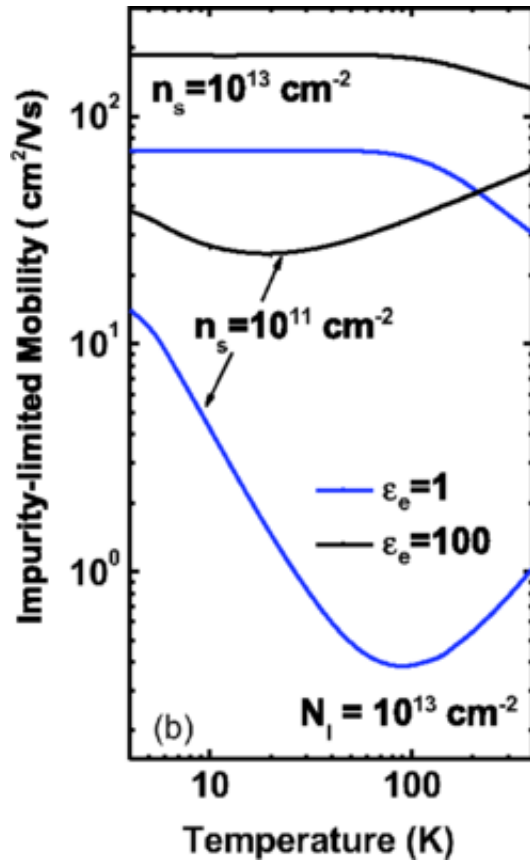
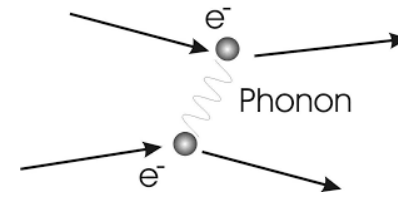
**$200 \sim 40 \text{ cm}^2 \text{V}^{-1} \text{s}^{-1}$**

# Charge Mobility of in MoS2: Substrate Effect

Charge impurity scattering



Phonon scattering

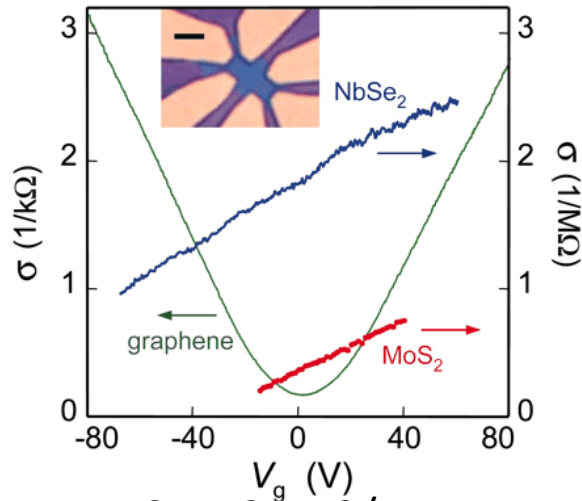


Phys. Rev. X 4, 011043

The ionized impurity scattering and remote phonon scattering are the major factors limiting the mobility

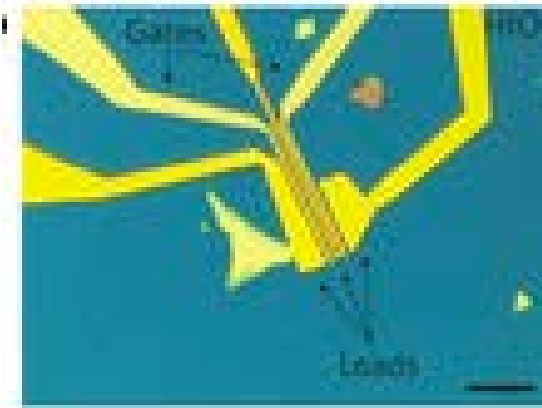
# Charge Mobility in MoS<sub>2</sub>: Experiments

A wide variation in the measured results



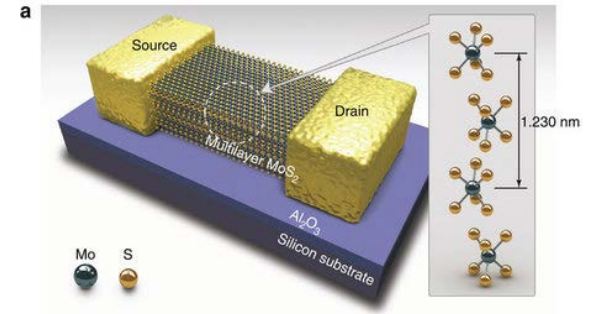
$0.5 - 3 \text{ cm}^2/\text{V}$

Proc. Natl. Acad. Sci. U. S. A. 102, 10451–10453



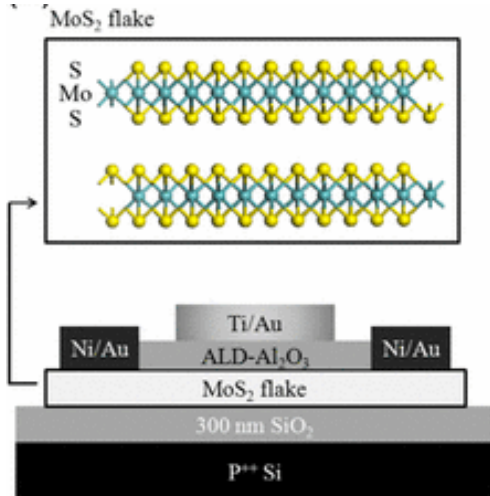
$200 \text{ cm}^2 \text{ V}^{-1} \text{ s}^{-1}$ ,

Nature Nanotechnology 6, 147–150 (2011)



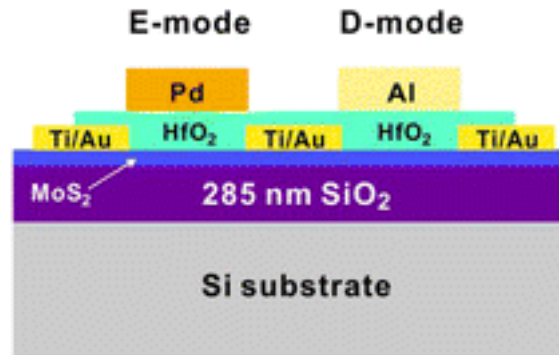
$>100 \text{ cm}^2 \text{ V}^{-1} \text{ s}^{-1}$

Nature Communications 3, 1011



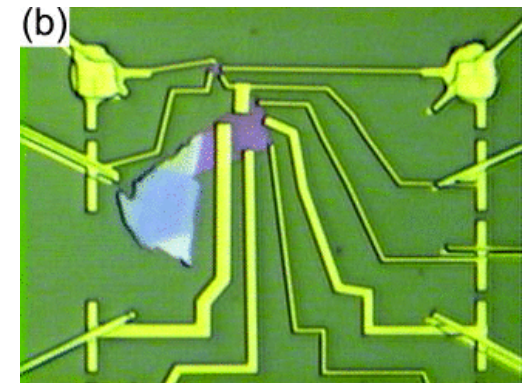
$517 \text{ cm}^2/\text{V}\cdot\text{s}$

IEEE Electron Dev. Lett. 33, 546–548 (2012)



$300 \text{ cm}^2 \text{ V}^{-1} \text{ s}^{-1}$

Nano Lett., 2012, 12 (9), pp 4674–4680



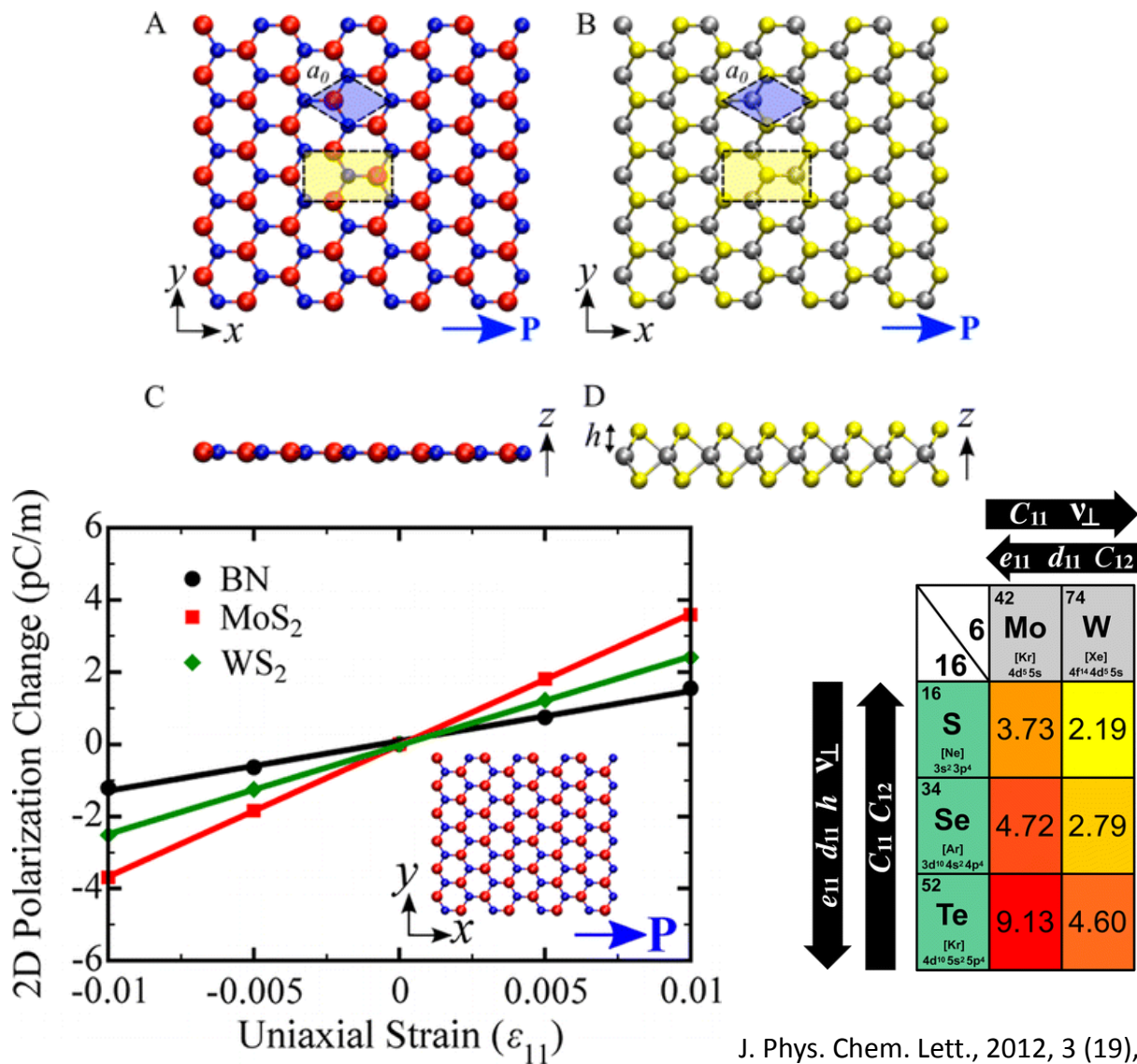
$\sim 10 \text{ cm}^2 \text{ V}^{-1} \text{ s}^{-1}$

J. Appl. Phys. 101, 014507 (2007)

## **III.3.3 Piezoelectricity**

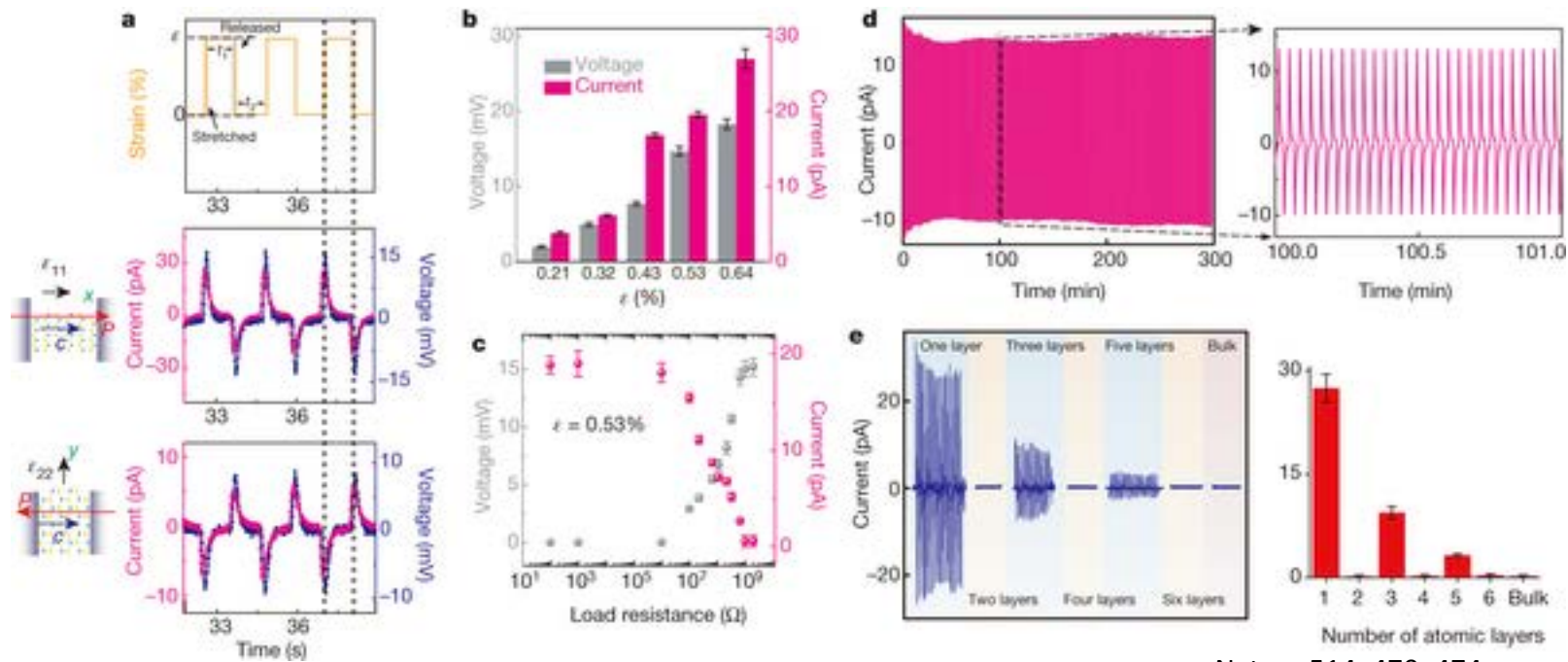


# Piezoelectricity in 2D TMDC Materials: Theory

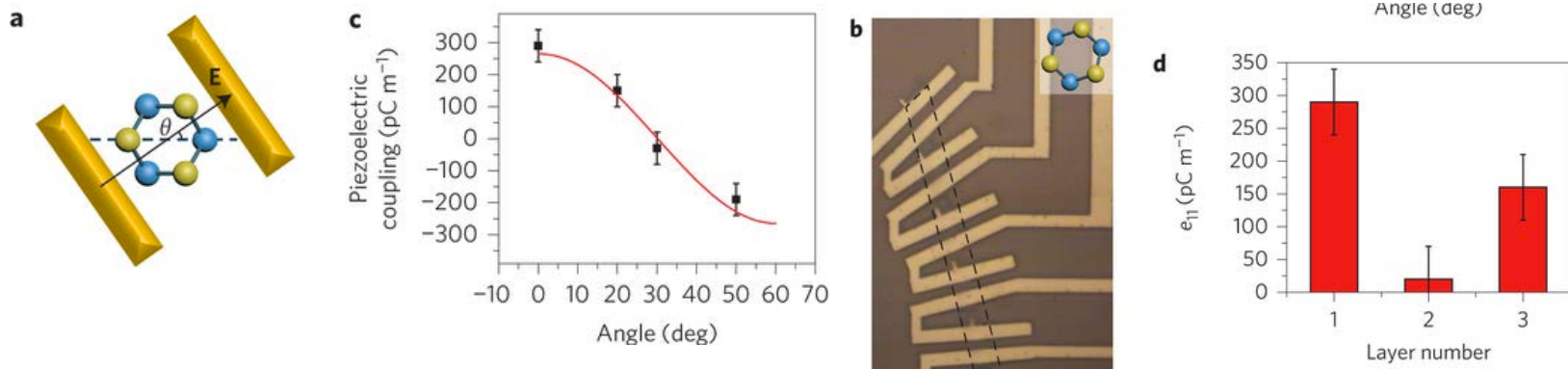


**Monolayer TMDC materials are piezoelectric**

# Piezoelectricity in MoS2: Experiments



Nature 514, 470–474

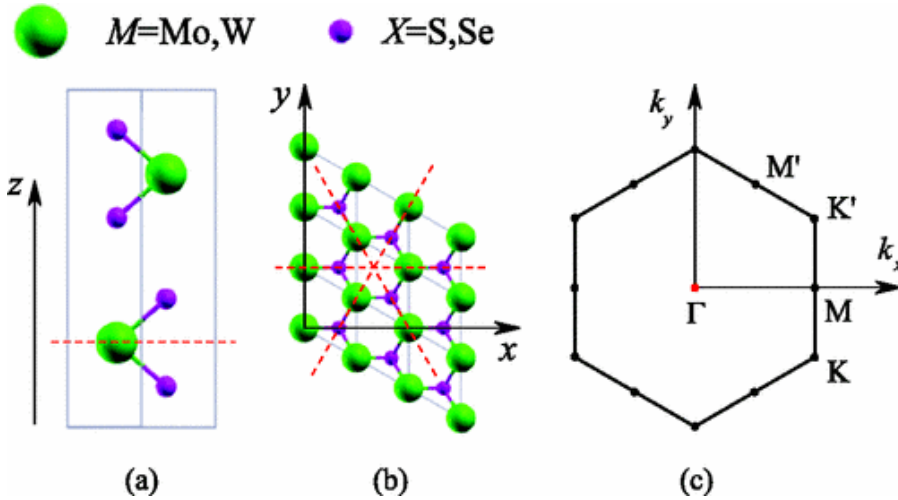


Nature Nanotechnology 10, 151–155 (2015)

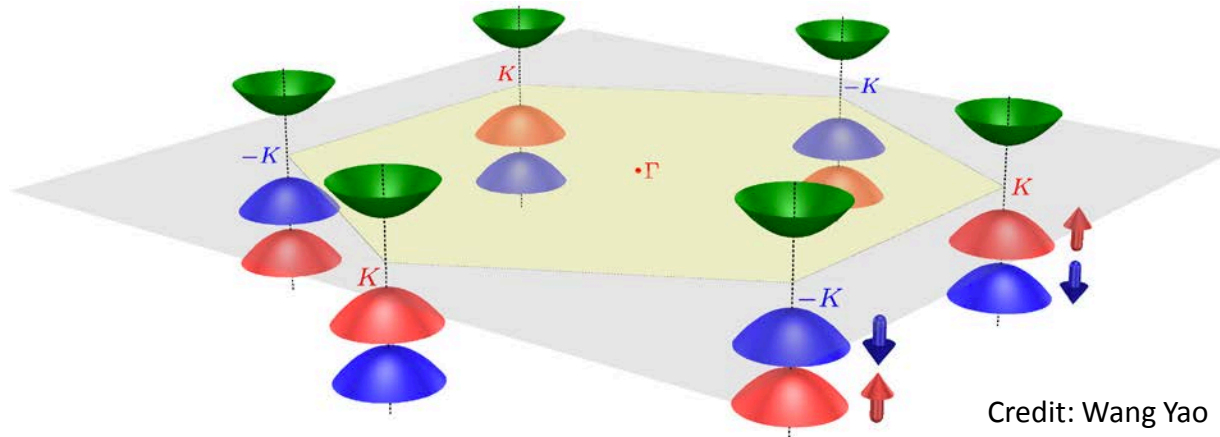
**Depend on if the layer number is odd or even.**

## **III.3.4 Spin-Valley Coupling**

# Coupled Valley-Spin of TMDCs (MoS2)

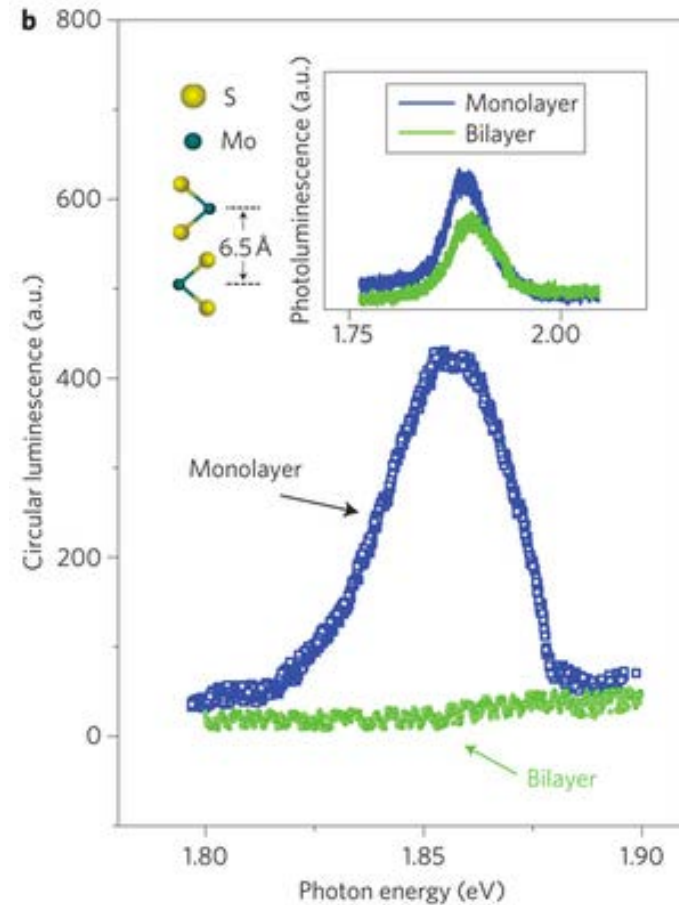
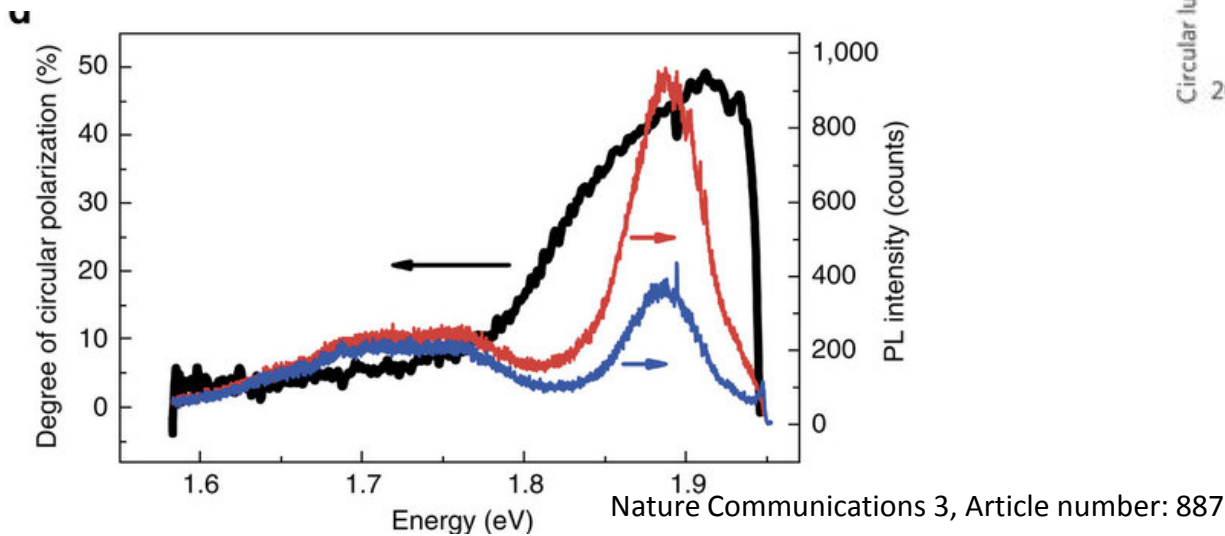
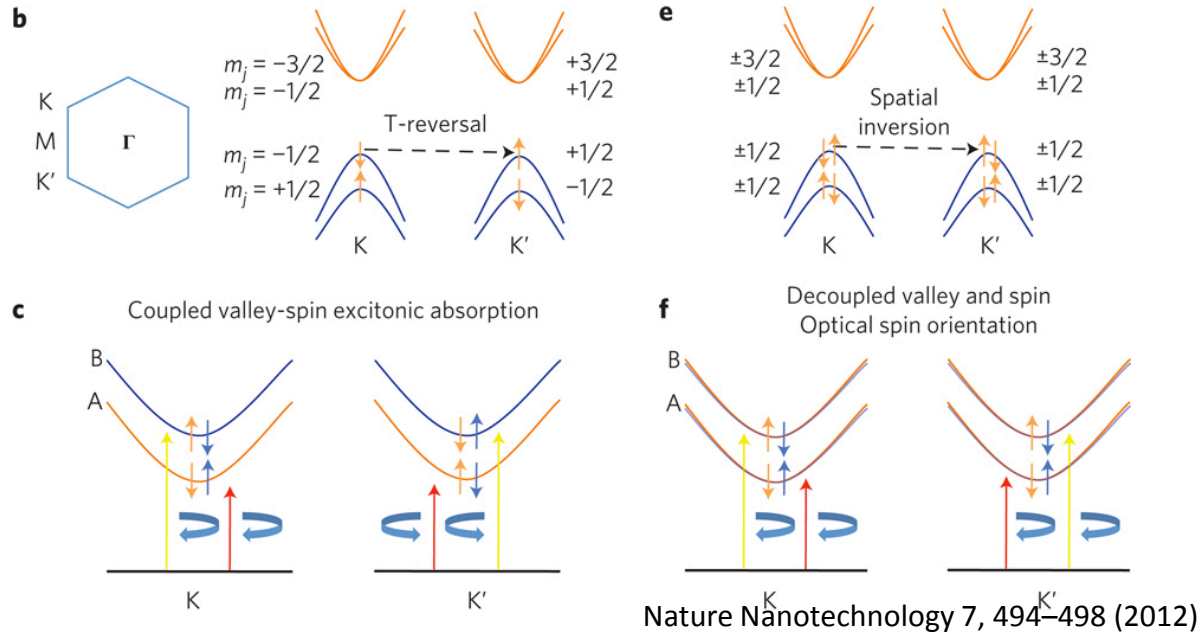


Phys. Rev. B 84, 153402



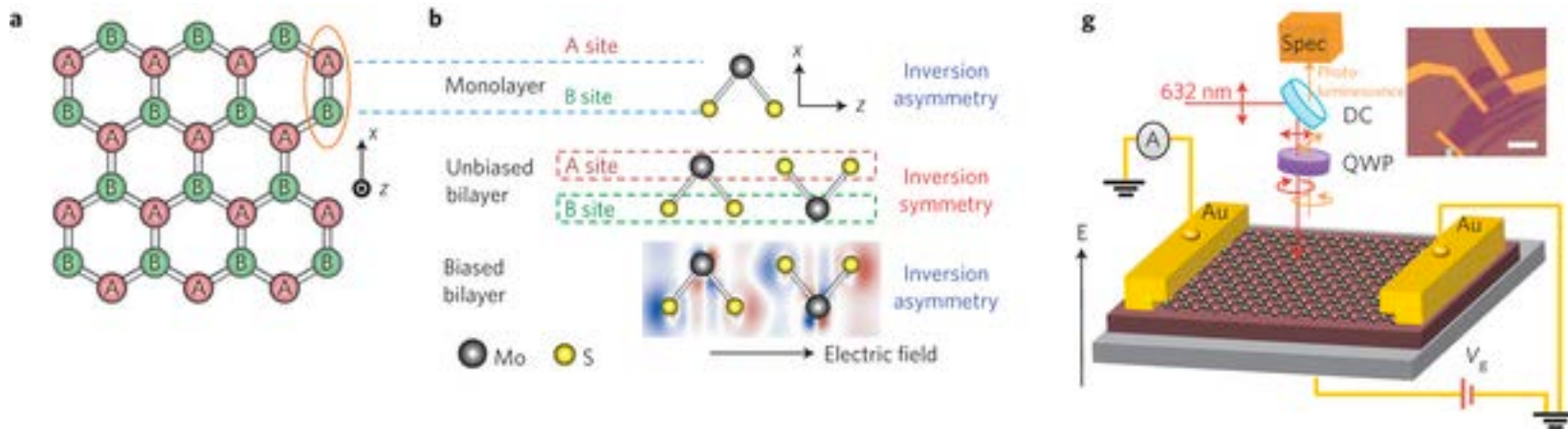
- At the  $K$  and  $K'$  valleys, the band edges are mainly of molybdenum d-orbital
- spin-orbit interactions split the valence bands by  $\sim 160$  meV in monolayer
- The valley and spin of the valence bands are inherently coupled in monolayers

# Valley-Spin Polarized Luminescence in Monolayer



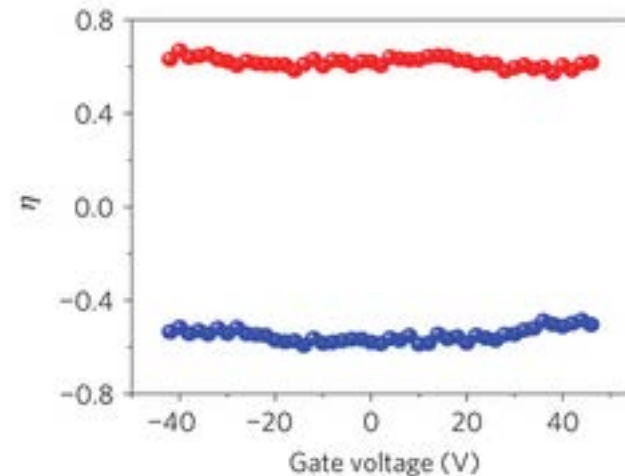
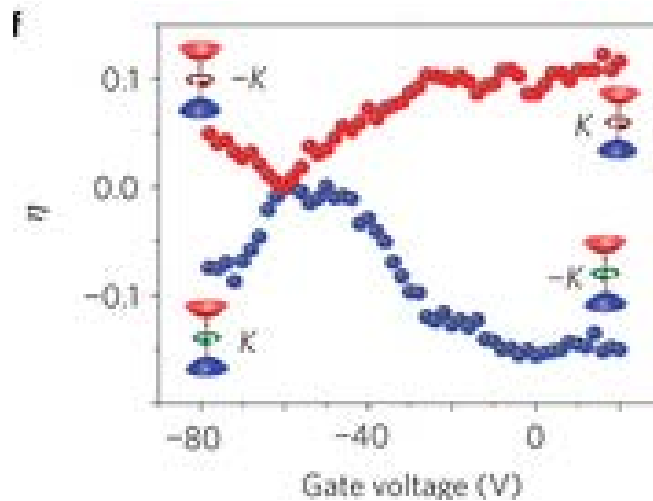
Left circularly polarized ( $\sigma^-$ ) and right circularly polarized ( $\sigma^+$ ) at the K and K' valleys

# Electrically Tuned Valley-Spin Polarization



**2L MoS2**

**1L MoS2**



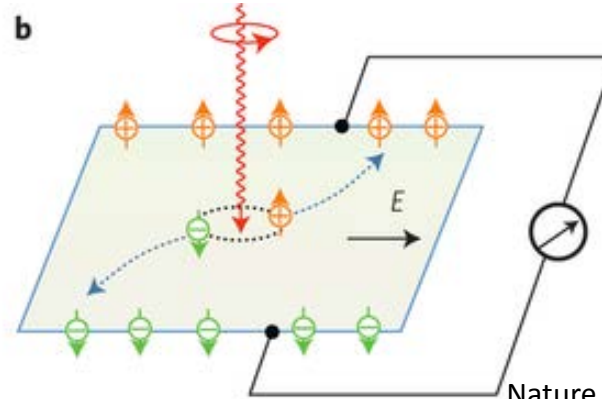
Nature Physics 9, 149–153 (2013)

$$\eta = (P(\sigma+) - P(\sigma-)) / (P(\sigma+) + P(\sigma-)).$$

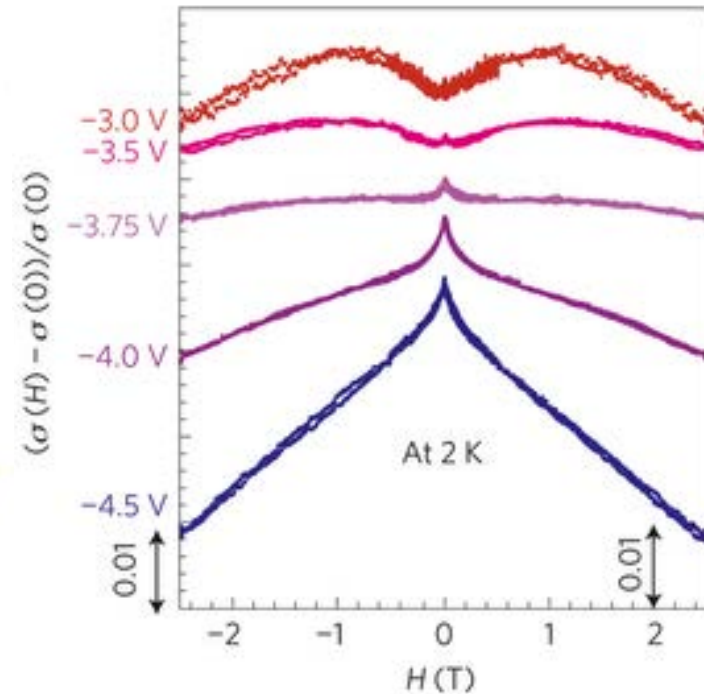
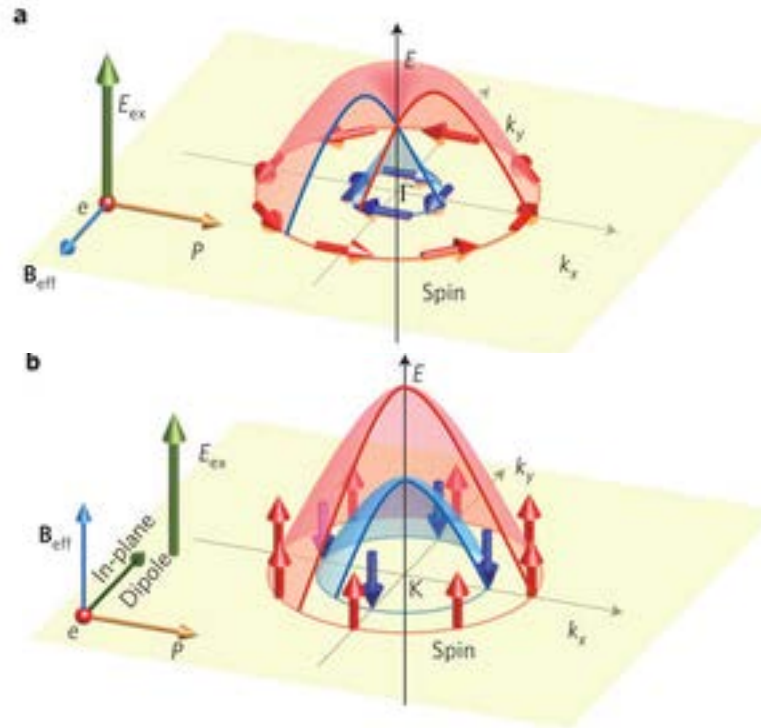
**Optical helicity can be continuously tuned from -15% to 15% as a function of gate voltage in 2L MoS2, but is gate independent in monolayer MoS2**

# Valley-Hall Effect and Zeeman-Type Splitting

Valley Hall effect.



Nature Physics 10, 343–350 (2014)



Nature Physics 9, 563–569 (2013)

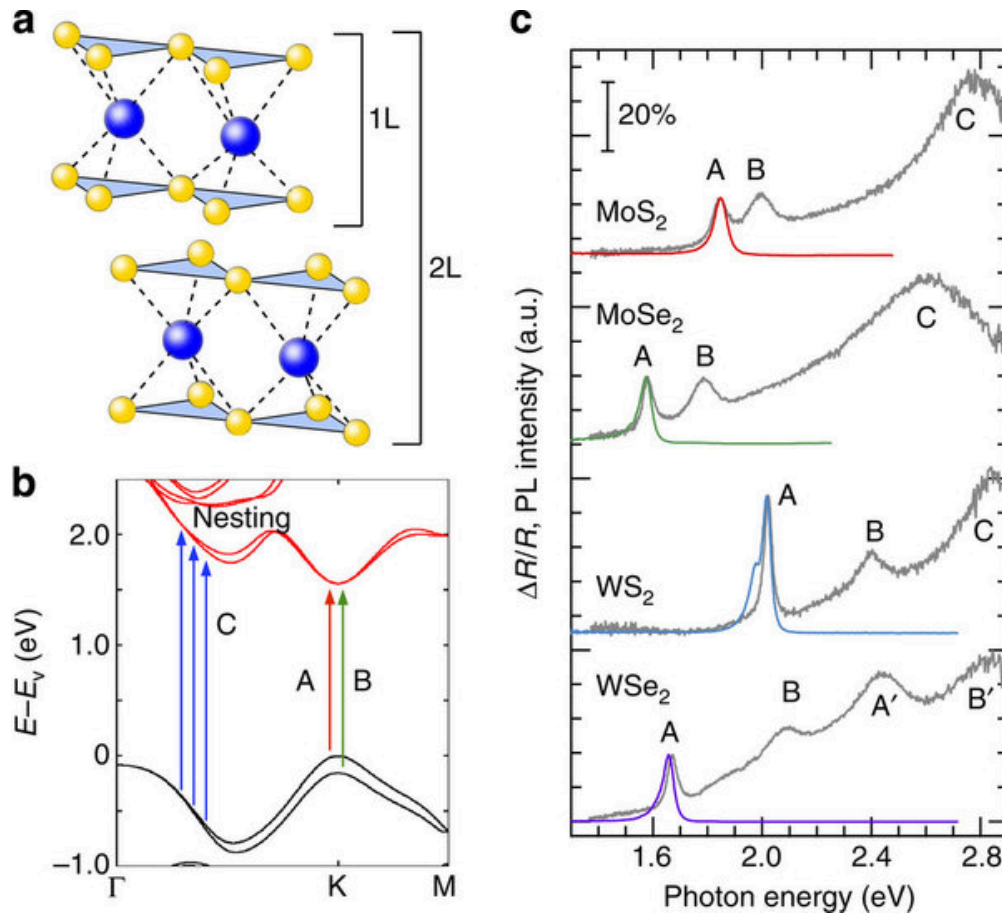
# **III. Fundamental Properties**

## **III.4 Optical Properties**



# **III.4.1 Exciton, Binding Energy & Radius**

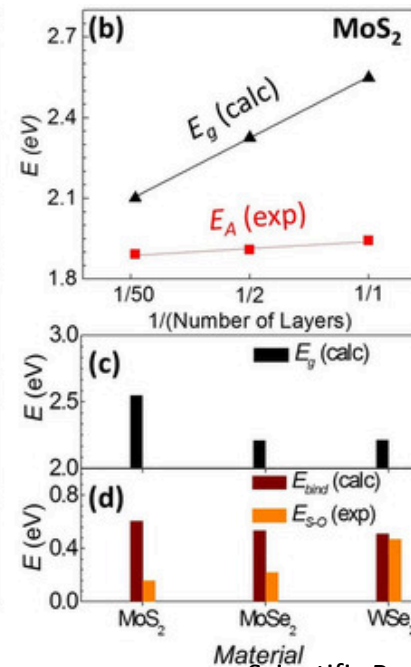
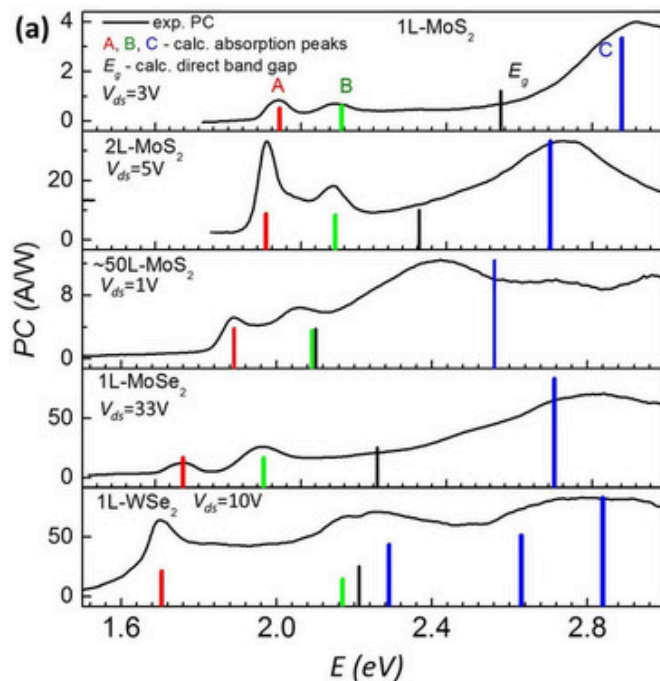
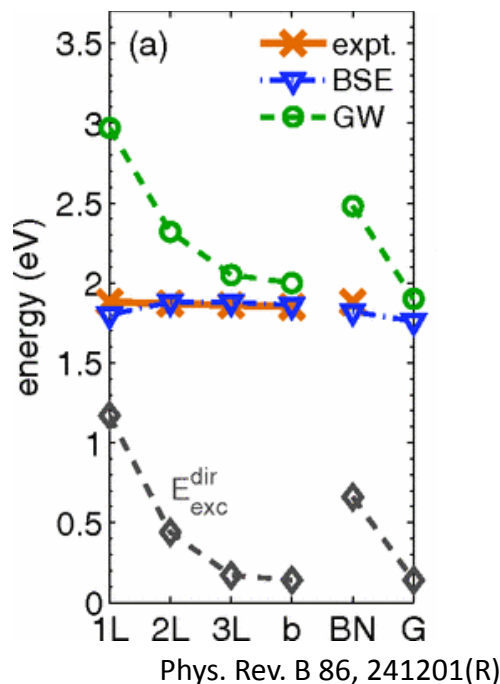
# Excitonic States



Nature Communications 5, 4543, (2014)

**A and B from interband transition of K/K' points, and C from transition in the Brillouin zone between  $\Gamma$  and  $\Lambda$**

# Extraordinarily Strong Binding Energy

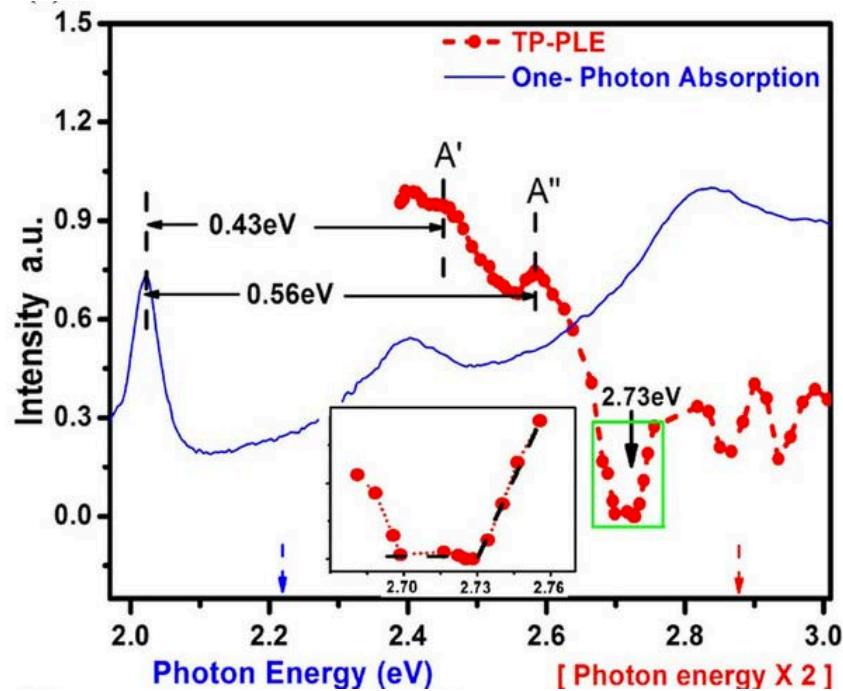
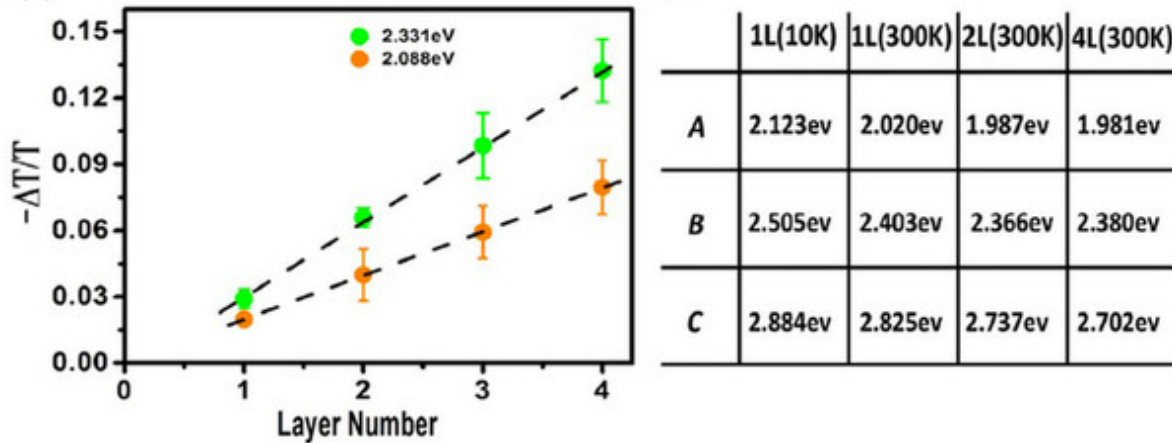


Scientific Reports 4, 6608, 2014

	Energy cutoffs	$k$ point	$E_g$	$E_g$ (optical)	Binding energy
Monolayer MoS <sub>2</sub> (3.160 Å)	400 and 200	6 × 6 × 1(SOC)	2.89	1.87	1.02
		6 × 6 × 1	2.99	1.96	1.03
		9 × 9 × 1	2.84	2.08	0.76
		12 × 12 × 1	2.78	2.16	0.62
		15 × 15 × 1	2.76	2.22	0.54
Monolayer MoS <sub>2</sub> (3.190 Å)	600 and 300	12 × 12 × 1	2.80	2.17	0.63
		12 × 12 × 1	2.66	2.04	0.62
Monolayer WS <sub>2</sub> (3.155 Å)	400 and 200	6 × 6 × 1(SOC)	3.02	1.97	1.05
		6 × 6 × 1	3.28	2.21	1.07
		9 × 9 × 1	3.12	2.34	0.78
		12 × 12 × 1	3.06	2.43	0.63
		15 × 15 × 1	3.05	2.51	0.54
Monolayer WS <sub>2</sub> (3.190 Å)	600 and 300	12 × 12 × 1	3.11	2.46	0.65
		12 × 12 × 1	2.92	2.28	0.64

The exciton binding energy in MoS<sub>2</sub> monolayer is reported ~ 0.4-1.1 eV

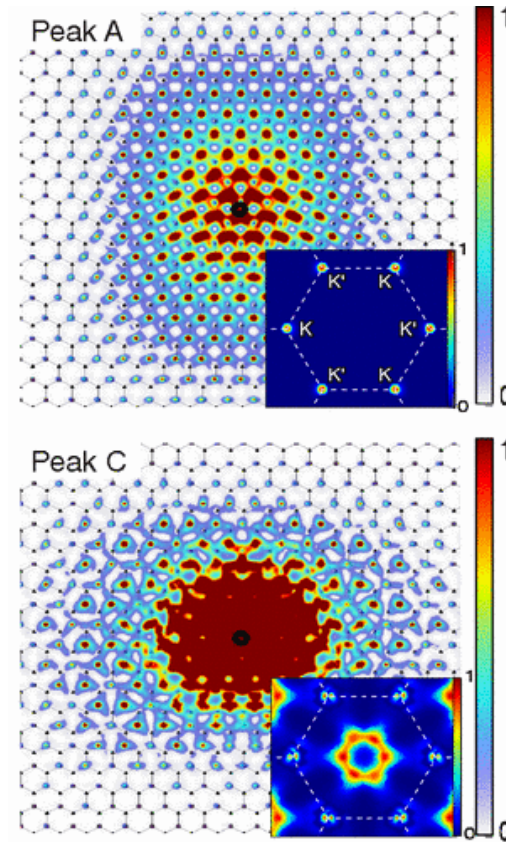
# Strong Binding Energy in WS2



Scientific Reports 5, 9218 (2015)

**The exciton binding energy in WS2 monolayer is  $0.71 \pm 0.01$  eV around K valley**

# Exciton Radius



Phys. Rev. Lett. 111, 216805

**The exciton radius is estimated to be 0.5-2 nm**

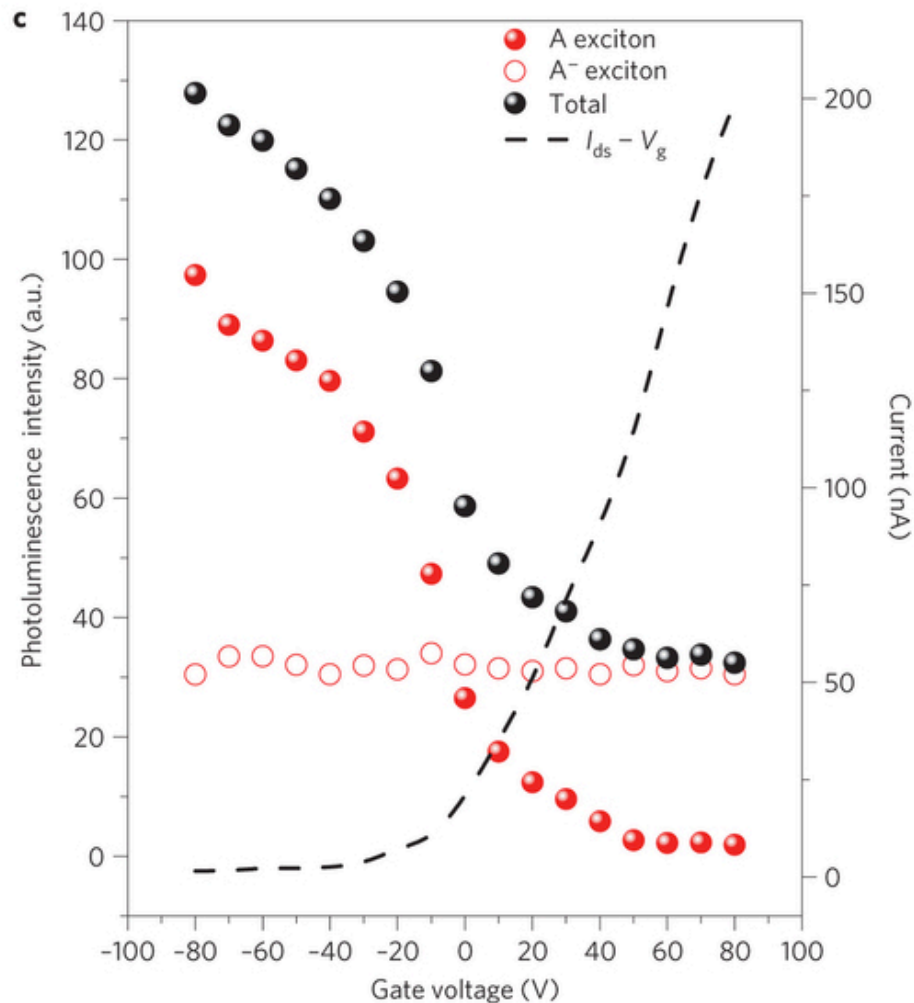
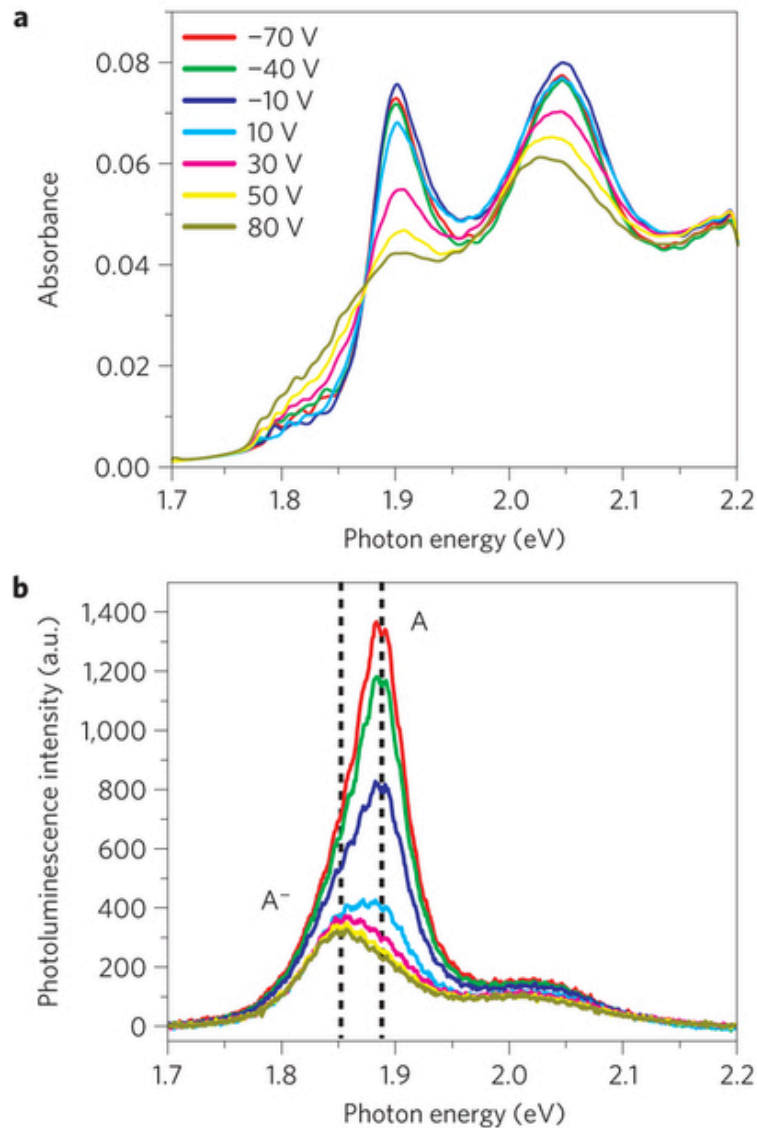
# Comment

**Most of the studies (binding energy, radius) focus on the A exciton**

**How these results could be applied to the B and C excitons is not clear.**

## **III.4.2 Neutral and Charged Excitons**

# Neutral and Charged Excitons

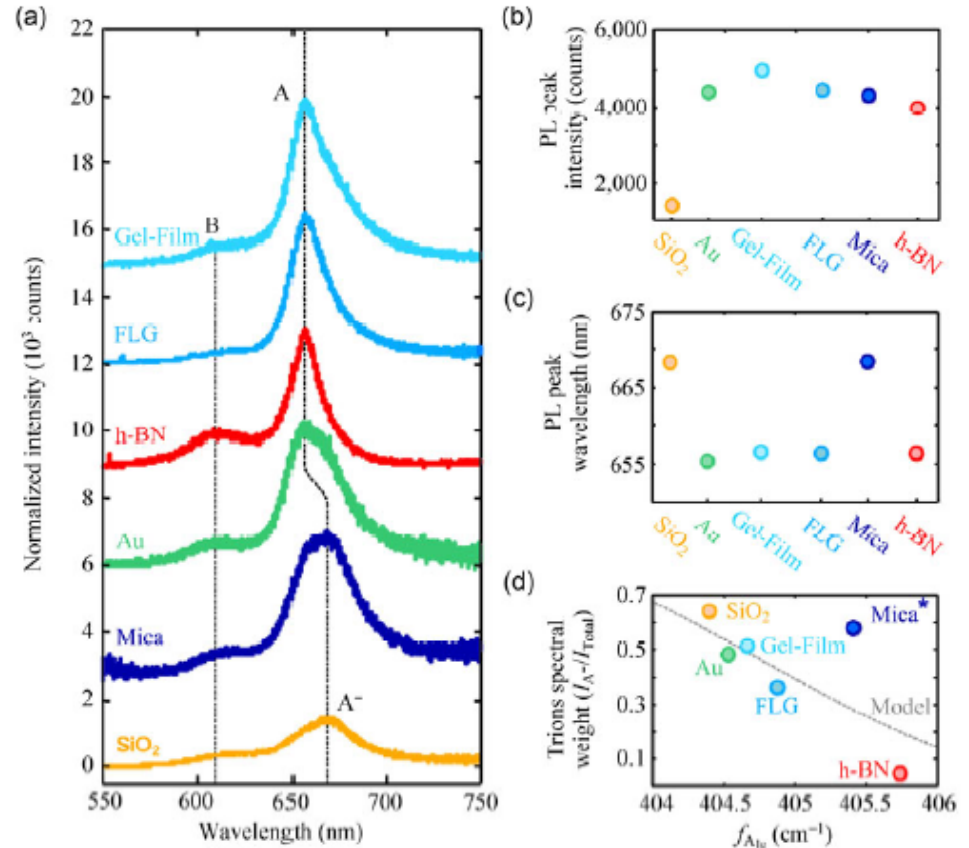
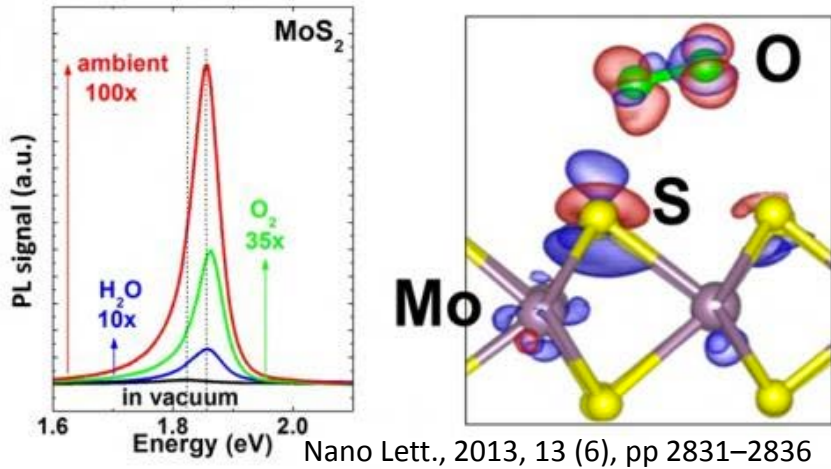


Nature Materials 12, 207–211 (2013)

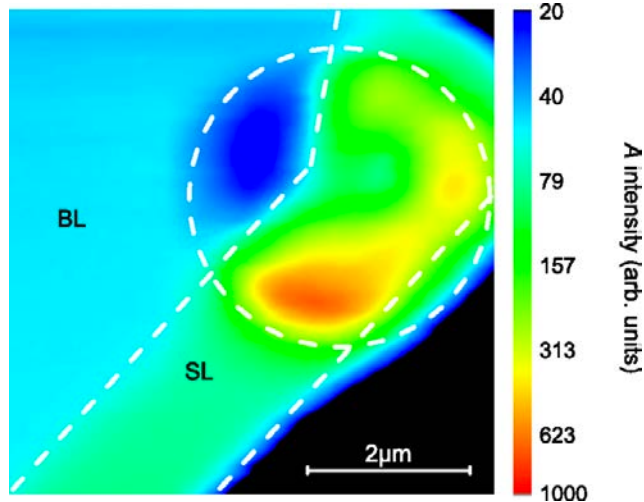
**Tightly bound negative trions, a quasiparticle composed of two electrons and a hole with a binding energy estimated to be ~20meV**



# Neutral and Charged Excitons: Effects of Doping



Nano Res. 2014, 7(4): 561–571

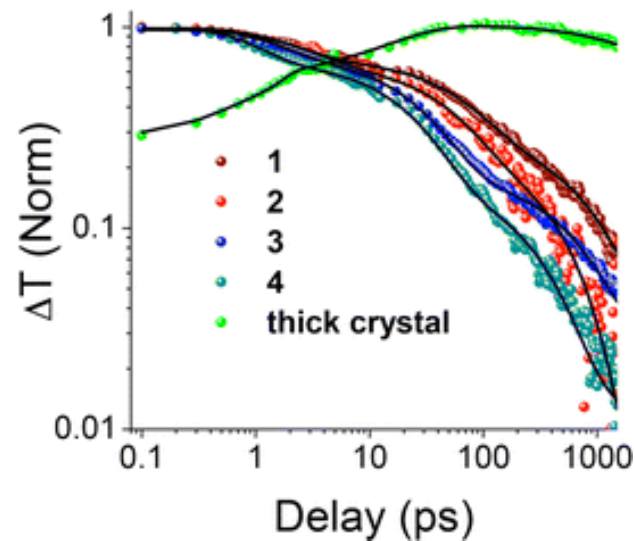
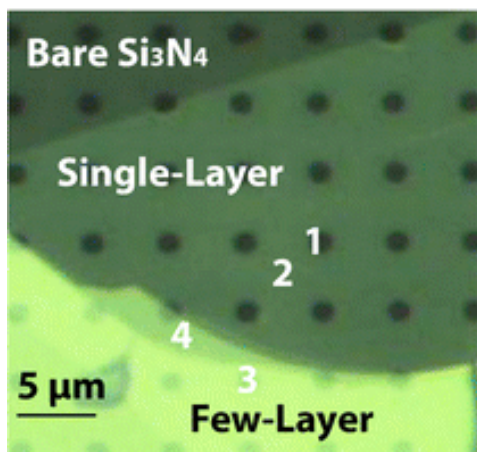


Phys. Rev. B 89, 125406

The PL intensity and position is subject to the effect of substrates and molecule adsorption, which may change doping level and the population of trions.

## **III.4.4 Exciton Dynamics and Manipulation**

# Exciton Dynamics

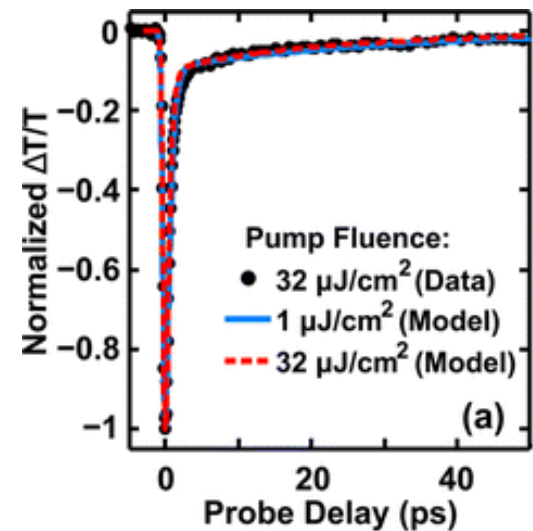
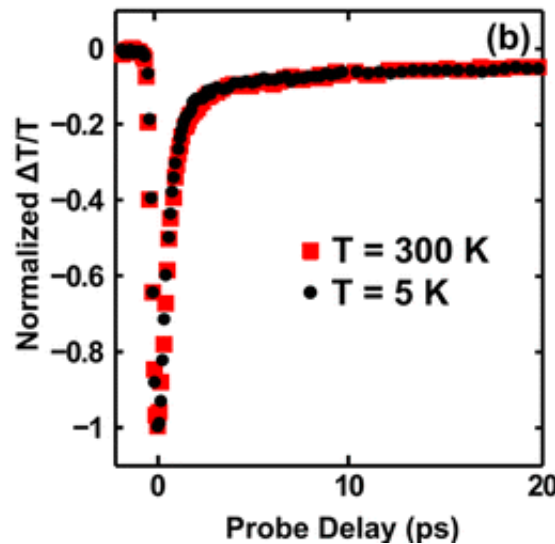
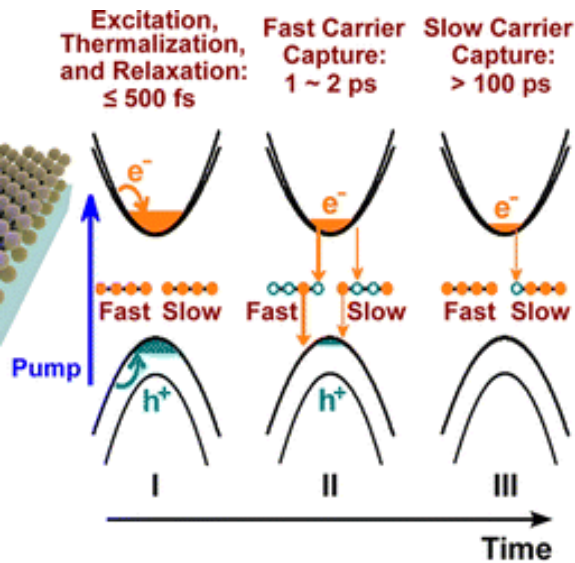


	$\tau_1$ (ps)	$\tau_2$ (ps)	$\tau_3$ (ps)
1 (suspended monolayer)	$2.6 \pm 0.1$ (39%)	$74 \pm 3$ (39%)	$850 \pm 48$ (22%)
2 (supported monolayer)	$3.3 \pm 0.2$ (40%)	$55 \pm 3$ (38%)	$469 \pm 26$ (22%)
3 (suspended few-layer)	$2.1 \pm 0.1$ (40%)	$34 \pm 1$ (47%)	$708 \pm 55$ (13%)
4 (supported few-layer)	$1.2 \pm 0.1$ (47%)	$29 \pm 2$ (41%)	$344 \pm 28$ (12%)
thick crystal	$1.8 \pm 0.6$ (19%) (rise)	$20 \pm 2$ (81%) (rise)	$2626 \pm 192$ (100%) (decay)

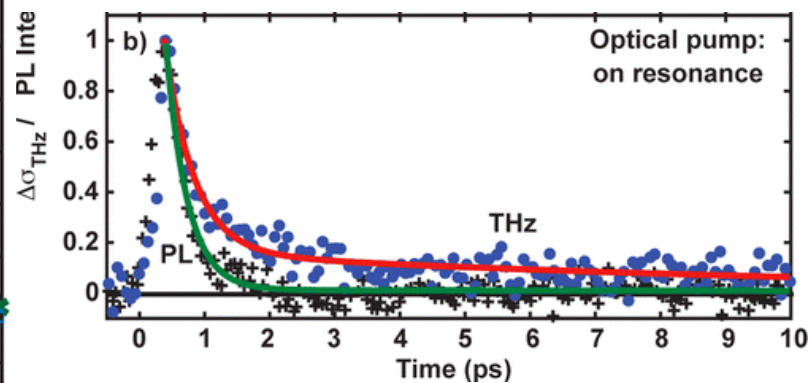
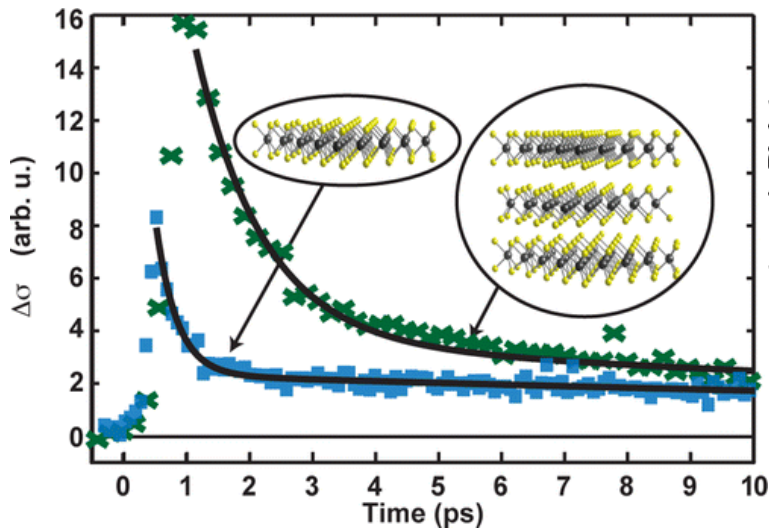
ACS Nano, 2013, 7 (2), pp 1072–1080

- **Nonradiative relaxation dominate**
- **Fast trapping of excitons by surface trap states**

# Exciton Dynamics



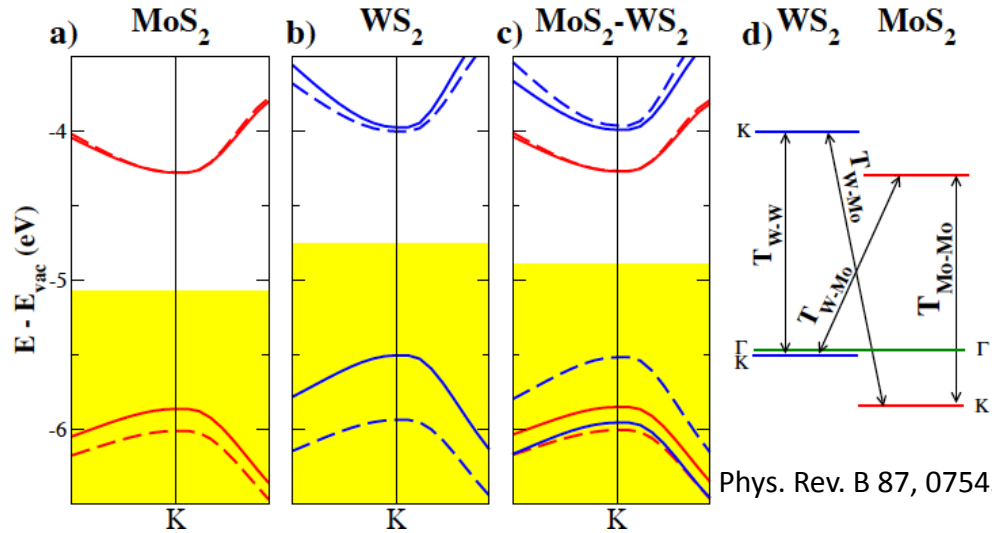
Nano Lett., 2015, 15 (1), pp 339–345



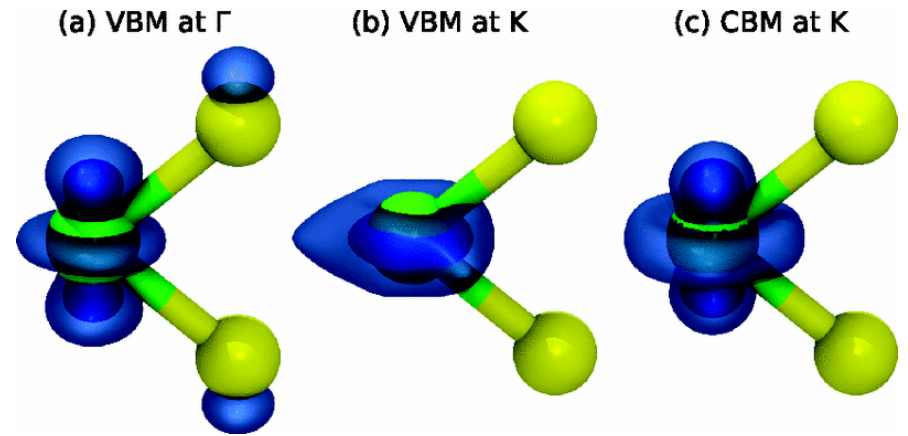
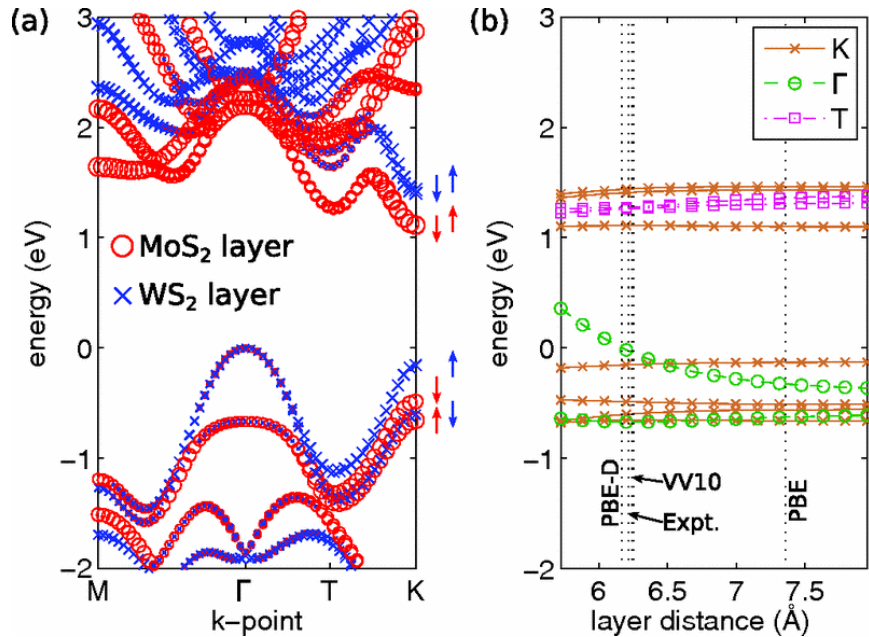
ACS Nano, 2014, 8 (11), pp 11147–11153

## Defect-Assisted Electron–Hole Recombination

# Band Structures in MoS<sub>2</sub>/WS<sub>2</sub> Heterostructures

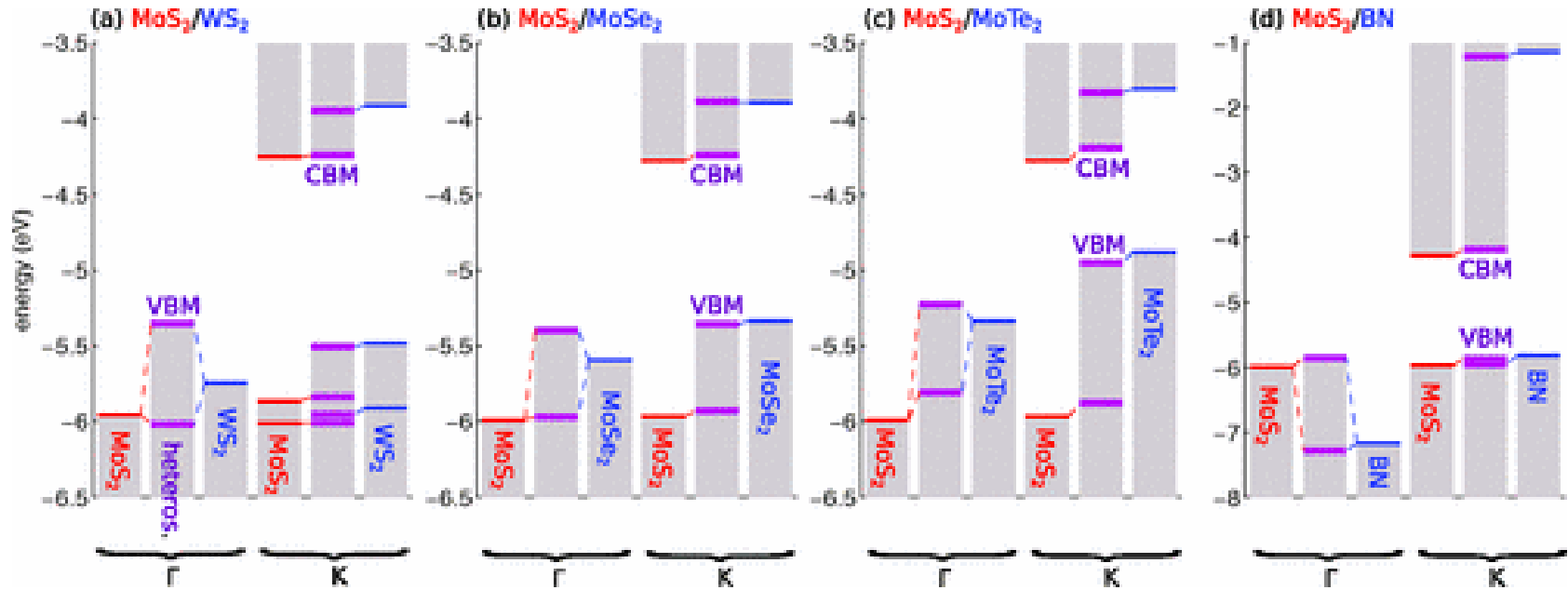


Phys. Rev. B 87, 075451 (2013)



Phys. Rev. B 88, 085318

# Band Structures in Other Heterostructures

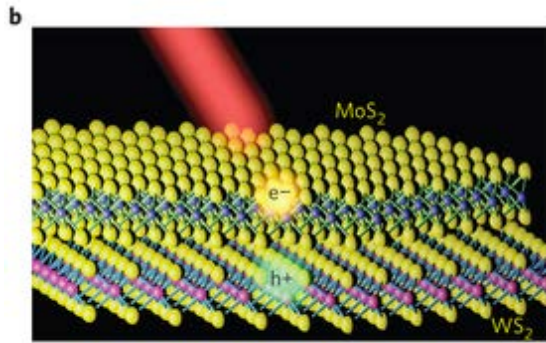


Phys. Rev. B 88, 085318

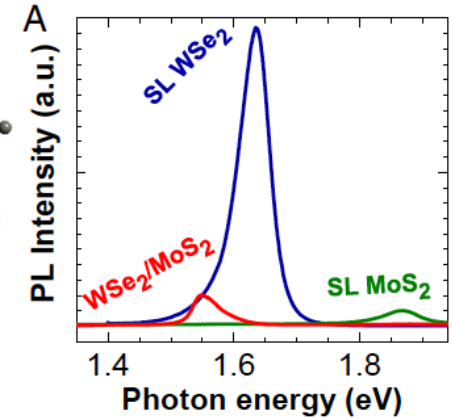
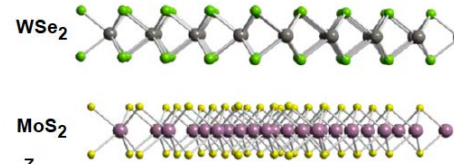
Table 1 | Direct and indirect (in parenthesis) band gaps in eV of hybrids of semiconducting transition metal dichalcogenides (STMD). Systems with a dominant direct band gap at the K point in the Brillouin zone have an asterisk. Cases with “+” show an indirect fundamental band gap  $\Gamma$ -K, and “&” corresponds to a dominant indirect gap K-I

Hybrid-Structure	Bilayer-Stacking A	Bilayer-Stacking B	Crystal- stacking A	Crystal- stacking B
WS <sub>2</sub> -MoS <sub>2</sub> Type 1	1.695(1.586 $\Gamma$ -I)	1.708(1.190 $\Gamma$ -I)	1.669(1.284 $\Gamma$ -I)	1.664 (0.764 $\Gamma$ -I)
WS <sub>2</sub> -WSe <sub>2</sub> Type 2	1.007(1.725 $\Gamma$ -I)*	1.068(1.314 $\Gamma$ -I)*	1.007(1.406 $\Gamma$ -I)*	1.037 (0.883 $\Gamma$ -I)
MoS <sub>2</sub> -WSe <sub>2</sub> Type 2	0.790(1.525 $\Gamma$ -I)*	0.891(1.147 $\Gamma$ -I)*	0.802(1.245 $\Gamma$ -I)*	0.883 (0.736 $\Gamma$ -I)
WS <sub>2</sub> -MoSe <sub>2</sub> Type 3	1.154(1.594 $\Gamma$ -I)*	1.180(1.052 $\Gamma$ -K) <sup>+</sup>	1.157(1.316 $\Gamma$ -I)*	1.155 (0.790 $\Gamma$ -I)
MoS <sub>2</sub> -MoSe <sub>2</sub> Type 3	0.945(1.560 $\Gamma$ -I)*	1.013(0.899 $\Gamma$ -K) <sup>+</sup>	0.949(1.260 $\Gamma$ -I)*	0.998 (0.699 $\Gamma$ -I)
WSe <sub>2</sub> -MoSe <sub>2</sub> Type 4	1.443(1.330 K-I)*	1.471(1.116 $\Gamma$ -I)	1.444(1.215 K-I)*	1.418 (0.761 $\Gamma$ -I)

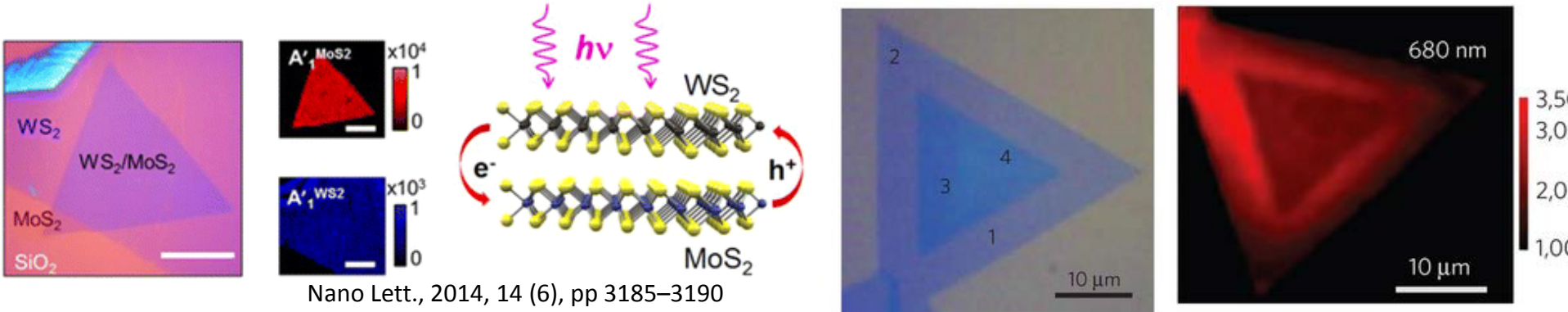
# Exciton Dynamics in Heterostructures



Nature Nanotechnology 9, 682–686 (2014)

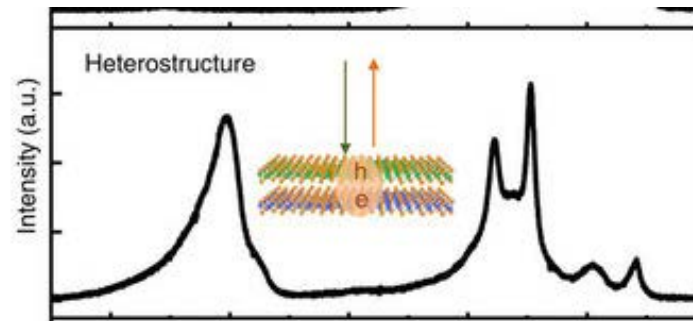
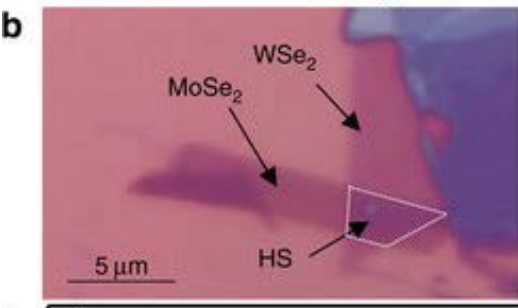


| PNAS | | vol. 111 | 6198–6202, 2014



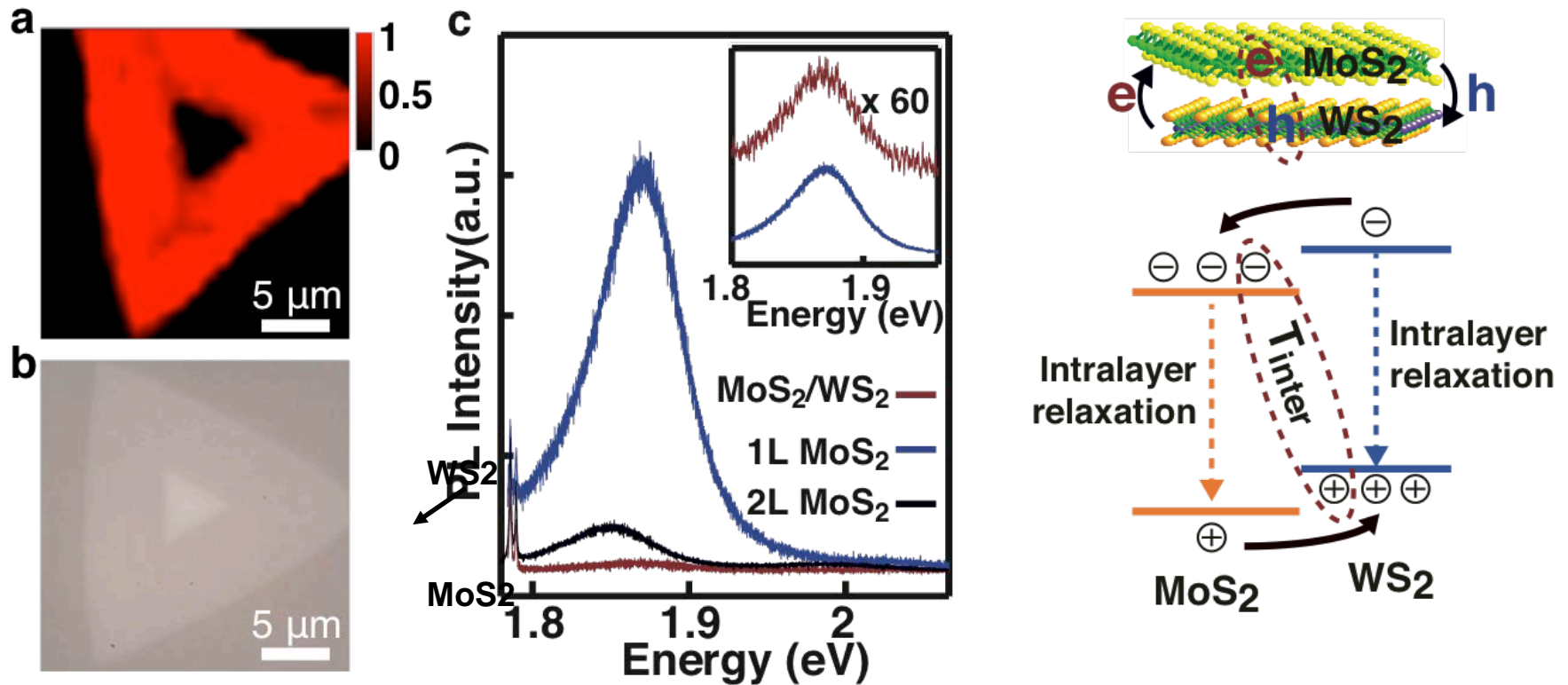
Nano Lett., 2014, 14 (6), pp 3185–3190

Nature Materials 13, 1135–1142 (2014)



Nature Communications 6, Article number: 6242

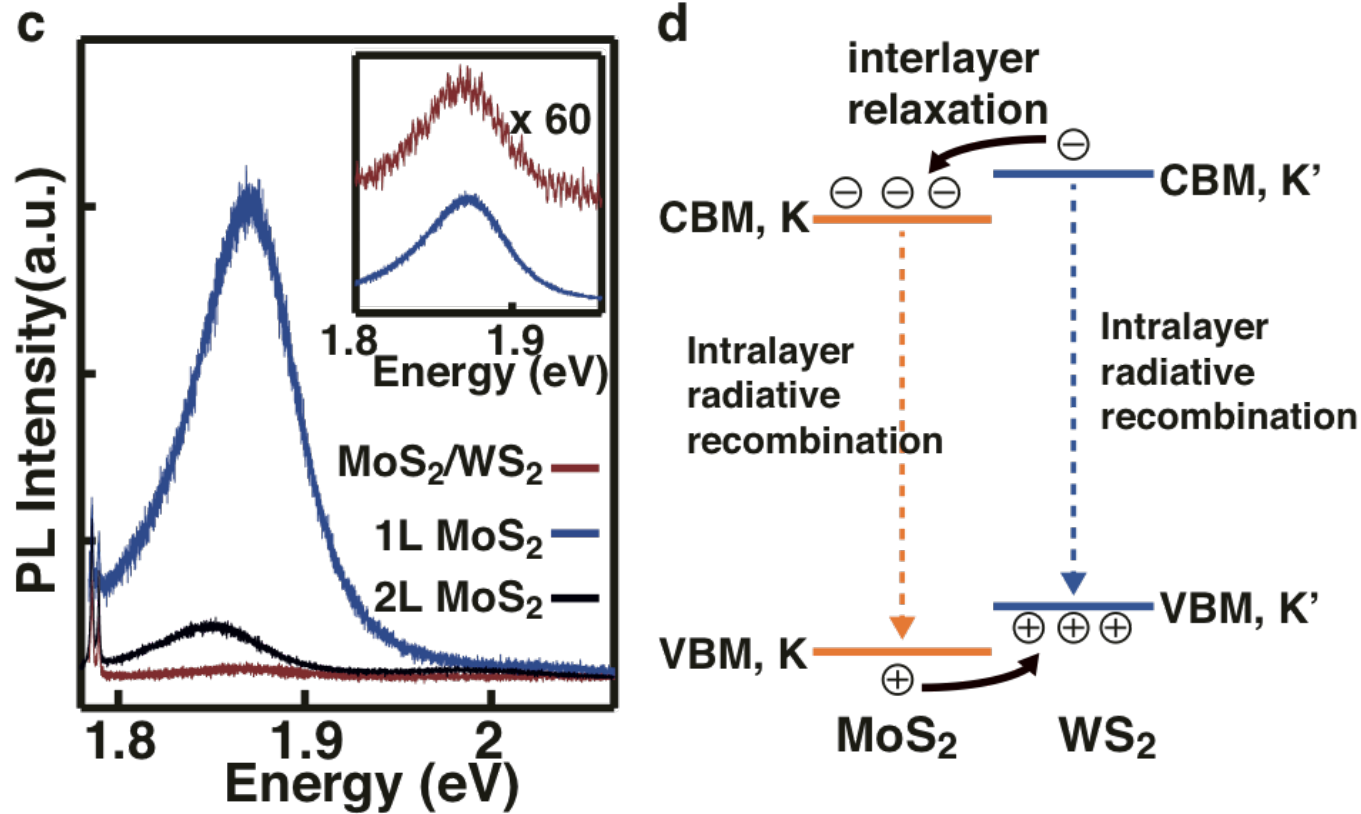
# Equally Efficient Interlayer Charge Transfer in Epitaxial and Non-epitaxial MoS<sub>2</sub>/WS<sub>2</sub> Heterostructures



**The PL in MoS<sub>2</sub>/WS<sub>2</sub> is two orders of magnitude less!**



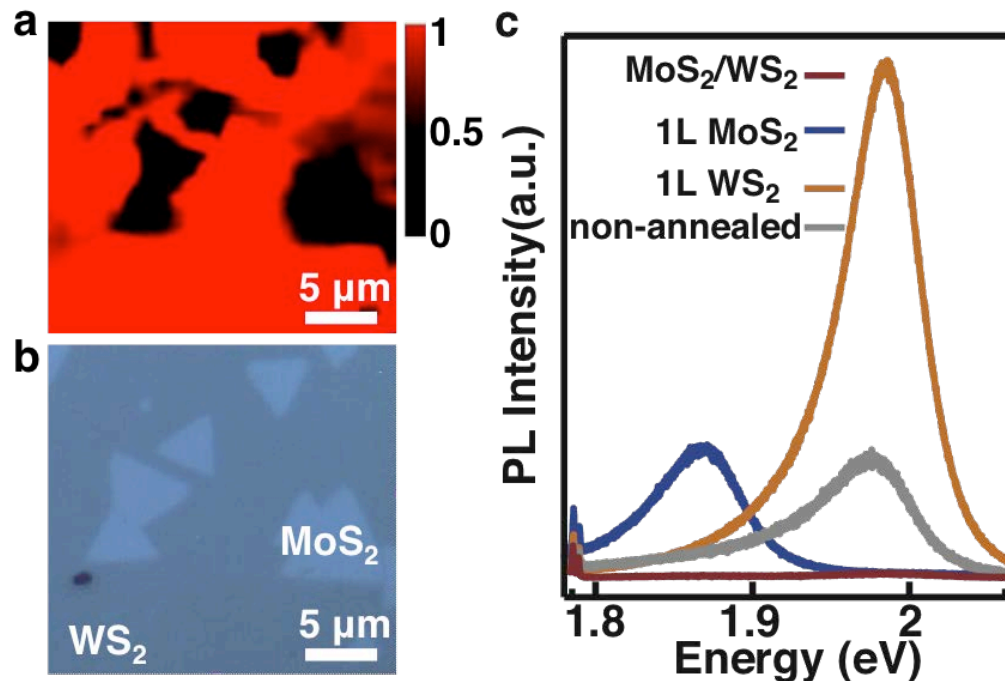
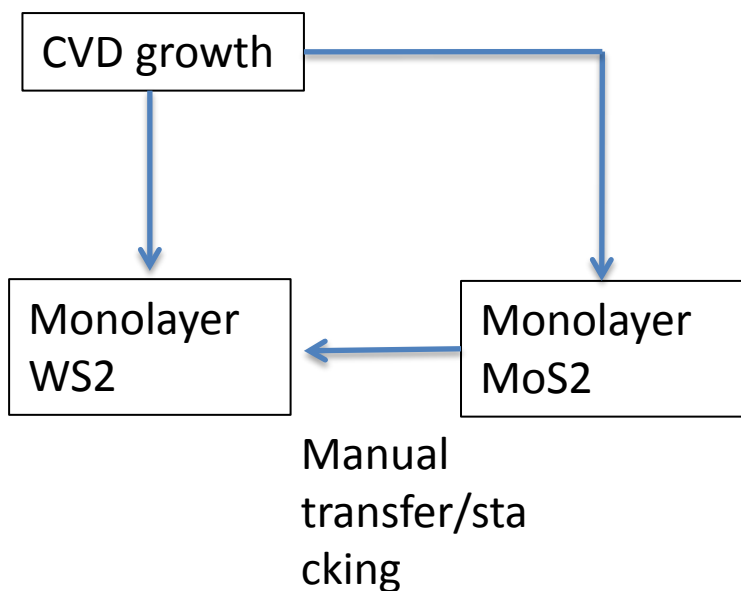
# Efficient Interlayer Exciton Relaxation



- The radiative lifetime of excitons in MoS<sub>2</sub> is around 1-5 ps.
- The PL is suppressed by 50 -100 times after the heterostructuring.

**The interfacial charge transfer is in scale of 10-100 fs!**

# Equally Efficient Interlayer Charge Transfer in Epitaxial and Non-epitaxial MoS<sub>2</sub>/WS<sub>2</sub> Heterostructures



**Efficient interlayer relaxation in non-epitaxial heterostructures!**

# Disclaimer

This tutorial is not meant to be comprehensive. The instructor would like to apologize for missing any important papers/works and would appreciate it if the missing work could be brought to the instructor's attention at [lcao2@ncsu.edu](mailto:lcao2@ncsu.edu).

**Thank You!**